



Characterisation of chromium interactions with *Aspergillus flavus*

AUTHOR(S)

Shilpi Vajpai

PUBLICATION DATE

01-09-2016

HANDLE

[10536/DRO/DU:30102724](https://hdl.handle.net/10536/DRO/DU:30102724)

Downloaded from Deakin University's Figshare repository

Deakin University CRICOS Provider Code: 00113B

Characterisation of chromium interactions with

Aspergillus flavus

by

Shilpi Vajpai

BSc. (Biotechnology), MSc. (Biotechnology)

Submitted in fulfilment of the requirements for the degree of

Doctor of Philosophy

Deakin University

September, 2016



**DEAKIN UNIVERSITY
ACCESS TO THESIS – A**

I am the author of the thesis entitled

“Characterisation of chromium interactions with *Aspergillus flavus*”

submitted for the degree of **Doctor of Philosophy**

This thesis may be made available for consultation, loan and limited copying

in accordance with the Copyright Act 1968.

*I certify that I am the student named below and that the information provided in
the form is correct*

Full Name: Shilpi Vajpai

Signed:

Signature Redacted by Library

Date: 6th September, 2016



**DEAKIN UNIVERSITY
CANDIDATE DECLARATION**

I certify the following about the thesis entitled

“Characterisation of chromium interactions with *Aspergillus flavus*” submitted for the degree of **Doctor of Philosophy**

- a. I am the creator of all or part of the whole work(s) (including content and layout) and that where reference is made to the work of others, due acknowledgment is given.
- b. The work(s) are not in any way a violation or infringement of any copyright, trademark, patent, or other rights whatsoever of any person.
- c. That if the work(s) have been commissioned, sponsored or supported by any organisation, I have fulfilled all of the obligations required by such contract or agreement.
- d. That any material in the thesis which has been accepted for a degree or diploma by any university or institution is identified in the text.
- e. All research integrity requirements have been complied with.

'I certify that I am the student named below and that the information provided in the form is correct'

Full Name: Shilpi Vajpai

Signed:

Signature Redacted by Library

Date: 6th September, 2016

ACKNOWLEDGEMENTS

My PhD. Journey... Well, I must say it has been an amazing, exuberant, and wonderful experience but at the same time most challenging and demanding years of my life, both professionally and personally. To reminisce, I have discovered the very essence of science, learnt to learn from failures, accomplished rewards, moved countries and most importantly embraced motherhood. This journey would have been a difficult one without the love and help of numerous people to whom I would like to express my gratitude and appreciation.

First and foremost I would like to thank my Indian lead supervisor Dr. Alok Adholeya for giving the opportunity to be a part of TERI Deakin PhD. Programme and sharing his vision about science and research. You have taught me the importance of efficient planning and self-criticism that has constantly helped to improve myself.

Words would not be enough to express my gratitude to a person with a beautiful soul, one who stood by me like a rock in the most difficult times, encouraged me and brought back my confidence when I almost gave up - my principal supervisor Professor Leigh Ackland. This PhD. would not have been completed without you. You believed in me and nurtured me like a mother during the entire phase of PhD and I thank you for that. I am grateful to you for always listening to my endless queries patiently and providing immediate solutions. Thank you so much for the constant support and guidance from the beginning till the very end that not only helped me to be a better researcher but a better human being.

A special note of thanks to Lee (Dr. Lee Hudek) for his generous help and support during my stay in Australia. I really appreciate your overall mentoring, from spending hours in teaching me bioinformatics to helping me with the experimental setups for real time PCR to arranging chemicals and primers to driving me to Geelong

several times for instrumental analysis. Working in a foreign lab would have been a struggle without your presence.

Dr Agnes Michalczyk, Dr. Philip Taylor and Mr. Anthony Sommers – thank you so much for extending your expertise in enhancing my knowledge and technical skills. I acknowledge and thank you for the timely help and invaluable suggestions you have provided.

Jeff and Avisia, thanks for being the most wonderful lab mates anyone can have and making me feel like home in Melbourne. Thanks for all those dinners and drives to wonderful Australian beaches.

Sandeep Sure, I can't thank you enough for being a great friend and a critic to my personal and professional traits. This long journey would have felt even longer without you in the lab.

I would also like to extend my thanks to the experts and professionals at TERI, India for carving my research knowledge further. Special thanks to Dr. Manab Das for introducing me to the rich details of Statistical analysis and Dr. Subhash Chandra Yadav (now at AIIMS) for all his wisdom and for seeding my noesis of Transmission Electron Microscopy.

My sincere thanks to Dr. Pushplata Singh and Dr. Mandira Kochar for sharing their expertise on Molecular Biology, Chandrakant Tripathi for Electron microscopy, and Dr. Sunil Kumar Deshmukh for his guidance. A lot of love along with ton of thanks to Priyanka, Deeprajni, Aditya, Aditi, Shloka, Nipanshu, Vatsala, Indu, and Palak for all your help and support and my labmates Leena, Shivani, Pavan, Ankita, Rita, Sreeparna, Shivankar for making it a memorable experience. I am thankful to Mr. Hetramji for always encouraging me to do better, Mr. D. Joshi and all the Lab technicians and assistants (Akhilesh, Lalu bhaiya, Ranjeet bhaiya, Chandan, Yashpal) without their support no stones can be turned.

Finally, I would like to dedicate this thesis to my entire family, my mother, Mrs. Madhu Vajpai, my father Mr. Ravindra Vajpai, my twinsies Monchu and Shipra. I have reached here only because of your unconditional love, faith, and support. Thank you for always encouraging me and letting me know that I am very close to success. You are my inspiration to pursue PhD. I owe my deepest gratitude to my maternal grandparents, “Nanaji and naniji”. Despite of your old age (85 and 80 years), you have provided tremendous support in taking care of my daughter when Ashutosh was in USA.

To my best friend, my companion, my critique, my enemy, my man - Mr. Ashutosh Jain. Thank you for everything. I learnt to do multitasking from you while always setting the right priorities of life in my mind. A big hug and thank you, for cooking dinner several times when I used to be too tired. Thank you for your compassionate attitude towards my infinite mood swings. Above all, I just cannot express how grateful I am to you for taking care of our daughter when I was busy with science. I love you.

Last but not the least, to my beautiful daughter “Samaira”. You have always welcomed me home with a bright smile on your face. Your amusing giggles, comforting cuddles and your sweet kisses have always wiped away my day’s enervation in just a fraction of seconds. You were the only person who made me smile when I wanted to cry. Thank you and God bless you always. I love you.

- Shilpi

PUBLICATIONS ARISING FROM THIS PROJECT

The data presented in this thesis is currently under preparation for publication.

Shilpi Vajpai, Philip E. Taylor, Alok Adholeya, M. Leigh Ackland. “*Characterization of chromium biosorption in SFL strain of A. flavus: Probing the mechanism*”. Manuscript under preparation.

Shilpi Vajpai, Philip E. Taylor, Alok Adholeya, M. Leigh Ackland. “Topographical characterization and *insitu* localization of cell-Cr interaction in *A. flavus*”. Manuscript under preparation.

Shilpi Vajpai, Lee Hudek, Michalczyk Agnes, Pushplata Prasad, Alok Adholeya and M. Leigh Ackland. “Bioinformatics and expression analysis of genes involved in chromium transport in *Aspergillus flavus*”. Manuscript under preparation.

Shilpi Vajpai, Alok Adholeya and M. Leigh Ackland. “Chromium transporters in microorganisms”. Manuscript under preparation.

CONFERENCES ATTENDED / PRESENTATIONS

1. Trends in Molecular and Cellular Applications of Nano-Sciences, 25th-26th April, 2010 at Centre for Cellular & Molecular Biology, Hyderabad, India.
2. 4th Winter School on Nanotechnology and Advance drug delivery at National Institute of Pharmaceutical education and Research (NIPER), 28th February-04th March 2011, Mohali, Punjab, India.
3. Deakin India Research Initiative (DIRI) symposium on “Frontiers in Science”, 21st -23rd November, 2011 at The Energy and Resources Institute, Gurgaon, India
4. International Conference on Mycology and Plant Pathology, Biotechnological Approaches, ICMPB-2012, 27th-29th February, 2012, at Banaras Hindu University, Varanasi, India.
5. SRC Molecular and Medical Research - Postgraduate Symposium, 20th September, 2012 at Deakin University, Burwood campus, Melbourne, Australia.
6. Conference on Agribiotechnology: Industrial Relevance of Genomics and Nanobiotechnology”, 27th November, 2012 at New Delhi, India.
7. Deakin India Research Initiative (DIRI) symposium on “Frontiers in Science” 2nd Edition, 28th -30th November, 2012 at The Energy and Resources Institute, Gurgaon, India.

TABLE OF CONTENTS

ACCESS TO THESIS – A	i
DECLARATION.....	ii
ACKNOWLEDGEMENTS	iii
PUBLICATIONS ARISING FROM THIS PROJECT	vi
CONFERENCES ATTENDED	vii
TABLE OF CONTENTS.....	viii
LIST OF ABBREVIATIONS	xiii
LIST OF FIGURES	xvi
LIST OF TABLES	xx
ABSTRACT	xxi
CHAPTER 1: Introduction.....	1
1.1 Background and foundation of thesis.....	1
1.1.1 The problem: Chromium - a toxic pollutant	1
1.1.2 The solution: Cr tolerant microorganisms	2
1.1.3 The missing link: Cellular and molecular mechanism of cell-Cr interaction.....	2
1.2 Hypothesis	3
1.3 Thesis Objectives	4
1.4 Thesis outline	4
CHAPTER 2: Literature review	6
2.1 Heavy metals.....	6
2.2 Conventional methods of heavy metal removal.....	6
2.2.1 Membrane filtration.....	7

2.2.1.1	Reverse Osmosis	7
2.2.1.2	Ultra-filtration	7
2.2.1.3	Nanofiltration.....	7
2.2.2	Electrodialysis	8
2.2.3	Ion-exchange	8
2.2.4	Chemical precipitation.....	8
2.2.5	Phytoremediation	9
2.3	Bioremediation	9
2.3.1	Non -metabolism dependent “biosorption”	10
2.3.1.1	Ion exchange	10
2.3.1.2	Complexation	11
2.3.2	Metabolism dependent “bioaccumulation	11
2.3.3	Biotransformation	12
2.4	Aspergillus flavus	12
2.5	Chromium.....	16
2.5.1	Uses of Cr: A boon or a curse.....	17
2.5.2	Chemistry of Chromium.....	19
2.5.3	Cr (VI) regulations	20
2.5.4	Biological impacts of chromium.....	20
2.5.4.1	Oxidative DNA damage.....	21
2.5.4.2	Cr (III)-DNA interactions	22
2.6	Toxic effects of Cr	22
2.7	Chromium resistant micro-organisms.....	23
2.7.1	Bacteria.....	23
2.7.2	Algae	23
2.7.3	Yeasts	24

2.7.4	Other fungi.....	24
2.8	Mechanism of Cr resistance in microorganisms.....	25
2.8.1	Chromium resistance in bacteria.....	25
2.8.2	Chromium resistance in algae.....	26
2.8.3	Chromium resistance in fungi.....	27
CHAPTER 3: Materials and Methods.....		29
3.1	Fungal strains and growth conditions.....	29
3.2	Determination of metal tolerance level	29
3.3	Determination of Chromium dose response in broth media.....	29
3.4	Cr (VI) depletion, biosorption and intracellular accumulation study.....	30
3.5	Determination of effect of metabolic inhibitors on Cr uptake.....	31
3.6	Trichloroacetic acid (TCA) protein precipitation and SDS PAGE analysis...	31
3.7	Scanning electron microscopy (SEM) and energy dispersive X-ray (EDX) Analysis	32
3.8	Transmission electron microscopy (TEM) and energy dispersive X-ray (EDX) analysis	33
3.9	Fourier transforms infrared (FTIR)	33
3.10	X-ray photoelectron spectroscopy (XPS).....	33
3.11	Bioinformatics analysis for the identification of Cr transporter genes from A1120 and SFL strain	34
3.12	Sequence retrieval of homologous Cr transporters genes	34
3.13	Sequence alignment using Clustal Omega	35
3.14	<i>In silico</i> identification of putative metal binding sites	35
3.15	Phylogenetic analysis	35
3.16	Membrane topology analysis	35

3.17 Total RNA (Ribonucleic acid) extraction, purification and synthesis of cDNA	36
3.18 Quantitative real time PCR.....	37
3.19 Statistical analysis	37
CHAPTER 4: Discrepant mechanism of cell-Cr interactions in two strains of <i>Aspergillus flavus</i>	39
4.1 Introduction.....	39
4.2 Results	41
4.2.1 Chromium tolerance study.....	41
4.2.2 Dose response study	43
4.2.3 Extracellular depletion of Cr (VI) by <i>A. flavus</i>	43
4.2.4 Total Chromium uptake and intracellular accumulation analysis.....	46
4.2.5 Identification of proteins involved in Cr binding	50
4.3 Discussion.....	53
CHAPTER 5: Topographical characterisation, <i>in situ</i> localization, and speciation of chromium in <i>A. flavus</i>	60
5.1 Introduction.....	60
5.2 Results	62
5.2.1 Localisation of Cr on the cell surface.....	62
5.2.2 Sub cellular localization of Cr.....	62
5.2.3 Identification of functional groups involved in Cr binding	66
5.2.4 Determination of Cr speciation by using X-ray photoelectron..... spectroscopy.....	69

5.3 Discussion.....	72
CHAPTER 6: Structural and functional characterisation of genes involved in chromium transport in <i>Aspergillus flavus</i> : Bioinformatics and gene expression	77
6.1 Introduction.....	77
6.2 Results	79
6.2.1 Identification of putative chromium transporter genes.....	79
6.2.2 Sequence homology analysis of Cr genes in A1120 and SFL strains, and <i>insilico</i> identification of putative metal binding sites.....	80
6.2.2.1 Sulphate uptake transporter	83
6.2.2.2 ABC iron exporter, Atm1.....	86
6.2.2.3 Vacuolar heavy metal transporter, Hmt1	87
6.2.2.4 ABC efflux transporter	90
6.2.3 Transmembrane domain (TMD) analysis of putative Cr transporters	90
6.2.4 Physicochemical properties of putative Cr transporters.....	99
6.2.5 Phylogenetic analysis of putative Cr transporters.....	100
6.2.6 Gene expression analysis	100
6.2.6.1 Sulphate uptake transporter.....	103
6.2.6.2 ABC iron exporter, Atm1.....	103
6.2.7.3 Vacuolar heavy metal transporter, Hmt1	105
6.2.7.4 ABC efflux transporter	105
6.3 Discussion.....	110
CHAPTER 7: Summary and Conclusion.....	120
REFERENCES.....	124

LIST OF ABBREVIATIONS

ABC	ATP binding cassette
ANOVA	Analysis of variance
ATCC	American type culture collection
ATP	Adenosine triphosphate
BLAST	Basic local alignment search tool
BOD	Biological oxygen demand
C- terminal	Carboxyl terminal
Cd	Cadmium
cDNA	Complementary deoxyribonucleic Acid
CHR	Chromate ion transporter
Co	Cobalt
CPCB	Central pollution control board
Cr	Chromium
Cu	Copper
DCCD	N, N-dicyclohexylcarbodiimide
DNA	Deoxyribonucleic Acid
DNP	Dinitrophenol
DPC	Diphenylcarbazine
EDTA	Ethylenediaminetetraacetic acid
EDX	Energy dispersive X-ray
FGSC	Fungal genetics stock center
FTIR	Fourier transform infrared spectroscopy
Hg	Mercury
LCHR	Long Chain chromate ion transporter

MEGA	Molecular Evolutionary Genetics Analysis
MEME	Multiple Em for Motif Elicitation
MIC	Minimum inhibitory concentration
MPL	Maximum permissible limit
N- terminal	Amino terminal
NaN ₃	Sodium azide
NBD	Nucleotide binding domain
NCBI	National Center for Biotechnology Information
Ni	Nickel
OP	Oxidative phosphorylation
PAGE	Polyacrylamide gel electrophoresis
Pb	Lead
PCR	Polymerase chain reaction
PDA	Potato dextrose agar
PDB	Potato dextrose broth
PMSF	Phenylmethane sulfonyl fluoride
ppm	Part per million
qRT-PCR	Quantitative real time polymerase chain reaction
RNA	Ribonucleic Acid
RT	Room temperature
SCHR	Short chain chromate ion transporter
SDS	Sodium dodecyl sulphate
SEM	Scanning electron microscopy
SPSS	Statistical analysis software package
STAS	Sulphate transporter and antisigma factor antagonist
TCA	Trichloroacetic acid

TEM	Transmission electron microscopy
TMD	Transmembrane domain
TMH	Transmembrane helix
TMHMM	Transmembrane hidden Markov model hidden
TNPCB	Tamil Nadu Pollution Control Board
US EPA	United States Environmental Protection Agency
UV-VIS	Ultraviolet–visible
WHO	World health organisation
XPS	X-ray photoelectron spectroscopy
Zn	Zinc

LIST OF FIGURES

Figure 2.1 Macroscopic features of <i>A. flavus</i> on potato dextrose agar.....	15
Figure 2.2 Scanning electron micrograph of <i>A. flavus</i>	16
Figure 2.3 General information about chromium.....	16
Figure 2.4 Various industrial applications of Cr and its compounds	17
Figure 4.1 Cr tolerance by <i>A. flavus</i>	42
Figure 4.2 Effect of increasing concentrations of Cr (VI) on the growth of <i>A. flavus</i>	44
Figure 4.3 Extracellular depletion of Cr (VI) by <i>A. flavus</i>	45
Figure 4.4 Bar graphs showing total Cr biosorption by <i>A. flavus</i> strains after 72 h in potato dextrose broth supplemented different concentrations of Cr (VI).....	47
Figure 4.5 Bar graphs showing Cr accumulation by <i>A. flavus</i> strains after 72 h in potato dextrose broth supplemented different concentrations of Cr (VI).....	49
Figure 4.6 Bar graphs showing the reduction in Cr accumulation by <i>A. flavus</i> strains in the presence of metabolic inhibitors.....	51
Figure 4.7 Detection of proteins expressed in <i>A. flavus</i> cells treated with 50 mg L ⁻¹ and 100 mg L ⁻¹ Cr (VI).....	52
Figure 5.1 SEM EDX analysis of <i>A. flavus</i> mycelia grown in broth media with or without 100 mg L ⁻¹ Cr (VI) supplement.....	63
Figure 5.2 TEM EDX analysis of <i>A. flavus</i> mycelia grown in broth media for 96 h with or without 100 mg L ⁻¹ Cr (VI) supplement.....	65
Figure 5.3 Point and Line EDX analysis of <i>A. flavus</i> cells treated with 100 mg L ⁻¹ Cr (VI)	66
Figure 5.4 FTIR spectra for 100 mg L ⁻¹ Cr (VI) treated <i>A. flavus</i> biomass.....	68
Figure 5.5 High resolution Cr2p spectra recorded after treating <i>A. flavus</i> biomass treated with 100 mg L ⁻¹ Cr (VI)	71

Figure 6.1a Sequence alignment of putative sulfate transporter from A1120 (XP_002374529.1) with amino acid sequence of putative sulphate permease 2 from SFL (scaffold_9G379).....	81
Figure 6.1b Sequence alignment of putative ABC iron exporter, Atm1 from A1120 (XP_002374920.1) with amino acid sequence of iron sulphur cluster transporter, Atm1 SFL (scaffold_12G096).....	82
Figure 6.1c: Sequence alignment of putative vacuolar heavy metal transporter, Hmt1 from A1120 (XP_002379308.1) with amino acid sequence of putative ABC transporter from SFL (scaffold_13G402).....	82
Figure 6.1d Sequence alignment of four putative ABC efflux transporters, A1120 (XP_002373430.1) with amino acid sequence of pleotropic drug resistant protein from SFL (scaffold_8G356).....	83
Figure 6.2: Multiple sequence alignment of alignment of putative sulfate transporter from A1120 (XP_002374529.1) and putative sulphate permease 2 from SFL (scaffold_9G379).....	85
Figure 6.3 Conserved motif analysis of sulfate uptake transporter.....	86
Figure 6.4 Multiple sequence alignment of putative ABC iron exporter, Atm1 from A1120 (XP_002374920.1) and iron sulphur cluster transporter, Atm1 from SFL (scaffold_12G096).....	88
Figure 6.5 Conserved motif analysis of ABC iron exporter ATM1.....	89
Figure 6.6 Multiple sequence alignment of putative vacuolar heavy metal transporter, Hmt1 from A1120 (XP_002379308.1) and putative ABC transporter from SFL (scaffold_13G402).....	91
Figure 6.7 Conserved motif analysis of vacuolar heavy metal transporter Hmt1.....	92

Figure 6.8 Multiple sequence alignment of putative ABC efflux transporter from A1120 (XP_002373430.1) and pleotropic drug resistant protein from SFL (scaffold_8G356).....	93
Figure 6.9 Conserved motif analysis of ABC efflux transporter.....	94
Figure 6.10 Predicted model for transmembrane domain analysis of putative sulfate uptake transporter in A1120 showing	95
Figure 6.11 Predicted model for transmembrane domain analysis of putative sulfate uptake transporter in SFL.....	96
Figure 6.12 Predicted model for transmembrane domain analysis of putative Atm1 transporter in A1120	96
Figure 6.13 Predicted model for transmembrane domain analysis of putative Atm1 transporter in SFL.....	97
Figure 6.14 Predicted model for transmembrane domain analysis of putative Hmt1 transporter in A1120	98
Figure 6.15 Predicted model for transmembrane domain analysis of putative Hmt1 transporter in SFL.....	98
Figure 6.16 Predicted model for transmembrane domain analysis of putative ABC efflux uptake transporter in A1120.....	99
Figure 6.17 Predicted model for transmembrane domain analysis of putative ABC efflux transporter in SFL.....	100
Figure 6.18 Molecular Phylogenetic analysis of putative Cr transporter by Maximum Likelihood method.....	102
Figure 6.19 Relative mRNA expression levels for putative sulphate uptake transporter gene in response to 50 and 100 mg L ⁻¹ Cr at time points of 0, 1, 6 and 24 hours	104

Figure 6.20 Relative mRNA expression levels for putative ABC iron exporter transporter, Atm1 gene in response to 50 and 100 mg L ⁻¹ Cr at time points of 0, 1, 6 and 24 hours	107
Figure 6.21 Relative mRNA expression levels for putative vacuolar heavy metal transporter, Hmt1 gene in response to 50 and 100 mg L ⁻¹ Cr at time points of 0, 1, 6 and 24 hours	108
Figure 6.22 Relative mRNA expression levels for putative ABC efflux transporter gene in response to 50 and 100 mg L ⁻¹ Cr at time points of 0, 1, 6 and 24 hours	109
Figure 6.23 Schematic representation of Cr interaction mechanism in SFL strain of <i>A. flavus</i>	119

LIST OF TABLES

Table 2.1 Summary of different mechanisms of bioremediation	14
Table 2.2 Microscopic features of <i>A. flavus</i>	15
Table 2.3 Different oxidation states of Cr and their characteristics	19
Table 3.1 Primes for quantitative real time PCR (qRT)	38
Table 5.1 Peak positions and allocation of FTIR bands in untreated (control) and Cr treated A1120 and SFL strain	70
Table 5.2 Peak position obtained in Cr _{2p} spectra	71
Table 6.1 Genes used for multiple sequence alignment.....	84
Table 6.2 General characteristics of putative Cr transport proteins	101

ABSTRACT

Widespread use of chromium (Cr) in industrial processes and its subsequent discharge has caused environmental pollution due to the toxic and mutagenic nature of this metal. Microorganisms populating in Cr contaminated environment possess diverse mechanisms for its detoxification. A detailed understanding of the molecular mechanism of Cr detoxification in filamentous fungi has not been reported. The work of this thesis characterized the underlying mechanisms of interaction of Cr in a Cr tolerant fungus, *Aspergillus flavus* strain SFL, isolated from tannery effluent loaded site, in comparison to a non-tolerant *Aspergillus flavus* strain A1120.

The SFL strain was found to tolerate substantially high levels of toxic Cr (VI) than A1120 strain and maintained growth in 100 mg L⁻¹ Cr while the growth of A1120 strain was impaired with 50 mg L⁻¹ Cr in the medium. The SFL strain showed complete depletion of Cr (VI) within 72 h at 100 mg L⁻¹ initial concentration whereas A1120 could reduce up to 85 % Cr (VI). SFL internalized more Cr into its cytoplasm whereas A1120 showed higher total uptake (cell wall bound as well as intracellular). Cr uptake was reduced in the presence of different metabolic inhibitors in SFL strain indicating metabolically active energy dependent chromium uptake system whereas in A1120 a passive mode of Cr uptake (not dependent on cells metabolism) was observed. Proteomic study revealed substantial differences between SFL and A1120 strain at the cellular level as indicated by differential expression pattern of proteins. Induction of ~35kDa protein (perhaps a glutathione synthetase) upon Cr treatment in SFL strain, not induced in A1120 indicated its potential involvement in conferring tolerance to Cr in SFL strain.

The characteristic physical and chemical interactions occurring at the cell surface between Cr and fungal cell were studied using scanning electron microscopy (SEM),

transmission electron microscopy (TEM), energy dispersive X-ray analysis (EDX), fourier transform infrared spectroscopy (FTIR) and X-ray photoelectron spectroscopy (XPS) were found to be similar in both SFL and A1120 strains. The combined SEM-EDX study revealed that the Cr (VI) exposed biomass of both SFL and A1120 was prominently different with irregular Cr deposits on the hyphal surfaces than the unexposed biomass having smooth surface. TEM-EDX study showed Cr is localized on fungal cell wall as well as in cell cytoplasm in both SFL and A1120 strain. The functional groups responsible for Cr (VI) binding was identified by fourier transform infrared (FTIR) spectroscopy which demonstrated involvement of carboxyl, amine and hydroxyl functionalities as main Cr binding sites present on the fungal cell wall in both the strain. Analysis of Cr speciation done via X-ray photoelectron spectroscopy (XPS) detected the presence of only Cr (III) corresponding to Cr (OH)₃ on the cell wall indicating, the reduced Cr (III) specie is precipitated on the cell wall in both the fungal strains.

Investigations using a genomic approach allowed the mapping of genes involved in Cr tolerance/accumulation. BLAST searches were carried out to identify putative Cr uptake and efflux genes namely, putative ABC efflux transporter, putative Atm1, putative Hmt1, putative sulphate transporter that might have a potential role in Cr resistance. These putative Cr transporter genes were tested for their responsiveness to short term Cr (VI) exposures at concentrations 50 mg L⁻¹ and 100 mg L⁻¹ by quantitative real time (qRT) PCR. Significant upregulation of sulphate uptake gene after 1 h of Cr exposure suggested it may have a potential role in uptake of Cr in both SFL and A1120 strains. A key finding of this study was the significant upregulation of Atm1 gene in SFL strain after Cr exposure suggesting it may function in mediating Cr tolerance in SFL by defending against mitochondrial damage and the non-responsiveness of this gene in A1120 suggested sensitivity to Cr by causing

mitochondrial toxicity. The role of ABC efflux and Hmt1 gene remained unclear which indicated the need for a long term Cr exposure study.

The data presented in this thesis provides preliminary data on the underlying molecular mechanisms of Cr tolerance in *Aspergillus flavus* fungi and demonstrates the presence of intrinsic intracellular mechanism of Cr accumulation as well as upregulation of genes mediating tolerance and survival at high Cr. This property can be genetically improved to use SFL as a potential tool for bioremediation and /or biomining purpose.

CHAPTER 1: Introduction

1.1 Background and foundation of thesis

1.1.1 The problem: Chromium - a toxic pollutant

Chromium (Cr) is an important heavy metal that occurs naturally in the environment. Today it is one of the most problematic environmental pollutants due to its toxicity (Mishra and Bhargava, 2016). Cr and its compounds are universally used in various industrial practices as diverse as leather tanning, chrome plating, wood preservation, textile dyeing and pigmentation, manufacturing pulp and paper etc. As a result, a large and alarming amount of Cr laden waste is discharged into the environment mainly to soils and waters that leads to Cr pollution, a serious environmental pollution problem worldwide (Gu et al., 2015, Ilias et al., 2011, Tripathi et al., 2011, Agrawal et al., 2006). The two most stable forms of Cr occurring in nature are the trivalent Cr, [Cr(III)] and the hexavalent Cr, [Cr (VI)] that differ in toxicity, bioavailability and mobility (UdDin et al., 2015). Cr (III) is scarcely soluble and less toxic form (Maqbool et al., 2015) and is an essential nutrient that plays a significant role in glucose metabolism (Cefalu and Hu, 2004). On the other hand, Cr (VI) is the most toxic state of Cr and commonly exists in the form of ions as chromate (CrO_4^{2-}) or dichromate ($\text{Cr}_2\text{O}_7^{2-}$). It is a strong oxidising agent, highly soluble, highly carcinogenic and teratogenic in nature has been listed as class-A human carcinogen according to the United States Environmental Protection Agency (US-EPA) (Maqbool et al., 2015, Desai et al., 2008). Efficient and environment friendly methods are thus needed to be developed to reduce the heavy metal content (Juang and Shiau, 2000, Yan and Viraraghavan, 2001).

1.1.2 The solution: Cr tolerant microorganisms

Several methods have been devised for the treatment and removal of heavy metals from aqueous streams including chemical precipitation, lime coagulation, ion exchange, reverse osmosis and solvent extraction (Ahalya et al., 2003). These techniques apart from being economically expensive have disadvantages such as incomplete metal removal, high reagent and energy requirements, and generation of toxic sludge or other waste products that require disposal (Juang and Shiau, 2000, Yan and Viraraghavan, 2001). The search for new technologies involving the removal of toxic metals from wastewaters has directed attention towards microorganisms populating heavy metal contaminated sites. These microbes adapt to survive in toxic conditions by developing tolerance/resistance are termed metal-tolerant (Morais et al., 2011, Krumov et al., 2009). A large number of Cr tolerant/resistant microorganisms including bacteria (Ran et al., 2016, Sharma and Adholeya, 2012; McLean and Beveridge, 2001), microalgae (Han et al., 2007, Deng et al., 2009), yeast (Ksheminska et al., 2008; Chatterjee et al., 2012, Ram'irez-Ram'irez et al., 2004) and fungi (Chang et al., 2016, Alonso et al., 2014, Shugaba et al., 2012, Sharma and Adholeya, 2011) have been identified and studied extensively for their possible role to remove Cr (VI) from aqueous solutions. Filamentous fungi in general are highly promising candidates well known for their ability to tolerate and remove metals from the environment by utilizing different mechanisms (Puglisi et al., 2012, Iram et al., 2013).

1.1.3 The missing link: Cellular and molecular mechanism of cell-Cr interaction

Despite numerous researches published on the use of fungi for Cr (VI) removal and various resistance mechanisms proposed to cope with chromate toxicity relying on

their capability to modulate the toxic concentrations of this metal ion there is insufficient or no information available on large scale industrial applications (Dhankhar and Hooda, 2011, Poljsak et al., 2010). The molecular mechanisms of Cr biotoxicity still remain unclear, which prevents the development of an optimal strategy for its detoxification and bioremediation of industrial wastewaters (Ksheminska et al., 2008). Moreover, a detailed understanding of the of Cr interactions in *Aspergillus flavus* (*A. flavus*), a potential remediation tool is still unexplored.

With this background, this thesis aims to probe the underlying mechanism of cell-Cr interactions in a filamentous fungus, *Aspergillus flavus* strain SFL previously isolated from Cr contaminated site. The study focuses on examining different facets of fungal interplay with Cr including physiological, topographical and molecular level. Overall, a model has been proposed that compares the cellular processing of Cr by two strains of *Aspergillus flavus*, the Cr tolerant SFL strain and the non-tolerant strain A1120.

1.2 Hypothesis:

The hypothesis of the present study originated from the fact that metal tolerant microbes develop specific strategies for their survival under stress. Based on this, I hypothesize that:

1. Cr-tolerant fungi possess active defense mechanisms of tolerance, reduction and intracellular transport of Cr which could lead to their application to develop a novel Cr hyper accumulator strain with enhanced Cr tolerance and accumulation properties.

2. Fungi able to accumulate Cr may also serve as potential biofactories for the synthesis of Cr (III) biocomplexes, probably in nano form with potential industrial and pharmacological applications.

1.3 Thesis Objectives

Keeping in view the many potential applications of Cr tolerant fungi in future, the following objectives are set forth for the proposed work:

1. To compare the chromium uptake and reduction rates in tolerant and non-tolerant strains of fungi.
2. To characterize the chromium complexes formed by fungi, their speciation and intracellular localization.
3. To identify chromium transporter genes and carry out expression analysis in tolerant and non-tolerant fungi.

1.4 Thesis outline

The thesis is divided into seven Chapters. Chapter 1 outlines the background and foundation of thesis, aim of the present study, research hypothesis and specific objectives. Chapter 2 discusses the review of literature related to aim of the thesis. In brief, heavy metal pollution, conventional and biological methods of metal removal, Cr toxicity and its biological impacts, various mechanisms of Cr resistance in different microorganisms has been discussed in detail. Chapter 3 describes the material and experimental methods used. Chapter 4 discusses the comparative analysis of Cr (VI) tolerance, physiological uptake and reduction in a Cr tolerant and non-tolerant strain of *A. flavus*. Chapter 5 demonstrates the surface phenomena of Cr interaction with the fungi, Cr localisation and speciation. Chapter 6 deals with the

identification, characterisation and expression analysis of Cr tolerant genes and delineates the molecular mechanism of Cr tolerance in *A. flavus*. Chapter 7 summaries the work done and highlights the major conclusions of the study. The gaps in the present study and the future direction for further research have been presented.

CHAPTER 2: Literature review

2.1 Heavy metals

Naturally occurring elements in the earth's crust having density greater than 5 g cm^{-3} are known as heavy metals and are comprised of 40 elements (Passow et al., 1961). Metal ions are required as trace elements for animals, plants and microorganisms; however they become toxic at high concentrations. Pollution caused by the discharge of excessive amount of heavy metals into the environment has become a serious issue worldwide because of the disastrous effect on living organisms. Recent technological developments and fast industrialization significantly contributes to the emission of heavy metals into the environment (Abbas et al., 2016). This poses a major threat to the environment and well as to public health (Cerbasi and Yetis, 2001). According to the World Health Organization, heavy metals that require urgent consideration include chromium (Cr), lead (Pb), cadmium (Cd), mercury (Hg), nickel (Ni), cobalt (Co), copper (Cu) and zinc (Zn), since they are prone to prevail and accumulate in the environment due to their non-biodegradable nature (WHO, Geneva 2010, Kobya et al., 2005).

2.2 Conventional methods of heavy metal removal

Due to this persistent problem of heavy metal pollution, a prior treatment of industrial wastewater is essential before release into the environment. Some widely used conventional methods for removal of heavy metals from polluted soil and water are explained below:

2.2.1 Membrane filtration:

Membrane filtration is an effective method for the industrial effluent treatment due to its ability to remove inorganic pollutants including heavy metals, as well as suspended solid and organic compounds. On the basis of particle size retained at the membrane during filtration process it is further categorised as (a) ultrafiltration, (b) nanofiltration and (c) reverse osmosis (Kurniawan et al., 2006).

2.2.1.1 Reverse Osmosis:

Reverse Osmosis is the process of removal of heavy metals using cellophane like semi-permeable membrane under high pressure. In this process the purified water is allowed to pass through the membrane while the contaminants are rejected (Fu and Wang, 2011). The main disadvantage of the process is the high cost involved (Ahalya et al., 2003).

2.2.1.2 Ultra-filtration:

Ultrafiltration is a pressure-driven purification process in which heavy metals, macromolecules and suspended solids are separated on an ultrafiltration membrane according to the pore size (5-20nm) and molecular weight of the compound. Low molecular weight particles/complexes are passed through the membrane while the larger and heavy molecules are retained (Fu and Wang, 2011, Vigneswaran et al., 2004). Generation of sludge is the major drawback of this process (Ahalya et al., 2003).

2.2.1.3 Nanofiltration :

Nanofiltration is a separation technique intermediary between reverse osmosis and ultrafiltration. In this process the ionic species are separated on a nanofiltration

membrane on the basis of charge and pore size (Seidel et al., 2001, Fu and Wang, 2011) where molecules as small as one nm in size can be retained on the nanofiltration membrane. Insufficient separation and membrane fouling are the main drawbacks of this method (Van Der Bruggen et al., 2008).

2.2.2 Electrodialysis:

Electrodialysis is a process where ionized species of heavy metal from the solution are separated using charged ion exchange membrane under the influence of electric field. When electric potential is applied between the electrodes, the anions migrate toward the anode and the cations toward the cathode, crossing the ion-exchange membranes (Chen, 2004). Corrosion of electrodes becomes a limiting factor and the generation of metal hydroxides that blocks the membrane is a major disadvantage of the process (Ahalya et al., 2003, Kurniawan et al., 2006).

2.2.3 Ion-exchange:

Ion-exchange includes the exchange of heavy metal ions from aqueous solutions by employing an ion exchanger, commonly a solid synthetic organic ion exchange resins with ions bound to the exchange resin by electrostatic forces. Incomplete removal of some ions is the disadvantages of this method (Kurniawan et al., 2006, Ahalya et al., 2003).

2.2.4 Chemical precipitation:

Chemical precipitation is the process in which heavy metals are precipitated from the aqueous solution as insoluble metal hydroxides (Wang et al., 2004). Precipitants like alum, lime, lime stone, iron salts and various organic polymers are added in order to precipitate heavy metals. It is relatively slow process that generates

voluminous amount of toxic sludge generated which needs further processing is the major drawback (Aziz et al., 2008, Ahalya et al., 2003).

2.2.5 Phytoremediation:

Phytoremediation is the process in which plants are used for the removal of contaminating pollutants and metals from soil, sediment, and water. Longer time required in cleaning up of metals and plant regeneration for continued accumulation is the main disadvantages (Ahalya et al., 2003).

These techniques have many disadvantages like partial removal of metal, high energy input, greater reagent need, and generation of sludge containing toxic substances that need disposal. There is a need to further develop them as economical and nature friendly procedures to minimize heavy metal content from the environment (Juang and Shiau, 2000, Yan and Viraraghavan, 2001). In search of new technologies for metal removal, researchers have directed their interest towards bioremediation, which rely on ability of various microorganisms to remove metals.

2.3 Bioremediation

It can be described as the capability of microbial biomass to remediate pollutants such as toxic organic compounds, heavy metals from soil, water, wastewater or any other contaminated site (EPA, 2016). Bioremediation of heavy metals such as Cr(VI), Cu(II), As(V), and Cd(II) depends upon their transformation to less toxic form and/or immobilisation is based on their conversion to a less toxic form and/or immobilization (Alvarez et al., 2016). There are some significant advantages of this method compared to the chemical treatments (Kratochvil and Volesky, 1998) such as: less costly, more efficient, minimum chemical and biological sludge generation, renewal capacity of biosorbent, and possibility of metal recovery.

Depending on the cellular metabolism there are two ways by which metals are removed by microorganisms, as indicated by their intricate cellular structure.

2.3.1 *Non -metabolism dependent “biosorption”*

The microbial biomass has an inherent capacity to adsorb metals due to the presence of functional groups such as -NH₂, -COOH, -SH, and -OH on microbial cell walls, which act as binding sites for interaction of metal ions (Kuyucak and Volesky, 1988). The microbial biosorbents can be specific for metal or have no specific priority. The microbial biomass can be from fungi, yeast, bacteria as by-product biomass or from marine algae and seaweeds (Volesky, 1994). Both prokaryotic and eukaryotic microorganisms such as bacteria, algae, fungi and yeasts have been used for metal biosorption (Volesky, 1986). In this process, the metal gets biosorbed on the cell wall of microbes as a result of different physical and chemical reactions. It occurs due to the presence of van der Waals' forces. The strong electrostatic forces between the metal ions and cell wall of microbes was assumed to be responsible for the biosorption of uranium, cadmium, zinc, and cobalt by non-living algal, fungal and yeast biomass (Kuyucak and Volesky, 1988). These interactions were proved to be associated with biosorption of Cu²⁺ by bacterium *Zoogloea ramigera* and alga *Chlorella vulgaris* (Aksu et al., 1992). This process is comparatively quicker and reversible (Kuyucak and Volesky, 1988). This further includes ion exchange and chemical sorption.

2.3.1.1. *Ion exchange:* In this process, the divalent cations interchange with the antagonistic ions of the polysaccharides of microbial cell wall. For example, the alginates of marine algae exist as salts of potassium, sodium, calcium and magnesium interchange with the antagonistic ions of cobalt, copper, cadmium and

zinc, leading to the sequestration of heavy metals by microorganisms (Kuyucak and Volesky, 1988). Fungus *Ganoderma lucidium* (Muraleedharan and Venkobachr, 1990) and *Aspergillus* (Ahalya et al., 2003) take up copper using this phenomena.

2.3.1.2 Complexation: Another method for metal removal from solutions is by formation of complexes on the cell surface once the metal and the dynamic groups interact. Both physical adsorption and formation of coordination bonds between metals and amino and carboxyl groups of the polysaccharides of cell wall, are involved in the biosorption of copper in *C. vulgaris* and *Z. ramigera* (Aksu et al., 1992). Complexation has been shown as the sole mechanism that enables calcium, magnesium, cadmium, zinc, copper and mercury to be accumulated by *Pseudomonas syringae*. In addition microorganisms also release acids like citric, oxalic, gluconic, fumaric, lactic and malic acids, that interchelate with toxic metals giving rise to metallo-organic complexes that renders dissolving of metal compounds ultimately removal from the surface (Ahalya et al., 2003).

2.3.2 Metabolism dependent “bioaccumulation”

The transport of heavy metal ions through the cellular membrane of microorganisms is a metabolism dependent biosorption, which implies that this type of phenomena occurs only in viable cells. The dynamic defence system of the microorganism, which responds in the presence of toxic metal, may be associated with this mechanism (Ahalya et al., 2003). It could be assumed that, the metabolism dependent biosorption is directed by the similar mechanism used for the import of metabolically essential ions like potassium, magnesium and sodium. Such ions having same charge and ionic radius may confuse the metal transport system (Ahalya et al., 2003).

2.3.3 Biotransformation:

Biotransformation is a crucial step that involves reduction of toxic metal to its less toxic form. This process is enhanced by employing metal reducing microorganisms. Biological reduction of metals is an effective mode of detoxification from polluted sites and therefore metal resistant microorganisms have a potential use in bioremediation (Jain et al., 2012). This can be further categorised into direct (enzyme mediated reduction) or indirect reduction (by reducing compounds produced by micro-organisms). A table summarising different mechanisms of bioremediation of heavy metals with special focus on Cr is given (Table 2.2).

2.4 *Aspergillus flavus*:

Kingdom Fungi is one of the most diverse groups of Eukaryotes. With approximately 5.1 million species present in this kingdom, about 100,000 species have been identified (Blackwell, 2011; Hibbett and Taylor, 2013, Kirk et al., 2008). Fungi are heterotrophic organisms that possess cell wall made up of chitin and grow in the form of single cells or as a network of multicellular mycelium. Most fungi can reproduce sexually and asexually via formation of spores although some species are not able to reproduce sexually and produce reproductive structures, but some species are not capable of forming specialized reproductive structures and populate entirely by vegetative growth (Wang et al., 2009). *Aspergillus flavus* is a filamentous fungi belonging to the class Euromycetes and order Eurotiales. It was first discovered by Link in 1809. Eurotiales are sac fungi possessing three families, 49 genera and 928 species (Kirk et al, 2008). All the sequenced genomes in order Eurotiales are *Aspergillus* species belonging to large genus "*Aspergillus*" and also including

Mechanism of bioremediation	Description	Heavy metals and microorganism	Reference
Biosorption	Adsorption of Cr (VI) to microbial cells	Cu, Zn, Cd, Pb (<i>Pseudomonas aeruginosa</i>) Cr(VI) (<i>Arthrobacter Viscosus</i>) U (<i>Pleurotus ostreatus</i>) Hg, Cu, Pb (<i>Cryptococcus sp.</i> AH-13, <i>Candida palmioleophila</i> KB-6) Hg (<i>Aspergillus versicolor</i>)	Zolgharnein et al., 2010 Hlihor et al., 2016 Zhao et al., 2016 Ngo, 2016 Das et al., 2009
Ion exchange	Metal cation interchange with the antagonistic ions of the polysaccharides of microbial cell wall	Cu (<i>Ganoderma lucidium</i>) Cu (<i>Aspergillus</i>)	Muraleedharan and Venkobachr, 1990 Ahalya et al., 2003
Complexation	Complex formation between metals and dynamic groups present on microbial cell	Ca, Mg, Cd, Zn, Cu, Hg (<i>Pseudomonas syringae</i>) Cu (<i>C. vulgaris</i> and <i>Z. ramigera</i>)	Ahalya et al., 2003 Aksu et al., 1992
Anionic adsorption	Electrostatic interaction where metal oxy anion bind to the cationic functional groups on the cell surface	Cr (VI) (<i>Pseudomonas putida</i>)	Garg et al., 2013
Adsorption-coupled reduction	Metal reduction followed by adsorption to biomass in the presence of acidic pH	Cr (VI) (<i>Coriolus versicolor</i>)	Sanghi et al., 2009
Anionic and cationic adsorption	Partial reduction of Cr(VI) to Cr (III) followed by adsorption of both cationic and anionic Cr specie	Cr (VI) (Agricultural solid waste)	Namasivayam and Sureshkumar, 2008
Reduction and anionic adsorption	Partial reduction of Cr (VI) to Cr (III) where only anionic Cr (VI) is adsorbed to cell biomass	Cr (VI) (<i>Larix leptolepis</i> Gold.)	Aoyama, M. and Tsuda, 2001

Table continues on next page...

Mechanism of bioremediation	Description	Heavy metals and microorganism	Reference
Bioaccumulation	Heavy metal transport across the cellular membrane of microbes	Cr (<i>Pichia guilliermondii</i>) Co^+ (<i>S. cerevisiae</i>)	Kaszycki et al., 2004 White and Gadd, 1986
Biotransformation/Bioreduction	Redox process which requires supply of electrons to reduce metals	Cr (VI) (<i>Sporosarcina saromensis</i> M52) Cr (<i>Aspergillus</i> , <i>Penicillium</i> , <i>Trichoderma</i>)	Zhao et al., 2016 Gouda, 2000; Acevedo-Aguilar et al., 2006, Morales and Cristiani, 2008

Table 2.1 Summary of different mechanisms of bioremediation of chromium.

Neosartorya fischeri, a telomorph of *Aspergillus fischeri* (Wang et al., 2009). The species belonging to the order Eurotiales are common and have various industrial and medicinal importances while some species are known human pathogen such as *Aspergillus fumigatus* (Yang et al., 2016). The genus *Aspergillus* can be identified by their characteristic conidiophores however the identification and differentiation of species is quite complex. Conventional taxonomy was based upon the morphological features along with molecular phylogenetics (Klich, 2002, Mangala et al., 2016). *A. flavus* is a saprophyte and has a world-wide distribution. It is found naturally in soil and over dead and decaying matter. Some microscopic features of *A. flavus* as described by Hedayati et al., 2007, are described below (Table 2.2). The culture of *A. flavus* on potato dextrose agar plate is shown (Figure 2.1). Scanning electron microscopy picture are shown in Figure 2.2.

Microscopic features	Description
Colony	Granular, flat, yellow to dark green in colour
Conidiophores	Thick walled, hyaline, coarsely roughened, ~1 mm in length
Vesicles	Subglobose to globose, 10–62 μm in diameters
Phialides	Uniseriate or biseriate
Primary branches	upto 10 μm in length
Secondary brances	upto 5 μm in length
Conidia	Globose to subglobose, 3.5 to 6 μm in diameter and conspicuously echinulate

Table 2.2 Microscopic features of *A. flavus* (Hedayati et al., 2007)



Figure 2.1 Macroscopic features of *A. flavus* on potato dextrose agar

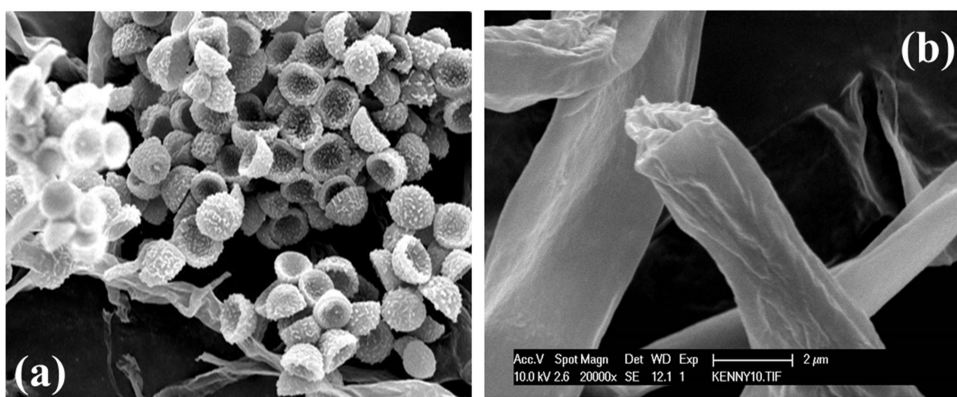


Figure 2.2 Scanning electron micrograph of *A. flavus* (a) spores (b) hyphae

2.5 Chromium

Chromium (Cr) having atomic number (24) and atomic weight (51.996) amu, is a d block element of the periodic table, that belongs to the group of transition metals (Figure 2.3). It occurs naturally in the earth's crust as chromite ore (FeOCr_2O_3). It also disperses in air, soil and water through volcanic discharge and erosions of Cr bearing rocks. Amongst most abundant elements on earth's crust, Cr acquires seventh position. French chemist Louis Nicolas Vauquelin first discovered Cr in a red lead mineral crocoite (PbCrO_4) in 1797 (Mishra and Bhargava, 2016).

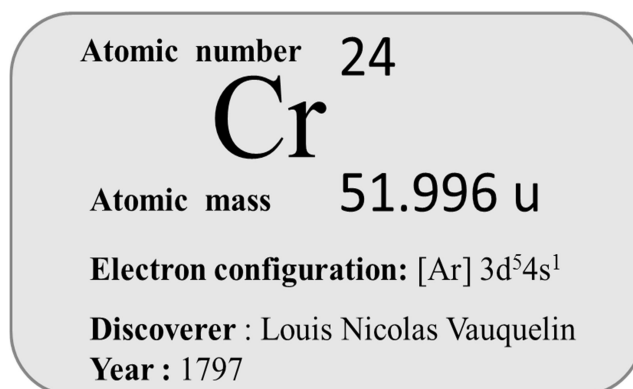


Figure 2.3: General information about chromium.

2.5.1 Uses of Cr: A boon or a curse?

Cr is an industrially important metal that is universally used in different industrial practices (Mishra and Bhargava, 2016, Pilon-Smits, 2005, Gao and Xia, 2011) in (Figure 2.4). The estimated yield of Cr in the world is around 10^7 tonnes per year; most of which (60-70%) is utilized in alloys, including stainless steel, and shown some (15%) in chemical industries, majorly in leather tanning process (Mishra and Bhargava, 2016, Cervantes et al., 2001, Polti et al., 2011). Due to its excessive use of this metal in different industrial applications a large amount of Cr is subsequently discharge into the environment Cr. As a result researcher's attention is mainly drawn towards Cr remediation (Zayed and Terry, 2003).

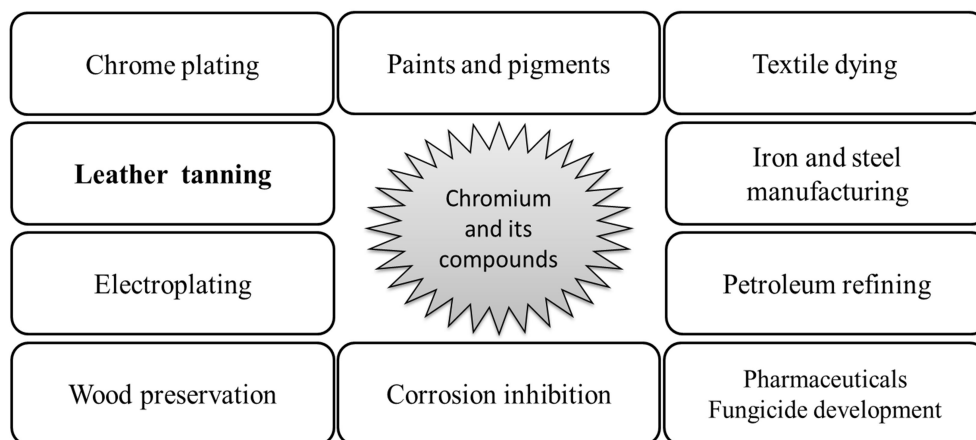


Figure 2.4: Various industrial applications of Cr and its compounds.

Amongst all industrial wastes, tannery industry which commonly uses Cr for tanning process is one of the major causes for high influx of this metal into the biosphere. Tannery industry is one of the oldest and fastest growing industries in India and there are about 2,161 tanneries excluding cottage industries, which discharge annual of $9,420,000 \text{ m}^3$ wastewater into the environment (Sharma, and Goyal, 2010). The process of tanning employs a Cr salt that convert hide to leather and the waste water

released from tanneries (tannery effluent) contain these Cr salts in excess (Sharma and Adholeya, 2011). The disposal of untreated effluent and sludge discharged by tanneries is one of the emerging problems as it contains high concentration of organic Cr which acts as pollutant (Apte et al., 2005). For instance, in India annually approximately 2000–3000 tones Cr discharges from tannery industries, having concentrations spanning between 2000 and 5000 mg L⁻¹ in the aqueous effluent as compared to the recommended permissible discharge limits of 2 mg L⁻¹ (Altaf et al., 2008). As per waste water discharge standard of Central Pollution Control Board, New Delhi, India (CPCB, 2000-2001), the discharge concentration of Cr should not exceed from 0.1 mg L⁻¹. As per the Pure Earth world's worst pollution problem reports 2015 Cr is ranked 4th amongst the top six toxic threats and approximately 16 million people are at risk to Cr exposures (Pure Earth, USA report 2015). The World's Worst Polluted Places reports released by Blacksmith Institute, USA in 2006 and 2007 also highlighted most polluted cities in India where chrome mining, chrome tanning, textile and other nearby industries discharge effluent containing higher concentration of toxic pollutants including chromium were reported. Places namely Sukinda valley in Orissa and Ranipet in Tamilnadu were among the top ten toxic threats in 2007. In Ranipet, India average concentration of chromium in surface water was found to be 247 µg L⁻¹, quintuple of the recommended permissible limit of 49 µg L⁻¹ (Srinivasa and Govil, 2008). It was noted that local tannery operations required manufacturing of Cr salts like sodium chromate (Na₂CrO₄), chromium (III) sulphate (Cr(H₂O)₆)₂(SO₄)₃ used as tanning agents, as a consequence around 15 lakh tons of solid waste aggregated in Ranipet over a period of last 20 years (Tamil Nadu Pollution Control Board (TNPCB), 2010). Whereas in Sukinda, approximately 70 % surface water and 60 % drinking water was found contaminated with hexavalent chromium which approximately twice the level of

national and international standards (Dhakate et al., 2008). In West Berkeley, California, USA, groundwater Cr (VI) contamination was found as a result of historical industrial activities. Similar finding was reported from Ljubijansko Poije aquifer in Slovenia due to industries in nearby area (Brilly et al., 2003).

2.5.2 Chemistry of Chromium:

In nature, Cr occurs in different oxidation states that range from -2 to +6 described in Table 2.1. But the frequently found oxidation states are Cr⁰, Cr (II), Cr (III) and Cr (VI) (Mishra and Bhargava, 2016). Of the various oxidation states, the trivalent, [Cr (III)] and the hexavalent state [Cr (VI)] are the most stable forms existing in the environment (Dayan and Paine, 2001, Thacker et al., 2006, Srivastava and Thakur, 2006).

Oxidation state	Properties
Elemental chromium	Biologically inert. Does not exist in nature
Univalent chromium	Unstable in nature
Divalent Cr (II)	A strong reducing agent which easily get oxidised to Cr ³⁺
Trivalent Cr (III)	Most stable and dominant specie of Cr. It is an essential nutrient required in glucose metabolism in humans.
Quadrivalent Cr (IV)	Intermediate specie of Cr formed during reduction of Cr (VI) to Cr (III). Toxic in nature.
Pentavalent Cr (V)	Intermediate specie of Cr formed during reduction of Cr (VI) to Cr (III). Toxic in nature
Hexavalent Cr (VI)	Second most stable form. It is a strong oxidising agent. Highly carcinogenic and mutagenic in nature.

Table 2.3 Different oxidation states of Cr and their characteristics.

Cr (III) is relatively insoluble and thus less toxic due to lesser availability for uptake (Leita et al., 2011, Beyersmann and Hartwig, 2008). On the other hand Cr(VI) is the

most harmful state of Cr, which commonly exists in the form of ions as hydro chromate (HCrO_4^-), chromate (CrO_4^{2-}) or dichromate ($\text{Cr}_2\text{O}_7^{2-}$). Cr (VI) is found in copious amount in deposits and surface waters, and is highly soluble and mobile in nature than Cr (III) and all other species of Cr (James 2002, USEPA 2005).

2.5.3 Cr (VI) regulations:

The United States Environmental Protection Agency (USEPA) has designated chromium as the priority pollutant due to its toxic mutagenic and carcinogenic properties which are significantly harmful to human health (USEPA, 2000, Thacker et al., 2006) and also listed among the 17 chemicals that presents biggest threat to humans (Marsh and McInerney, 2001). Slightly elevated amount of Cr can cause serious negative impact on the environment. Hence strict regulations have been enforced by various government bodies. The maximum threshold level of Cr (III) in waste and ground waters is 5 mg L^{-1} (Acar and Malkoc, 2004). For Cr (total), the maximum permissible limit (MPL) of total Cr is 2 mg L^{-1} for surface waters (Park et al., 2004) and that for Cr (VI) in drinking water has been established at a concentration of 0.05 mg L^{-1} on the basis of health considerations (Yadav et al., 2005, WHO, 2004) whereas as per environment protection agency (EPA) drinking water standards, the MPL of total Cr in drinking water is 0.1 mg L^{-1} (US EPA, 2011).

2.5.4 Biological impacts of chromium

The biological impact of chromium is related to its interaction with the biological matter. Depending upon the speciation of Cr and the representative organisms studied, diverse effects have been displayed (Poljsak et al., 2010). Though living membranes are virtually impenetrable for Cr (III), it may enter the cells by promptly

forming composites in aqueous environment with the most biologically applicable ligands (Poljsak et al., 2010). Once inside the cells Cr (III) takes part in DNA-DNA cross-linking (Snow and Xu, 1989) DNA-protein cross-linking (Kortenkamp et al., 1992), DNA condensation, and decreases DNA replication fidelity (Bridgewater et al., 1994). Cr (VI) has pronounced toxicity effects upon entering the cellular system, in both prokaryotic and eukaryotic cells. The mechanism most likely contribute to the genotoxicity of Cr (VI) is related to the formation of transient, short lived Cr (IV) and/or Cr (V) complexes and free radicals during its intracellular reduction to Cr (III) with the aid of the cytoplasmic reductants such as ascorbate and glutathione (Costa M., 2003, Xu et al., 2004, Xu et al., 2005). Since Cr (VI) is not able to interact with DNA directly, DNA damage is caused during such reduction reaction inside the cell which can be grouped into two categories: (a) oxidative DNA damage and (b) Cr (III)-DNA interactions (Arakawa et al., 2012, Sobol and Schiestl, 2012).

2.5.4.1 Oxidative DNA damage

Cr (V) so produced inside the cytoplasm is oxidized back to Cr (VI) leading to generation of reactive oxygen species (ROS) which includes hydrogen peroxide (H_2O_2), superoxide superoxide ($O_2^{\cdot-}$), hydroxyl radical (OH^{\cdot}) and singlet oxygen (O_2^{\cdot}) (Cheng et al., 2009, McNeill and McLean, 2012). As a result of oxidative stress in cells and the DNA protein cross-links formed, significant promutagenic effects are induced in cells (Quievryn et al., 2003, Reynolds et al., 2009). Cr (VI) is known to alter normal physiological functions of the cell by binding to cellular materials and Cr (VI) species along with hydroxyl radicals cause DNA lesions in vivo (Pesti et al., 2000, Cervantes et al., 2001, Zhitkovich, 2001).

2.5.4.2 Cr (III)-DNA interactions:

During Cr (III)-DNA interactions, the magnitude of DNA damage is greater as stable complexes are formed between the intracellularly trapped Cr (III) with proteins and nucleic acids. This is due to the weak membrane permeability and greater binding efficiency of Cr (III). The formation of binary and ternary Cr (III)-DNA adducts (L-cysteine-Cr (III)-DNA and ascorbate-Cr (III)-DNA) and related highly reactive (OH^{\bullet}) radical induce severe cellular DNA damages and play a key role in increasing both genotoxicity as well as mutagenicity in human cells (Valko et al., 2005, Quievryn et al., 2002, Quievryn et al., 2003).

2.6 Toxic effects of Cr:

Excessive concentrations of Cr (VI) in the organic matter in soils modifies the biological structure of soil microbial communities that greatly impacts the microbial biomass thus affecting microbial activities related to decomposition of organic matter, cycling of nutrients etc. (Zhou et al., 2002, Shi et al., 2002). Cr (VI) easily crosses the cellular membranes, both in prokaryotic and eukaryotic cells, resulting in loss of membrane integrity and/or inhibition of the electron transport chain (Codd et al., 2001, Francisco et al., 2010). In plants, Cr concentration above 2 ppm was found to have inhibitory effects on plant growth, seed germination and leading to necrosis. Plants growing in the neighbourhood of chromium discharging factories have reported diminished photosynthesis and change in chloroplast structure in vegetable and fruit trees (Yadav et al., 2006). Cr (VI) is also highly hazardous to human health and affects through inhalation, skin contact, and ingestion, being highly toxic, carcinogenic and mutagenic to living organisms, even in very low amounts. Its compounds are known to cause irritation in the lining of the nose, breathing problems, allergy reactions, skin rashes, reproductive problems, anaemia,

irritation and ulcer in small intestine and sometimes cancer and tumours in stomach, intestinal tract and lung, etc. (Kozlowski and Walkowrak, 2002, Agency for Toxic Substances and Disease Registry, 2008).

2.7 Chromium resistant micro-organisms:

Elevated concentration of toxic metals has deleterious effects on the functionalities of microbial communities that inhabit contaminated environments. In order to survive in toxic conditions, concentration of these metals (Habi and Daba, 2009, Ahmad, 2012). Over a period of time, several Cr resistant microorganisms has been identified and studied extensively for their potential as Cr removing agents.

2.7.1 Bacteria

Some of the recently identified Cr resistant bacterial strains are *Zobellella denitrificans* (He et al., 2016), *Rhizobacteria* (CrS2) (Pramanik et al., 2016), *Sporosarcina saromensis* M52 (Ran et al., 2016), *Bacillus methylotrophicus* (Mala et al., 2015), *Bacillus dabaoshanensis* sp. nov. (Cui et al., 2015) *Brevibacterium casei* (Verma and Singh, 2013), *Serratia* sp. Cr-10 (Zhang and Li, 2011), *Leucobacter chromiirestiens* sp. nov., (Sturm et al., 2011). Several others include bacteria belonging to genera *Escherichia*, *Bacillus*, *Pseudomonas*, *Pantoea*, *Cellulomonas*, *Micrococcus*, *Staphylococcus*, *Achromobacter* and *Ochrobactrum* (Narayani and Shetty, 2013).

2.7.2 Algae

Comparatively lesser data is available Cr tolerance and biosorption using algal species than other microorganisms. Some examples are *Dictyosphaerium chlorelloides*, a laboratory strain trained to be Cr (VI)

resistance (D'ors et al., 2016), *Spirulina platens* (Zinicovscaia et al., 2016), *Rhizoclonium hookeri* (Kayalvizhi et al., 2015), and *Cladophora albida* (Deng et al., 2009), *Ceramium virgatum* (Sari and Tuzen, 2008), *Chlorella miniata* (Han et al., 2007), *Scenedesmus acutus* (Torricelli et al., 2004) and *Spirogyra* species (Gupta et al., 2001).

2.7.3 Yeasts

Several yeast strains have been isolated from different Cr polluted sites and are known for chromate resistance. These include *Cyberlindnera fabianii*, *Wickerhamomyces anomalus* and *Candida tropicalis* (Bahafid et al., 2013), *Rhodotorula mucilaginosa* (Chatterjee et al., 2012), *Candida maltose* (Ramírez-Ramírez et al., 2004), *Pichia guilliermondii* ATCC 201911 (L2) (Ksheminska et al., 2008), *Saccharomyces cerevisiae* (Fedorovych et al., 2009), *Schizosaccharomyces pombe* (Czakó-Veér et al., 1999).

2.7.4 Other fungi

A large amount of data is available on Cr resistance by fungal system and many Cr resistant fungi have been identified including *Cladosporeum perangustum*, *Penicillium commune*, *Fusarium equiseti* (Sharma and Malviya, 2016) *Trichoderma asperellum* (Chang et al., 2016), *Penicillium griseofulvum* MSR1 (Samuel et al., 2015), *Aspergillus niger* (Gu et al., 2015, Alonso et al., 2014), *Paecilomyces lilacinus* (Sharma and Malviya, 2016, Sharma and Adholeya, 2011), *Termitomyces clypeatus* (Ramrakhiani et al., 2011, Das et al., 2009), *Coriolus versicolor* (Sanghi and Srivastava, 2010), *Aspergillus versicolor* (Das et al., 2008) and many more.

2.8 Mechanism of Cr resistance in microorganisms

Metal resistance is defined as the ability of an organism to respond to concerned metal species by means of mechanisms to promote their survival in a toxic metal environment. In different organisms different mechanism of Cr (VI) resistance has been demonstrated. In general, three main strategies adopted by the microorganism to confer Cr (VI) resistance are reduction, uptake and efflux (Joutey et al., 2015). In this section, mechanism of Cr (VI) resistance by different microorganisms has been explained.

2.8.1 Chromium resistance in bacteria:

Bacteria exhibits transmembrane efflux of chromate as one of the survival mechanism which has been well documented. In species like *Pseudomonas* (Bopp et al., 1983, Cervantes and Ohtake, 1988, Summers and Jacoby, 1978) and *Alcaligenes* (Nies et al., 1989) a plasmid-determined resistance to chromate has been shown. In these organisms the plasmid-specified resistance phenotype was determined by ChrA, a hydrophobic protein with 12 proposed transmembrane-spanning domains (Cervantes et al., 2001, Cervantes et al., 1990, Nies et al., 1990) ChrA is a membrane protein belonging to chromate ion transporter (CHR) superfamily that confers chromate resistance by pumping chromate out of the cell in an energy dependent process (Alvarez et al., 1999). Two families of CHR proteins have been reported, a bidomain long chain chromate ion transporter or LCHR, approximately 340-500 amino acid long and a monodomain short chain chromate ion transporter or SCHR approximately 120-250 amino acid long. Both families of CHR transporters are known to mediate chromate efflux in bacteria. Phylogenetic analysis of CHR protein revealed several homologous membrane found in all three domains of life; bacteria, archea and eukaryota (Díaz-Pérez et al., 2007).

Another Cr resistance mechanism reported in bacterial species is reduction of Cr (VI) to Cr (III). Chromate reductases secreted by these organisms mediate the conversion of hexavalent Cr to its trivalent form via electron transfer reactions by its cytosolic form under aerobic conditions and by its membrane bound component under anaerobic conditions (Camargo et al., 2003). In *Bacillus methylotrophicus* extracellular chromate reductase activity has been reported (Mala et al., 2015). In *Shewanella oneidensis* MR-1, involvement of outer membrane bound cytochromes in the extracellular reduction of Cr (VI) to insoluble Cr (III) precipitate has been reported (Belchik et al., 2011).

2.8.2 Chromium resistance in algae

Little is reported about the Cr resistance in algae with no information on tolerance mechanisms. Possibly, the exudates secreted by algal cells form complexes with Cr (VI) to reduce its toxic effects (Gorbi et al., 2004). It was described in *S. acutus* that after treatment with chromate, asexual reproduction does not occur and tolerance to Cr (VI) is acquired resulting in a Cr-resistant offspring by sexual reproduction (Corradi et al., 1995a). This species when incubated with Cr (VI) results in the formation of agglomerates; which when dissipates, biflagellate cells are released, allowing cell survival (Corradi et al., 1995a). Interaction of Cr with plastidial metabolism was demonstrated in *Scenedesmus* (Corradi, and Gorbi, 1993), *Chlorella* (Wong, and Chang, 1991) and *Euglena* (Fasulo et al., 1983). There are reports that in the presence of Cr, plastid-deprived gametes were induced (Corradi et al., 1995b). Surprisingly, diminished chromium uptake and Cr (VI) resistance were not correlated in *Scenedesmus* (Gorbi et al., 1996).

2.8.3 Chromium resistance in fungi

In filamentous fungi and yeasts, mutations in the laboratory strain were induced to determine the mechanism of Cr resistance (Marzluf, 1970, Czako-Veř et al., 1999). Non-functionality of sulphate transport system was also described in the chromate-resistant mutants of filamentous fungus *Neurospora crassa* (Marzluf, 1970) indicating the role of sulphate transport system in Cr tolerance. Mutations affecting a single copy glutathione reductase gene (*pgr*⁺¹) resulted in enhanced Cr (VI) tolerance in fission yeast *Schizosaccharomyces pombe*. Glutathione reductase facilitates the reduction of Cr (VI) to the reactive intermediate Cr (V) and subsequently generating reactive oxygen species (peroxides and superoxides and hydroxyl radical) that lead to cytotoxic and genotoxic effects on the cell. Hence, a diminished glutathione dependent glutathione reductase activity coupled with decreased production of hydroxyl radicals induced Cr (VI) tolerance in *S. pombe* (Gazdag et al., 2003). For the chromate-resistant strains of *Candida maltosa*, it was found that a NAD-dependent chromate-reducing activity took place mainly in the soluble protein fraction, and was less active in the membrane fraction (Ramirez-Ramirez et al., 2004). In another study, it has been discovered that a significant role in Cr (VI) detoxification belongs to extracellular reducing substances, which are secreted by the yeast cells (Ksheminska et al., 2006). It was shown that extracellular pathways leading to Cr (VI) reduction are also an important factor in providing the resistance of the cells to chromate (Ksheminska et al., 2008). In a separate study, it was observed that the sequestration of Cr (possibly in vacuoles) is increased due to the activity of a putative transcriptional activator MSN1 in yeast, seen when its disruption decreases Cr sequestration, regardless of the content of Cr (Chang et al., 2003). The role of metabolically active vacuoles in heavy metals resistance was shown in *S. cerevisiae* where mutants with non-functional vacuole, mutants lacking

vacuole-like structures as well as mutants devoid of a particular subunit of vacuolar (V)-H⁺-ATPase demonstrated high sensitivity to chromate and tellurite (Gharieb, and Gadd, 1998). Studies on *Aspergillus* in the past have conclusively proven its biosorption abilities, also another species from same genera, *A. niger* showed chromate reduction of the more toxic Cr (VI) to less toxic Cr (III) and indicated that this process was not an enzyme mediated process (Park et al., 2005a, b). In *A. parasiticus* and *A. niger* uptake and reduction of Cr (VI) has been described as a mechanism of Cr detoxification (Shugaba et al., 2012).

Hence it can be concluded that fungi exhibit different mechanisms of Cr resistance. To investigate the potential for fungi to be used either as an environmental heavy metal remediator or as a biomining tool it is necessary to characterize the cellular and molecular mechanism related to Cr (VI) tolerance and detoxification. This thesis describes an analysis of the mechanisms of Cr resistance/tolerance in a strain of *Aspergillus flavus* (SFL) isolated from a Cr-contaminated site in comparison to the laboratory *A. flavus* strain (A1120). Firstly the two fungal strains were compared for their ability to tolerate, accumulate and reduce Cr (VI). Further investigations were done to characterize the surface configuration of fungi in relation to Cr binding and different functional groups potentially involved in the binding process were identified. Localisation and Cr speciation analysis was done. To further delineate the mechanism at molecular level, putative genes encoding Cr transporters were identified. *In silico* analysis was carried out to analyze the structural and functional characterization of these transporters and gene expression studies were done to test the responsiveness of putative gene to Cr exposures. Overall a model of Cr tolerance in SFL strain of *A. flavus* has been proposed.

CHAPTER 3: Materials and Methods

3.1 Fungal strains and growth conditions

The well-characterized reference strain *A. flavus* (FGSC A1120, henceforth A1120) was obtained from Fungal Genomics Stock Group, Kansas City, Kansas, U.S.A. Chromium tolerant *A. flavus* (SFL), previously isolated from tannery effluent, was provided by the Centre for Mycorrhizal Research at TERI, New Delhi, India. Cultured plates were grown and maintained on potato dextrose agar (PDA) (Hi-media Lab. Ltd., Mumbai, India) plates at 30°C in a BOD incubator.

3.2 Determination of metal tolerance level

Tolerance to chromium was determined for both reference and tolerant fungal strains. PDA medium (Hi-media Lab. Ltd., Mumbai, India) was prepared and supplemented with various amounts of potassium dichromate ($K_2Cr_2O_7$) (Hi-media Lab. Ltd., Mumbai, India) ranging from 100 mg L⁻¹ to 3200 mg L⁻¹. The PDA plates, containing different concentrations of chromium, were each inoculated with a 10 mm disc taken from the edge of actively growing fungal colony and incubated at 30°C for 10 days. Fungi grown on PDA plates containing no Cr (VI) were used as controls. The tolerance level to Cr (VI) was determined by measuring the diameter of fungal growth (Zafar et al., 2007, Ezzouhri et al., 2009). The experiment was performed using three biological replicates.

3.3 Determination of Chromium dose response in broth media

To establish the effect of Cr (VI) on growth in a submerged culture, the fungus was grown in potato dextrose broth (PDB) containing 50 mg L⁻¹, 100 mg L⁻¹, 250 mg L⁻¹ and 500 mg L⁻¹ Cr (VI) concentrations and incubated in a continuous rotatory shaker

incubator (Kuhner Shaker X, Lab-Therm LT-X) at 140 rpm at 30°C for 144 h. After every 24 h, the biomass was harvested by sieving through 300 µ mesh and placed in hot air-oven at a temperature of 60°C for drying till the constant weight arrived. The constant dry weight was recorded. Biomass of fungi grown in media not supplemented with any Cr was used as the control. The experiment was performed using three biological replicates.

3.4 Cr (VI) depletion, biosorption and intracellular accumulation study:

The capacity of Cr (VI) to be removed from the media by actively growing A1120 and SFL strains was examined by cultivating each fungus in 250 ml Erlenmeyer flasks containing 100 ml PDB, in a continuous rotatory shaker at 140 rpm at 30°C. At the mid exponential phase (48 h), the mycelial biomass was separated from the culture broth by sieving through 300µm mesh and re-suspended in 100 ml of fresh media supplemented with 50,100 and 250 mg L⁻¹ K₂Cr₂O₇ solution, and again incubated at 30° C in a rotatory shaker at 140 rpm for 96 h. After every 24 h, the biomass was harvested, washed with sterile water to remove the loosely bound Cr (Ahmad et al., 2003), centrifuged and divided into two halves. One half was used immediately after the treatment (contains total Cr taken up by the fungus). The remaining half was treated with 20 mM ethylenediaminetetraacetic acid (EDTA) for 30 min (to remove cell wall bound Cr). Samples were dried in hot air oven at 60°C and later digested in concentrated nitric acid for 2 h. Total Cr was detected in the acid digested samples with flame atomic absorption spectrophotometer (TJA Solutions Solaar M5 series Model). Results were analysed using three replicates.

Residual Cr (VI) in the supernatant was determined using 1, 5-di-phenylcarbazide method (DPC) (Greenberg et al., 1981). Briefly, to 950 µl sample, 20 µl of 0.5% w/v 1, 5-di-phenylcarbazide (prepared by dissolving 250 mg DPC in

50 ml acetone) was added. Few drops of 10 % H₂SO₄ were added to give a pH of 2 ± 0.5 in a total reaction volume of 1 ml. The reaction mixture was left at room temperature for 10 min for full colour development and Absorbance was measured in a UV-VIS spectrophotometer (UV-2450, SHIMADZU, USA) at 540 nm. Cr (VI) concentration was calculated by preparing a Cr (VI) standard curve using K₂Cr₂O₇ solution in the range of 0.5 - 5 mg L⁻¹. Total Cr was determined by flame atomic absorption spectrophotometer (TJA Solutions Solaar M5 series Model). Cr (III) was determined in the supernatant by subtracting the remaining Cr (VI) from the total Cr (Gu et al., 2015, Shen et al., 2012). Media not inoculated with fungi was taken as control. Three replicates of each culture were taken.

3.5 Determination of effect of metabolic inhibitors on Cr uptake:

To study the effect of metabolic inhibitors on Cr uptake, experiments were carried out according to (Das et al., 2009) with some modifications. Briefly actively growing fungus was incubated in 100 ml of PDB supplemented with 50, 100 and 250 mg L⁻¹ K₂Cr₂O₇ solution, and containing 200 uM N,N'-dicyclohexylcarbodiimide (DCCD), 1 mM sodium azide (NaN₃) and 1mM 2,4-dinitrophenol (DNP) at 30° C in a rotatory shaker at 140 rpm. The biomass was then harvested and processed as described in the previous section. Three replicates of the culture were taken. The biomass not incubated with inhibitors was taken a control.

3.6 Trichloroacetic acid (TCA) protein precipitation and SDS PAGE analysis

The TCA precipitation of protein protocol was based on Carpentier et al., 2005 with some modifications. Briefly, fungal biomass was grown to mid log phase (new growth material); harvested by centrifugation, water washed and approx. 2 g

maximum wet weight was grounded in powder using liquid nitrogen. The powdered biomass was suspended in 50mM phosphate buffer (pH 7.2), vortexed and centrifuged at 10000 rpm to collect the debris. To the supernatant, 10 % (w/v) TCA dissolved in acetone containing 1mM phenylmethane sulfonyl fluoride (PMSF) and 0.07 % β -mercaptoethanol was added. This suspension was kept at -20°C for 1 h and stirred at regular intervals. Total protein was precipitated by centrifugation at 4°C for 20 minutes at 14000 rpm. The protein pellet was then washed with 100 % acetone, air dried and redissolved in 50 mM phosphate buffer. The concentration of protein was determined using Bradford method; 250 μ l Bradford reagent (Sigma-Aldrich, USA) was added to 10 μ l protein sample. Absorbance was read in HIM microplate reader (Biotek, USA) at 595nm. Approximately 15 μ g of protein was electrophoresed on 15 % SDS-PAGE gel and the bands were visualised after staining with Coomassie Brilliant Blue R-250 stain. The experiment was performed using three biological replicates.

3.7 Scanning electron microscopy (SEM) and energy dispersive X-ray (EDX) analysis:

Fungal strains treated with Cr for up to 96 h and controls were freeze dried and mounted onto aluminum stubs and coated with gold in a sputter coater (Polaron SC7610, Fisons Instruments) and examined under SEM (Philips XL20). Duplicate samples were carbon-coated (Polaron CA7615, Fisons Instruments) and analyzed under SEM with energy-dispersive x-ray spectroscopy (EDS, X-Max 50 mm², Oxford Instruments) to detect Cr signals in the fungal mycelia. Data was processed with Aztec Nanoanalysis Software (Oxford Instruments).

3.8 Transmission electron microscopy (TEM) and energy dispersive X-ray (EDX)

analysis:

For TEM, duplicate samples of Cr treated and untreated cells were fixed in 1.5 % glutaraldehyde buffered with sodium phosphate buffer (50 mM, pH 7.2). Primary fixation was done for 3 h at 4°C. The cells were then washed with fresh buffer several times. Secondary fixation was done in 0.75 % Osmium tetroxide for 1 h. The cells were again washed several times with buffer. Dehydration of cells were done in graded acetone solutions and followed by engrafting in spur resin. An ultra cut E, Ultramicrotome (PowerTome, RMC Products, USA) was used to cut ultrathin sections of approximately 60–80 nm in thickness. Electron scattering provided by the adsorbed metal ions acted as the contrasting agent. Electron micrographs were recorded in a transmission electron microscope (Technai 20 G2 STEM, 200KV FEI Company, The Netherlands) at 80 kV (Das et al., 2008, Srivastava and Thakur, 2006) and EDX analysis was done at 200 kV. Gatan's Digital Micrograph software was used for processing the images.

3.9 Fourier transforms infrared spectroscopy (FTIR):

For FTIR study fungal biomass treated with and without Cr were harvested by centrifugation and washed with deionized water several times and freeze dried. The infrared spectra of duplicate samples were recorded on Nicolet 6700 FTIR spectrometer in the region of 400–4000 cm^{-1} with 500 scans at a resolution of 2 cm^{-1} .

3.10 X-ray photoelectron spectroscopy (XPS):

For XPS study fungal biomass treated with and without Cr were harvested by centrifugation and washed with deionized water several times and freeze dried. XPS

analysis was performed at LaTrobe University, Melbourne, Australia using a Kratos Nova with an Al K α energy source at 1486.6 eV. Scans of duplicate samples were conducted using an anode voltage of 15 kV and a current of 10 mA. The pass energy was set to 20 eV for high resolution scans. The binding energy was calibrated by referencing the charge to the hydrocarbon C 1s peak at 284.8 eV.

3.11 Bioinformatics analysis for the identification of Cr transporter genes from A1120 and SFL strain:

To identify putative Cr transporter genes present in *A. flavus* protein sequences encoding metal ion transporters were retrieved from the sequenced genome of reference (A1120) *Aspergillus flavus* (NCBI Accession number; AAIH00000000.2) obtained from NCBI genome database. Four putative transporters were selected based on the designed hypothesis and the related literature search. The identified putative Cr transport sequences, from A1120 strain, were used as bait to pull out putative Cr transporter amino acid sequences from the recently sequenced (at TERI) and putatively annotated genome of Cr tolerant SFL strain (unpublished) on the basis of maximum sequence similarity and percent identity.

3.12 Sequence retrieval of homologous Cr transporters genes:

For a comparative sequence analysis basic local alignment search tool (BLAST) searches were carried out to retrieve homologous sequences in other fungal species *Aspergillus oryzae*, *Aspergillus parasiticus*, *Talaromyces marneffie* and *Penicillium italicum* as the genome of these fungi are fully sequenced and *Saccharomyces cerevisiae*, *Arabidopsis thaliana* as these are the two well studied model organisms.

3.13 Sequence alignment using Clustal Omega

Multiple sequence alignment were produced using sequence alignment tool Clustal Omega (Higgins and Sharp, 1988, Sievers et al., 2011). NCBI conserved domains database search (Marchler-Bauer A et al., 2015) was carried out for the identification of conserved regions in the aligned species.

3.14 Insilico identification of putative metal binding sites:

Putative metal binding sites were identified by using Multiple Em for Motif Elicitation MEME programme (Version 4.11.2) (Bailet et al., 2009). Following parameters were used: the maximum number of motifs to be found, 5. Minimum width of motifs was set as 5 and the maximum width of motif was set as 15.

3.15 Phylogenetic analysis:

For the construction of phylogenetic tree MEGA (Molecular Evolutionary Genetics Analysis) version 6 was used (Tamura et al., 2013). The evolutionary history was inferred by using the available Maximum Likelihood algorithm based on the JTT matrix-based model. For a reliable assessment, 1000 bootstrap replicates were taken.

3.16 Membrane topology analysis:

The amino acid sequences were submitted to Transmembrane Hidden Markov Model (TMHMM) online programme for the prediction of total number of transmembrane domains (TMDs and the physicochemical properties of putative Cr transporters were determined using Expasy's ProtParam tool.

3.17 Total RNA extraction, purification and synthesis of cDNA:

A1120 and SFL strains were grown for 48 h in PDB media. The biomass was then harvested and treated with 50 mg L⁻¹ and 100 mg L⁻¹ Cr (VI) for 1 h, 6 h, and 24 h. Total RNA was extracted using PureLink RNA mini kit (Ambion). The kit protocol followed as described below: Approximately 100 mg of frozen fungal pellet was grounded into fine powder using liquid nitrogen in RNase free motor and pestle. Liquid nitrogen was allowed to evaporate. Immediately 1 ml of lysis buffer containing β-mercaptoethanol was added and homogenised and transferred to RNase free Eppendorf tube and centrifuged at ~2,600 × g for 5 minutes at room temperature (RT). The supernatant was transferred to a new RNase free tube. Approx. 0.5 volume of 96 % ethanol was added to the volume of homogenate and thoroughly mixed on vortex. The mixture (700 µl) was transferred to spin cartridge and spun for 15 s at high speed. The flow through was discarded and this step was repeated 3 to 4 times until the entire sample was processed. The flow through was discarded and 700 µl of wash buffer I was added directly to the Spin Cartridge and centrifuged for 15 s at 12,000 × g at RT. The flow through and the collection tube was discarded and the spin cartridge was placed into a new collection tube. To this 500 µL Wash Buffer II containing ethanol was added and again spun for 15 s at 12,000 × g at RT. The flow through was discarded and this step was repeated twice. The membrane was dried by spinning the spin cartridge along with the collection tube at 12,000 × g for 1 minute at RT. The flow through was discarded and spin cartridge was reinserted into a new eppendorf tube. 11. Finally, RNA was eluted in 50 µl RNase-Free Water added directly to the center of the Spin Cartridge, incubated at RT for 1 minute, spun for 2 minutes at ≥12,000 × g at RT. Approximately 1.5 mg of isolated RNA was then treated with DNase I (Sigma-Aldrich, USA) as per the given protocol and used for cDNA synthesis using the iScript cDNA synthesis kit

(Bio-Rad Laboratories, Inc.) using following PCR conditions: 5 minutes at 25°C, 30 minutes at 42°C and 5 minutes at 85°C. RNA and cDNA quantification was done using the HIM microplate reader (Biotek, USA). The experiment was performed using three biological replicates.

3.18: Quantitative real time PCR

The response of putative Cr transporter genes to Cr (VI) exposure was tested by qRT-PCR. Primer Express software (Applied Biosystems, Primer Express version 2.0) was used to design the real time primers. Primers were bought from Sigma-Aldrich (Melbourne, Australia) (Table 3.1). The efficiency of primers were tested by amplification of template cDNA as control at concentrations of 1, 2, 4 and 8 $\mu\text{g ml}^{-1}$ and comparing the cycle time on a log scale. The binding efficiencies of all primers were >0.1 . qRT PCR analysis was executed using: cDNA 50 ng; 10X Sso Fast Eva Green Supermix Dye (Bio-Rad Laboratories, Inc.), 10 μl ; forward and reverse primers, 0.3 μM with the final volume of reaction mixture, 20 μl . qRTPCR analysis was carried out on a CFX96 Touch Real-Time PCR Detection System (Bio-Rad Laboratories, Inc.). β -tubulin was taken as internal control for the normalization of targeted gene expression. Three replicates of each sample were taken and a no template control reactions lacking template cDNA was included.

3.19 Statistical analysis

All the experiments were carried out in triplicates. The data are presented as standard error of mean ($\pm\text{SEM}$). The data analysis for Cr reduction and uptake studies was done using one-way analysis of variance (ANNOVA) and independent t-test. A non-parametric Kruskal-Wallis test and Tukey's post hoc analysis were performed for gene expression study data. Significance of difference was tested

against the probability values (p-value) of <0.05. SPSS version 22.0 was used for all statistical analyses.

Name	Sequence of primers (5'-3')
BTub qRT (F)	GCCGCTTTTGGACTTGCTCC
BTub qRT (R)	ACTGATTGCCGATACGCTGG
Sul qRT (F)	GGGCGATCTCAAAACCAAAA
Sul qRT (R)	AAATAACGGCCCACCTGATG
Atm1 qRT (F)	ACAGCGACCAAATCCTTGACTAAA
Atm1 qRT (R)	ATCGAGCTCAAGAAGTTCACGAT
Vac qRT (F)	GCTTTGGTTGTCACTATTGTCACA
Vac qRT (R)	GCTTTGGTTGTCACTATTGTCACA
ABC qRT (F)	GGGCGCACTCTGGTTATGA
ABC qRT (R)	CACTGGAGAAATGCTGGAACAA

Table 3.1 Primes for quantitative real time PCR (qRT). The primers used for gene expression study are listed as forward (F) and reverse (R). BTub represents internal control β -tubulin. Sul represents sulphate uptake gene. Atm1 represents Atm1 gene, Vac represents vacuolar Hmt1 gene and ABC represents ABC efflux gene.

CHAPTER 4

Discrepant mechanism of cell-Cr interaction

in two strains of *Aspergillus flavus*

4.1 Introduction:

The capacity of microorganisms to acquire different resistance/detoxification mechanisms to deal with the toxic effects of metals enables them to tolerate and survive in high concentrations of polluting heavy metals (Gadd, 2001, Krumov et al., 2009). These different detoxification strategies are therefore of great significance in metal removal processes. Extrapolation of various mechanisms of metal tolerance/resistance might lead to development of microbes with high intrinsic tolerance and promising metal accumulation potential (Chang et al., 2016, Shugaba et al., 2012).

Various detoxification mechanisms have been proposed in relation to Cr (VI) tolerance. Cr studies in various filamentous fungi have demonstrated either adsorption and/or Cr (VI) reduction mechanism for Cr removal. Biosorption and/or bioaccumulation of Cr (VI) has been reported in a number of filamentous fungi including: *Aspergillus foetidus* (Prasenjiti and Sumathi, 2005), *Aspergillus niger* (Kovacevic et al., 2000), *Termitomyces clypeatus* (Das et al., 2009), *Aspergillus sp.* (Congeevaram et al., 2007), *Hirsutella sp.* (Srivastava and Thakur, 2006a) and *Rhizopus* (Bai and Abraham, 2001). Reduction of Cr (VI) to less toxic Cr (III) was investigated in actively growing the filamentous fungi: *Aspergillus sp.*, *Penicillium sp.* (Acevedo-Aguilar et al., 2006, Fukuda et al., 2008) and *Trichoderma inhamatum* (Morales and Christiani, 2008). In *Aspergillus* and *Rhizopus sp.*, an “adsorption coupled reduction” mechanism for Cr(VI) removal has been described whereby Cr

(VI) is completely reduced to Cr (III) by the fungal biomass and then adsorbed to the cell surface (Park et al., 2005, 2007, Sanghi et al., 2009). In *Paecilomyces lilacinus* (Sharma and Adholeya, 2011), *Aspergillus niger* (Alonso et al., 2014, Gu et al., 2015), *A. flavus* (Singh and Bishnoi, 2015, Singh et al., 2016) both Cr (VI) reduction and adsorption has been demonstrated but reduction has been reported as the main mechanism. The events of intracellular accumulation of Cr have not been explored in detailed in filamentous fungi. Moreover, the mechanisms of interaction of Cr (VI) with *A. flavus* are not well studied.

Hence, to gain an understanding of the mechanisms of Cr interaction with fungi, I evaluated Cr (VI) tolerance and detoxification via biotransformation or reduction, sorption and intracellular accumulation in the filamentous fungi, *Aspergillus flavus* strain SFL, previously isolated from a tannery effluent-loaded site containing high concentrations of chromium, in comparison to a laboratory reference strain of *A. flavus* A1120. This knowledge will form the basis to study the interaction of Cr with fungal cell at cellular and molecular level and develop a novel Cr hyper accumulator strain with enhanced Cr tolerance and accumulation property.

My project examined three different pathways of Cr biosorption: 1) extracellular depletion of Cr (VI), 2) cell surface sorption and 3) intracellular accumulation. The effect of increasing concentration of Cr (VI) on the growth of fungi was examined and the maximum Cr (VI) tolerance level was determined in comparison to the reference strain. Cr (VI) reduction by the two fungal strains was studied in the extracellular growth medium. Cr biosorption and accumulation study was carried out by determining the amount of total Cr uptake by the cell as well as that taken up inside the cell. The intracellular accumulation of Cr is an energy-dependent process and to confirm this, metabolic inhibitor study was done. Further, SDS-PAGE analysis was carried out to visualise proteins expressed under Cr stress.

In addition, a qualitative comparison was done to identify differences between A1120 and SFL strain with respect Cr interaction. Overall, substantial differences in the mechanism of Cr tolerance exhibited by SFL and A1120 strain have been shown.

4.2. Results

4.2.1 Chromium tolerance study:

Cr tolerance was measured in the reference (A1120) and tolerant (SFL) fungi grown in potato dextrose agar media containing increasing concentration of Cr (VI) ranging from 100 mg L⁻¹ to 3200 mg L⁻¹ over a period of 10 days (Figure 4.1).

A prominent difference in the response to Cr (VI) tolerance was observed between the two strains. The A1120 strain showed 27% reduction in growth at 100 mg L⁻¹ Cr (VI) (Figure 4.1a_{iii}) compared to control containing no Cr (VI) in the media (Figure 4.1a_i). No growth was observed above 100 mg L⁻¹ Cr (VI) (Figure 4.1a_{iii, iv}). In contrast, the SFL strain showed no significant reduction in growth up to 400 mg L⁻¹ (Figure 4.1b_{i-iii}). With Cr (VI) above 400 mg L⁻¹ a progressive reduction in growth of the SFL strain was found and the SFL strain could tolerate up to 1600 mg L⁻¹ Cr (VI) (Figure 4.1b_{iv-vii}). No growth was observed at 3200 mg L⁻¹ Cr (VI) (Figure 4.1b_{viii}). The dark green powdery mass of spores observed in the untreated A1120 strain (Figure 4.1a_i) was reduced at 100 mg L⁻¹ Cr (VI) (Figure 4.1a_{iii}). In comparison, no reduction in sporulation was seen in the tolerant strain at concentration from 100-400 mg L⁻¹ (Figure 4.1b_{i-iii}). With the increase in concentration from 800 mg L⁻¹ onwards, a gradual reduction in sporulation was seen (Figure 4.1b_{iv-vii}).

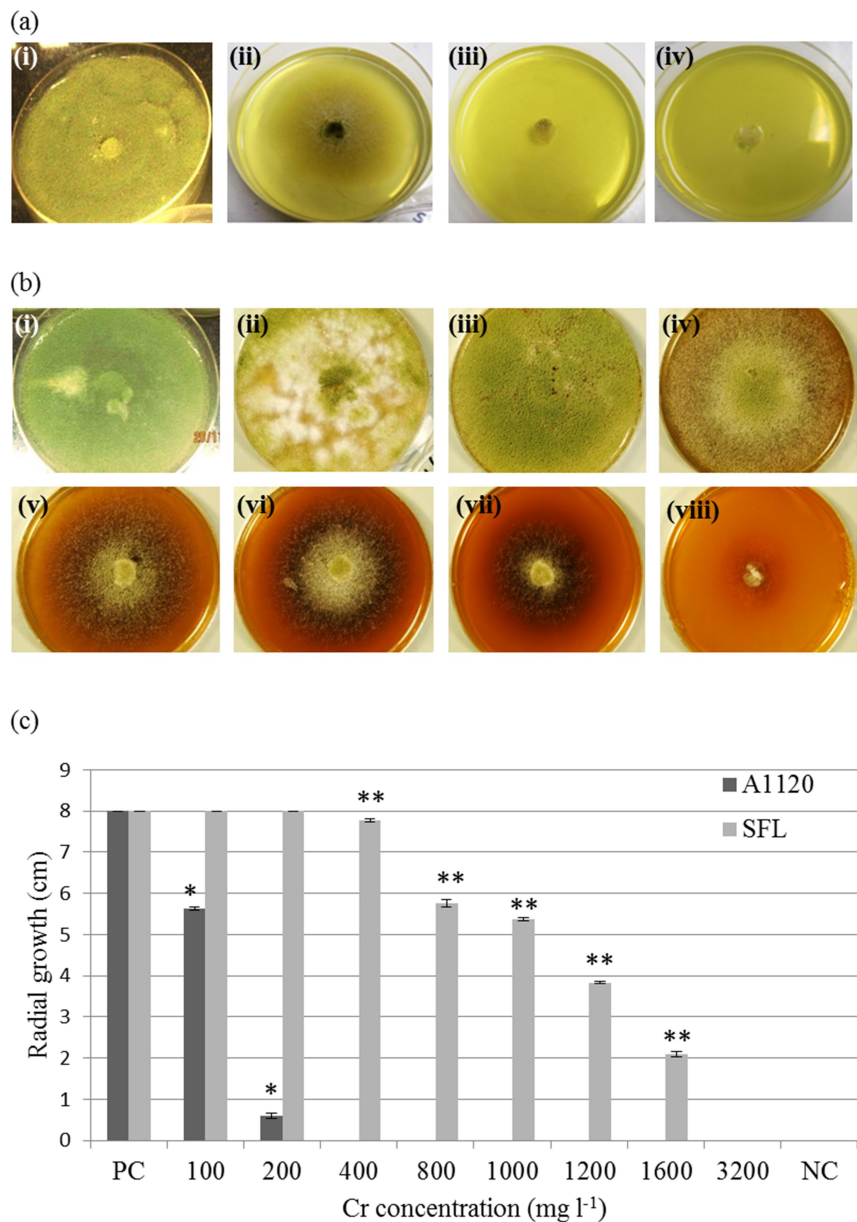


Figure 4.1 Determination of Cr tolerance in *A. flavus* by observing the growth on PDA plates supplemented with different concentration of Cr (VI) after 10 days of incubation (a) photographs of A1120 strain exposed to (i) no chromium (ii) 100 mg L⁻¹ (iii) 200 mg L⁻¹ (iv) 400 mg L⁻¹, showing complete inhibition of fungal growth at 200 mg L⁻¹ (b) photographs of SFL strain exposed to 0 to 1600 mg L⁻¹ (i) to (viii) showing gradual reduction in fungal growth up to 1600 mg L⁻¹ (c) graph of radial growth of each strain, relative to control versus Cr (VI) exposures from 0 to 3200 mg L⁻¹ where PC is a positive control [media not supplemented with Cr (VI)] and NC represents a 10 mm stub of *A. flavus* taken as negative control just before incubation. Significant difference in radial growth was observed between A1120 and SFL strain. Mean ± SEM of three replicates are shown. Significance of difference (p < 0.01) is denoted by (*) for A1120 and (**) for SFL strain.

4.2.2 Dose response study:

A dose-response relation of the filamentous fungus to Cr was tested by growing the fungus in broth media, the fungi were grown in potato dextrose broth (PDB) containing Cr (VI) at concentrations of 50, 100, 250 and 500 mg L⁻¹. In broth media, only vegetative mycelia were found, devoid of the reproductive structures that are frequently observed on solid media. The A1120 strain grown without Cr (VI) showed a relatively rapid increase in growth between 24 h and 72 h followed by a stationary phase up to 120 h and autolysis at 144 h (Figure 4.2a). When treated with 50 mg L⁻¹ Cr (VI), reduced growth was seen up to 24 h, and then a rapid increase in growth was observed until 72 h. This growth rate then significantly reduced until 144 h. At exposure to 100 mg L⁻¹ Cr (VI), a reduction in growth was also observed over the first 48 h. Growth was inhibited by approximately 84% by 72 h, but partially recovered to 44 % inhibition after 144 h compared to the control. Negligible growth was observed at exposures to 250 mg L⁻¹ over 144 h. Growth was completely inhibited at 500 mg L⁻¹.

The growth pattern of SFL strain was not affected at 50 and 100 mg L⁻¹ Cr (VI) supplemented broth (Figure 4.2b). However, at 250 mg L⁻¹ Cr (VI) exposure, growth was impaired by approximately 89 % at 96 h, but partially recovered to 61 % inhibition after 144 h, relative to untreated control. No growth was observed at exposures of 500 mg L⁻¹ Cr (VI).

4.2.3 Extracellular depletion of Cr (VI) by *A. flavus*:

A time course study was carried out to determine the Cr depletion efficiency of the fungal strains in the liquid culture. The filtrate was collected after separating the biomass from media following treatment with different concentrations of Cr (VI) in

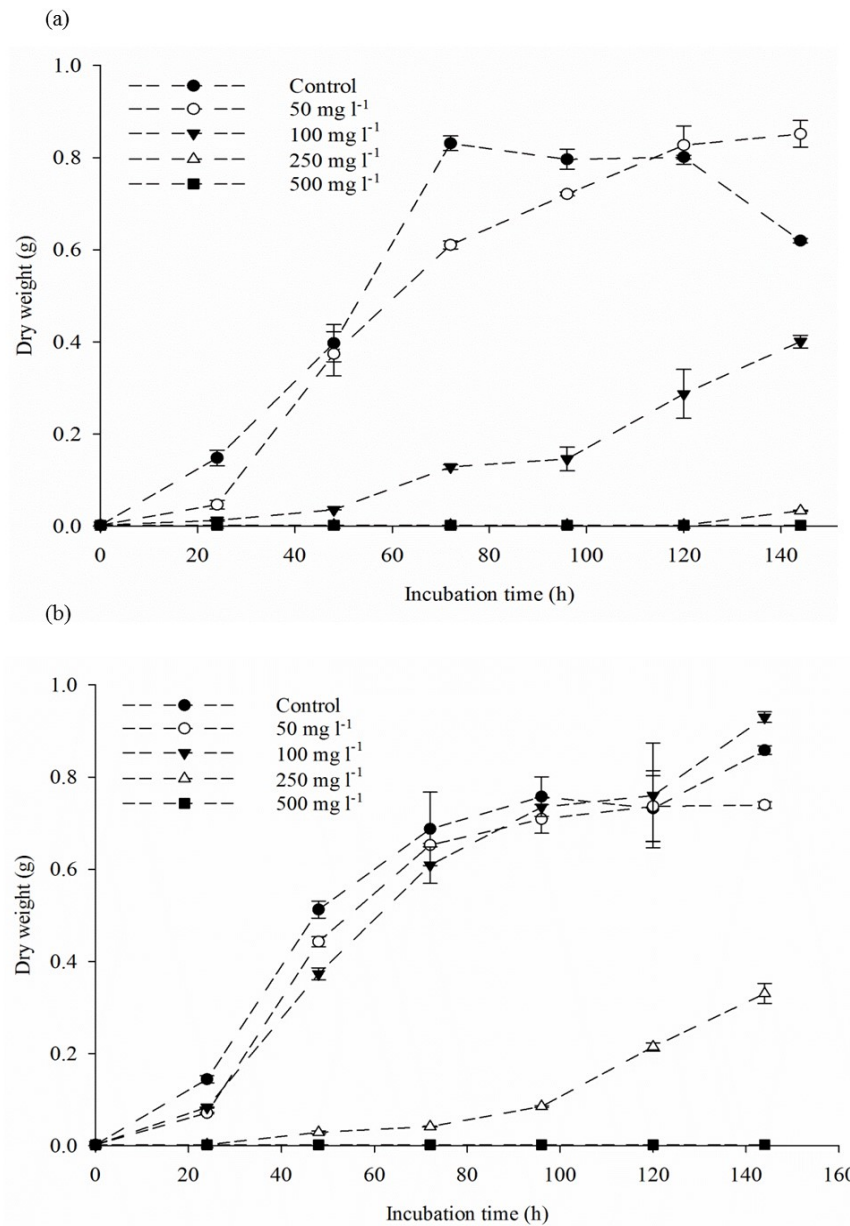


Figure 4.2 Effect of increasing concentrations of Cr (VI) on the growth of *A. flavus*. The fungal biomass was grown for up to 144 h in potato dextrose broth supplemented with 0 to 500 mg L⁻¹ Cr (VI) and its effect on growth was determined by measuring the dry weight of biomass (a) graph showing growth inhibition of A1120 strain. Around 84% growth inhibition was observed after 72 h of exposure at 100 mg L⁻¹ and complete growth inhibition at 250 mg L⁻¹ (b) graph showing inhibition of growth in SFL strain. Approximately 89 % growth inhibition was observed after 96 h at 250 mg L⁻¹. The data are presented as mean \pm SEM of three biological replicates.

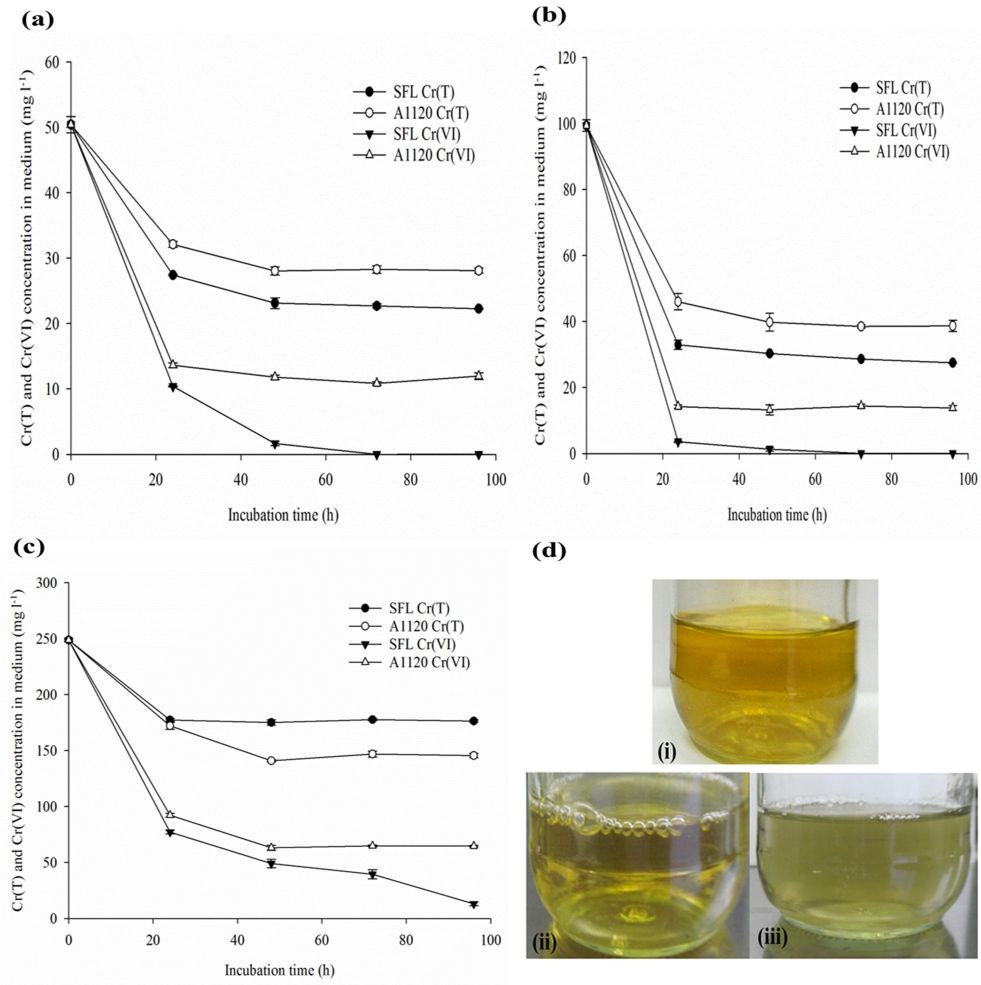


Figure 4.3 Extracellular depletion of Cr (VI) by *A. flavus*.

Graphs showing significant ($p < 0.001$) depletion of Cr (VI) by A1120 and SFL strain, from the extracellular medium spiked with different concentration of Cr (a) at 50 mg L^{-1} and (b) at 100 mg L^{-1} , (c) 250 mg L^{-1} . The data are presented as mean \pm SEM of three replicates. (d) representative photograph showing the disappearance of pale yellow colour indicative of $\text{K}_2\text{Cr}_2\text{O}_7$ (Cr VI), and appearance of greenish colour in the extracellular filtrate at 100 mg L^{-1} , confirming the biotransformation of Cr (VI) to Cr (III) (i) abiotic control showed no significant change in Cr concentration as well as no change in colour ruling out the possibility of abiotic Cr (VI) reduction by any of the media component (ii) A1120 strain, (iii) SFL strain.

PDB. The depletion of Cr (VI) and total Cr [Cr (T)] concentration in PDB spiked with 50 , 100 and 250 mg L^{-1} Cr (VI) over a period of 96 h is shown (Figure 4.3).

Significant reduction ($P < 0.001$) in the Cr (VI) concentration was observed in both the strains at 24 h intervals. At 50 mg L^{-1} the SFL strain showed complete removal of Cr (VI) from the media within 72 h, representing 100% detoxification whereas Cr

(VI) was reduced to $10.84 \pm 0.28 \text{ mg L}^{-1}$ by the A1120 strain, showing 78% removal. The amount of total Cr reduced sharply ($P < 0.001$) within 24 h and remained unchanged after 72 h. After the complete reduction of Cr (VI), the final concentration of Cr (T) in the medium remained at $22.68 \pm 0.31 \text{ mg L}^{-1}$ in SFL and $28.29 \pm 0.56 \text{ mg L}^{-1}$ in A1120 strain (Figure 4.3a). At 100 mg L^{-1} Cr (VI) initial concentration also SFL strain showed complete removal of Cr (VI) from the media within 72 h. In contrast at this concentration, Cr (VI) was reduced to $14.38 \pm 0.59 \text{ mg L}^{-1}$ by A1120 strain showing 85 % removal. After 72 h the final amount of Cr (T) in the medium was $28.61 \pm 0.12 \text{ mg L}^{-1}$ in SFL strain and $38.50 \pm 0.44 \text{ mg L}^{-1}$ in A1120 strain (Figure 4.3b). Further, at 250 mg L^{-1} , a maximum of 95% and 74 % Cr (VI) removal was observed after 96 h by SFL and A1120 strain, respectively with remaining Cr (VI) amount of $13.08 \pm 3.09 \text{ mg L}^{-1}$ and $64.61 \pm 1.05 \text{ mg L}^{-1}$, respectively in the medium (Figure 4.3c). In both the strains, the amount of total Cr [Cr (T)] in the medium also decreased significantly ($p < 0.001$) within 24 h which then became constant without significant change ($p > 0.05$). The decrease in the amount of Cr (VI) coincided with the disappearance of the pale yellow colour from the media, a general indicator of $\text{K}_2\text{Cr}_2\text{O}_7$ corresponding to Cr (VI) and appearance of greenish colour indicative of Cr(III) which was not initially present in the medium (Figure 3.3d). There was no significant change in Cr concentration in the abiotic control (biomass free PDB spiked with Cr) along with any change in the colour of media. This observation eliminates the possibility of Cr reduction by media components or degradation by UV or light.

4.2.4 Total Chromium uptake and intracellular accumulation analysis:

To determine the amount of total Cr uptake by hyphae, the fungal cells were grown in PDB supplemented with 50 mg L^{-1} , 100 mg L^{-1} and 250 mg L^{-1} Cr (VI). Post Cr

(VI) treatment biomass was harvested, dried and acid digested. Total Cr concentrations in the acid digested samples were recorded using atomic absorption spectroscopy (AAS). The biosorption capacity of the two fungi increased significantly ($p < 0.05$) with an increase in Cr (VI) concentration from 50 to 250 mg L⁻¹ (Figure 4.4).

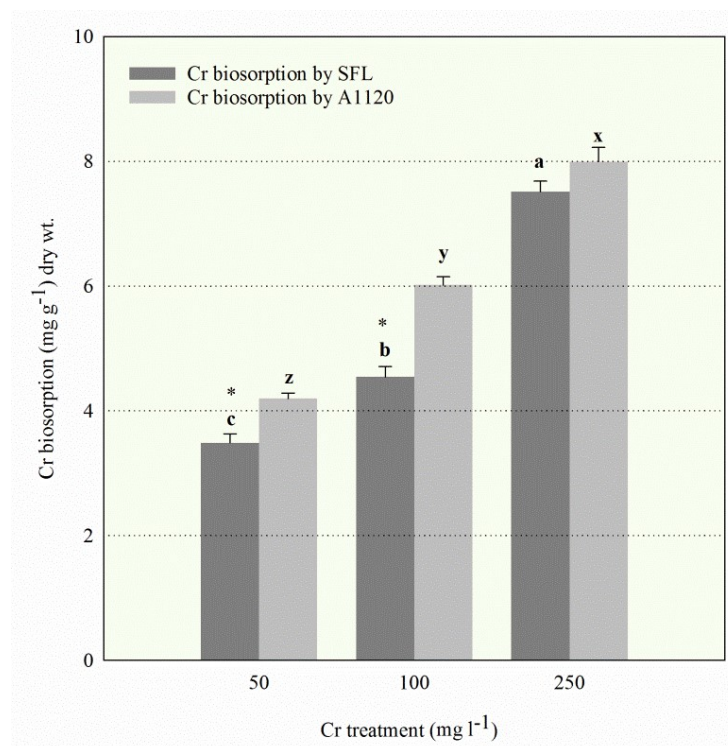


Figure 4.4: Bar graphs showing total Cr biosorption by *A. flavus* strains after 72 h in potato dextrose broth supplemented different concentrations of Cr (VI). The fungal biomass was then harvested, dried and acid digested. The Cr concentrations were analysed in the digested sample. The amount of total Cr taken up by fungal cells increased significantly ($p \leq 0.05$) with the increase in Cr (VI) concentration. Data are presented as mean \pm SEM of each of three replicates ($n = 3$). Significant difference ($p \leq 0.05$) in the Cr biosorption capacity of SFL denoted by superscript (a, b, c) and by A1120 denoted by superscript (x, y, and z). Significant difference ($p \leq 0.05$) in the Cr biosorption between the two strains at each concentration is denoted by asterisk (*).

This suggests that both the strains are able to take up Cr from the medium. Following treatment with 50 mg L⁻¹ Cr (VI), a maximum biosorption of 4.19 mg g⁻¹ and 3.48 mg g⁻¹ dry weight of A1120 and SFL strain occurred. At 100 mg L⁻¹, a

maximum biosorption of 6.01 and 4.54 mg g⁻¹ dry weight was observed by A1120 and SFL strain. With the further increase in Cr concentration to 250 mg L⁻¹ the Cr biosorption increased to a maximum of 7.99 mg g⁻¹ and 7.51 mg g⁻¹ dry weight by A1120 and SFL strain. The sorption values in A1120 strain were significantly higher (P<0.05) than SFL strain at 50 and 100 mg L⁻¹ Cr (VI) concentration.

The intracellular uptake capacity of fungi was determined by incubating Cr treated fungi with EDTA to remove cell wall bound Cr. The EDTA washed biomass was acid digested and analysed for Cr by using AAS. Internalization of 0.88 mg g⁻¹ and 2.25 mg g⁻¹ dry weight was observed by A1120 and SFL strains, respectively at 50 mg L⁻¹ Cr (VI). With the Cr (VI) concentration at 100 mg L⁻¹, accumulation of 2.41 mg g⁻¹ and 3.68 mg g⁻¹ dry weight and at concentration 250 mg L⁻¹, internalization of 3.39 mg g⁻¹ and 6.17 mg g⁻¹ was observed by the A1120 and SFL strains, respectively (Figure 4.5).

Overall, SFL fungus showed complete removal of 50 mg L⁻¹ and 100 mg L⁻¹ Cr (VI) in 100 ml growth media [i.e, net removal of 5 mg and 10 mg Cr (VI) in 100 ml media]. Out of total 5 mg of extracellularly removed Cr (VI) at 50 mg L⁻¹ Cr (VI), a maximum accumulation of 2.26 mg Cr by 0.65g dry biomass (calculated as total accumulation in mg g⁻¹ by fungi × total biomass of fungi in g) was achieved. At 100 mg L⁻¹ Cr (VI), out of total 10 mg of extracellularly depleted Cr (VI) a maximum uptake of 2.76 mg Cr by 0.61 g dry biomass has been observed. At 250 mg L⁻¹ Cr (VI) [with a total of 25 mg Cr present in the medium] about 23.69 mg Cr (VI) was removed and out of which 1.22 mg Cr was taken up by 0.16 g dry SFL biomass. On the other hand in A1120 strain at 50 mg L⁻¹, 3.92 mg Cr was removed extracellularly out of which only 1.67 mg Cr uptake was achieved by 0.61g dry biomass and at 100 mg L⁻¹, out of 8.57 mg of extracellularly removed Cr, a total of 0.78 mg Cr uptake was achieved by 0.12 g dry fungal biomass. At 250 mg L⁻¹, about 18.53 mg Cr (VI)

was removed from the growth medium out of which 0.31 mg accumulation was achieved by 0.03g dry biomass. Interestingly, SFL strain showed significantly higher ($P < 0.05$) intracellular Cr uptake than A1120 at all Cr concentrations.

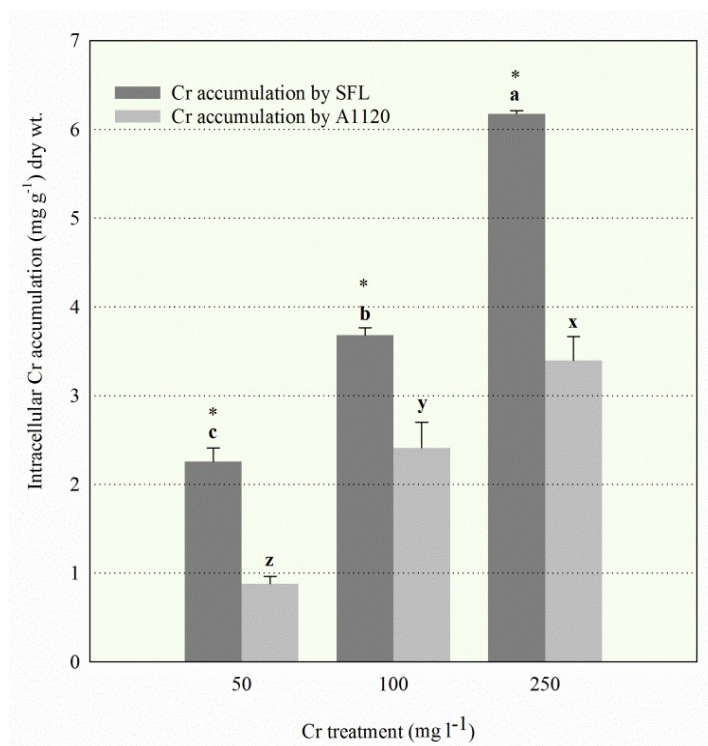


Figure 4.5: Bar graphs showing Cr accumulation by *A. flavus* strains after 72 h in potato dextrose broth supplemented different concentrations of Cr (VI). Cr treated biomass was incubated with 20mM EDTA to remove the cell wall bound Cr, dried and acid digested. The Cr concentrations were analysed in the digested sample. Cr accumulation by fungal cells increased significantly ($p \leq 0.05$) with the increase in Cr (VI) concentration. Data are presented as mean \pm SEM of each of three replicates ($n = 3$). Significant difference ($p \leq 0.05$) in Cr accumulation capacity of SFL denoted by superscript (a, b, c) and of A1120 denoted by superscript (x, y, and z). Significant difference ($p \leq 0.05$) in the Cr accumulation between the two strains at each concentration is denoted by asterisk (*).

Further to confirm the role of fungal active metabolism in transport of Cr to the cells, the inhibitory effects of the respiratory chain inhibitor sodium azide (NaN_3), an uncoupler of oxidative phosphorylation 2,4 Dinitro phenol (DNP) and an ATP

synthetase inhibitor N,N-Dicyclohexylcarbodiimide (DCCD) on Cr accumulation was studied (Figure 4.6).

In the presence of 1 mM DNP, the uptake was inhibited by 69%, 76% and 78% in SFL strain at 50 mg L⁻¹ (Figure 4.6a) 100 mg L⁻¹ (Figure 4.6b) and 250 mg L⁻¹ (Figure 4.6c) Cr (VI) respectively. In A1120 strain, 51 %, 41 % and 12 % inhibition was observed at 50 mg L⁻¹ (Figure 4.6a) 100 mg L⁻¹ (Figure 4.6b) and 250 mg L⁻¹ (Figure 4.6c) Cr (VI) respectively. In the presence of 200 µM DCCD the uptake of Cr was reduced to approximately 71-72 % at 50 mg L⁻¹ (Figure 4.6a) and 100 mg L⁻¹ (Figure 4.6b) Cr (VI) and 80 % at 250 mg L⁻¹ (Figure 4.6c) Cr (VI) in SFL strain. In contrast, a 48 %, 42 % and 15 % inhibition was observed by A1120 strain at 50 mg L⁻¹ (Figure 4.6a) 100 mg L⁻¹ (Figure 4.6b) and 250 mg L⁻¹ (Figure 4.6c) Cr (VI) respectively. The respiratory chain inhibitor NaN₃ (1mM) showed 59 %, 61 % and 75 % inhibition in SFL strain and 37 %, 19 % and only 8 % inhibition in Cr accumulation at the three Cr concentrations used (Figure 4.6a-c).

4.2.5 Identification of proteins involved in Cr binding:

SDS-PAGE analysis of the two *A. flavus* strains was done to identify the proteins expressed upon exposure of 50 mg L⁻¹ and 100 mg L⁻¹ Cr (VI) in A1120 and SFL strain. The fungal mycelia was harvested from the mid-log phase and used for TCA-acetone precipitation. The coomassie blue stained PAGE gels showed protein band patterns containing up to 20 discrete bands. The protein bands ranged from ~12 kDa to 95 kDa in molecular weight on 15 % PAGE gel. The electrophoresis observations showed considerable changes in expression of different proteins in Cr treated samples in comparison to the untreated (without Cr) samples (Figure 4.7). The expression of ~12 kDa and 23 kDa protein decreased in both the strains after Cr treatment in comparison to the corresponding untreated protein band, as observed by

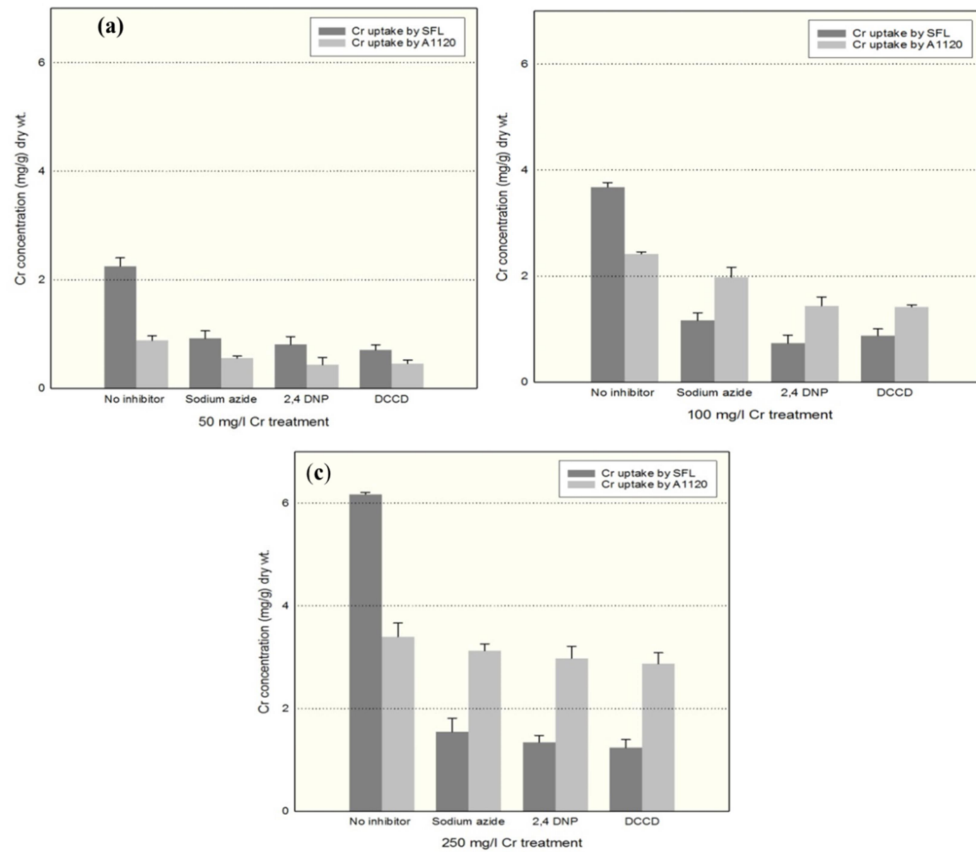


Figure 4.6 Bar graphs showing the reduction in Cr accumulation by *A. flavus* strains in the presence of metabolic inhibitors. Actively grown fungal biomass was incubated with 1 mM NaN_3 , 1mM 2, 4 DNP and 200 μM DCCD, harvested, dried and acid digested. Cr concentration was detected in the acid digested samples. a) at 50 mg L^{-1} b) at 100 mg L^{-1} c) at 250 mg L^{-1} SFL strain.

a reduction in protein band density on the PAGE gel (indicated by red arrow). The expression of $\sim 25 \text{ kDa}$ and $\sim 29 \text{ kDa}$ proteins was induced after Cr treatment in SFL compared to the untreated, indicated by increase in band density. In contrast, these proteins were either not expressed or expressed in low quantity in Cr treated A1120 strain (indicated by green arrow) and hence not much visible on the gel. Relative to other proteins, a strong protein band of $\sim 35 \text{ kDa}$ was present in untreated A1120 strain and its expression was slightly decreased after Cr treatment. On the contrary, this 35 kDa protein band was less prominent in untreated SFL and increased in density after Cr treatment but still less prominent in comparison to A1120 (indicated

by yellow arrow). Differential expression of proteins of approx. 45 kDa, 51 kDa, 62 kDa and 80 kDa was observed in SFL and A1120 where these proteins were strongly expressed in SFL as observed by increase in band density after Cr treatment as compared to A1120 in which the band density remained same or have decreased (indicated by blue arrow).

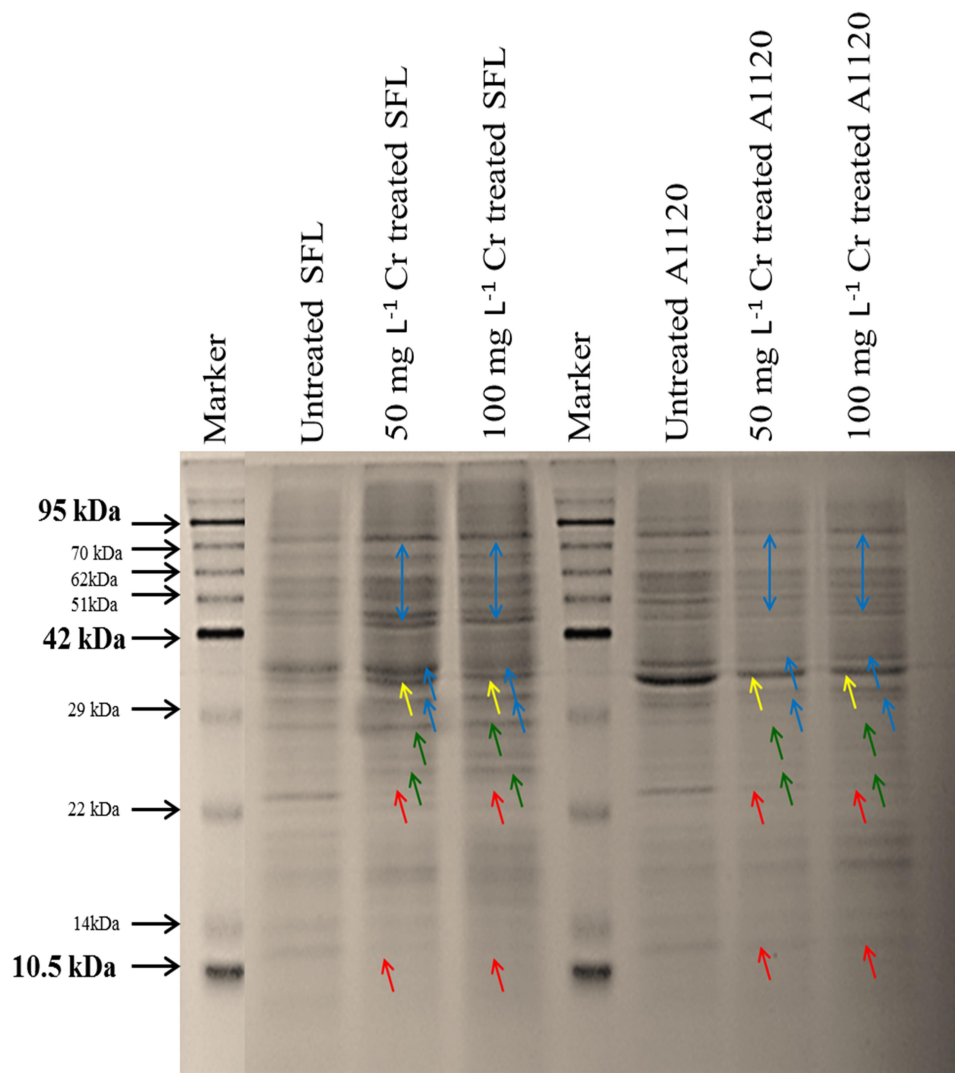


Figure 4.7 Detection of proteins expressed in *A. flavus* cells treated with 50 mg L⁻¹ and 100 mg L⁻¹Cr (VI). Intracellular proteins were isolated from untreated and Cr treated mycelia and analysed and separated on 15% SDS-PAGE gels. Approximately, 15 ug of total protein was loaded in each lane. Bands were visualized using coomassie blue stain. Differentially expressed proteins are shown by different coloured arrows.

4.3 Discussion:

In *A. flavus*, the mechanism of Cr (VI) detoxification is not well understood. Two main mechanisms found in fungi include biotransformation of Cr (VI) to Cr (III) and cell wall adsorption. The events of Cr sequestration inside the cell, however, remained unexplored. The filamentous fungus *Aspergillus flavus*, strain SFL, isolated from Cr contaminated tannery site was used to investigate Cr tolerance, uptake and reduction in comparison to a reference strain of *A. flavus*, A1120. In the metal tolerance study carried out in solid media after 10 days of incubation, the SFL strain showed remarkably high Cr (VI) tolerance of 1600 mg L⁻¹ Cr (VI), although there was a gradual reduction in visible radial growth. Conversely, A1120 could tolerate a maximum of 100 mg L⁻¹ but the growth is significantly reduced, however A1120 showed biosorption at 250 mg L⁻¹ Cr (VI) concentration (mentioned below) which could be because of the presence of more number of dead cells. In *Aspergillus lentulus*, *Penicillium sp.*, and *Fusarium solani* a tolerance level of 1000 mg L⁻¹ Cr (VI) have been reported (Fukuda et al., 2008; Sen, 2012). In another study, *A. terreus* was found to tolerate Cr (VI) up to 1200 mg L⁻¹ (Mishra and Malik, 2014).

The lowest concentration of metal that completely inhibits the visible growth of the isolate was termed “minimum inhibitory concentration” (MIC) (Chang et al., 2016). In this study, the MIC for SFL strain was found to be 3200 mg L⁻¹ and 200 mg L⁻¹ for A1120. Thus, a substantial difference in the Cr (VI) tolerance capacity between the two fungal strains was observed on solid media where SFL strain was found to be approximately 16 times more tolerant than A1120 strain. The results indicated the capacity of the SFL strain to tolerate a broad range of Cr concentration and survive at high levels of toxic Cr (VI), compared to the A1120 strain. Similar to this, variable tolerance to Cr (VI) has also been reported in two strains of

Trichoderma asperellum (PTN7 and PTN10) having high homology where PTN7 was 1.5 times more tolerant than PTN10 (Chang et al., 2016).

Growth inhibition of 84% was observed in A1120 strain grown for 72 h in 100 mg L⁻¹ Cr, and partial recovery to 44 % inhibition was found after 144 h compared to the control (biomass grown in broth media not spiked with Cr). In contrast, SFL strain grew well in liquid media containing up to 100 mg L⁻¹ Cr (VI). At exposures to 250 mg L⁻¹ over 144 h, negligible growth of A1120 strain was observed. This is in contrast to the 89 % growth inhibition in SFL that occurred at 96 h which was reduced to 61% after 144 h at 250 mg L⁻¹ Cr (VI). This suggests that in liquid media fungal cells can become tolerant over time where their growth is restored after certain period of adaptation. Growth inhibitory effects of 51 mg L⁻¹ Cr (VI) in laboratory strains of yeast *Pichia guilliermondii* (Ksheminska et al., 2003), 15 and 20 mg L⁻¹ Cr (VI) in *A. flavus* and *A. parasiticus* strains, isolated from landfill and sludge samples, respectively (Shugaba et al., 2010) and 15.3 mg L⁻¹ in the aerobic cultures of bacterial strain *Shewanella oneidensis* MR-1 (Middleton et al., 2003) have been reported. Our newly described strain of *A. flavus* (SFL) demonstrated a higher tolerance than found in these examples.

Both the strains were found capable of reducing Cr (VI) to Cr (III) from the extracellular medium, however significant differences (p<0.001) in the reduction capacity between the two strains were observed. SFL showed complete reduction of Cr (VI) in the growth medium supplemented with 50 mg L⁻¹ and 100 mg L⁻¹ Cr (VI) within 72 h of exposure and approximately 95 % reduction occurred at 250 mg L⁻¹ after 94 h. Cr (VI) is most likely to be enzymatically reduced to Cr (III) in the medium. This is consistent with the disappearance of the pale yellow colour from the media, and subsequent appearance of greenish colour indicative of Cr (III) which was not initially present in the medium. Chromate reductases secreted by

microorganisms most likely mediate the conversion of hexavalent Cr to trivalent Cr via electron transfer reactions occurring in the cytosol under aerobic conditions and by a membrane bound component under anaerobic conditions (Camargo et al., 2003, Mala et al., 2015). Chromium reduction by various *Aspergillus* species has previously been reported in a range of media conditions. Reductions of 96.3 % and 91.6 % Cr were attained by *A. niger* and *A. parasiticus*, respectively, within 72 h at 20 mg L⁻¹ Cr (VI) (Shugaba et al., 2012). A 97 % decrease occurred from an initial concentration of 5 mg L⁻¹ Cr (VI) after 92 h by *A. foetidus* (Prasenjit and Sumathi, 2005 et al., 2005). Complete removal of 50 mg L⁻¹ Cr (VI) was also reported for *A. tubingensis* after 72 h (Acevedo-Aguilar et al., 2006). The SFL strain investigated in the current study was found to be more efficient compared to other reported *Aspergillus* species. The fungal strains also demonstrated partially adsorption and /or accumulation Cr by the biomass as one of the mechanism of Cr (VI) detoxification. This was inferred by the sharp decrease in the amount of Cr (T) within 24 h that subsequently levelled off.

To determine Cr adsorption and /or accumulation capacity of *A. flavus* cells, a Cr biosorption study was carried out. Biosorption of Cr is a complex phenomenon involving metabolism-independent surface adsorption or “passive uptake”, which takes place either in living or dead biomass, followed by metabolism-dependent intracellular uptake or “active uptake” where metal is transported across the cell membrane, occurring only in viable cells (Malik, 2004). The Cr biosorption capacity of 7.99 mg g⁻¹ and 7.51 mg g⁻¹ dry weight by the two *A. flavus* strains was found to be higher than most of the other reported *Aspergillus* species where Cr biosorption of 2.99 mg g⁻¹ was reported in *A. niger* (Kovacevic et al., 2000), 1.56 mg g⁻¹ and 1.2 mg g⁻¹ by a tolerant and a less tolerant *Aspergillus* sp., respectively (Zafar et al., 2007), 0.587 mg g⁻¹ and 0.082 mg g⁻¹ by *A. niger* and *A. parasiticus* (Shugaba et al.,

2012), 2 mg g⁻¹ by *A. foetidus* (Prasenjit and Sumathi, 2005 and Sumathi, 2005). Our newly described strain SFL and A1120 showed approximately 5 fold higher biosorption.

The intracellular accumulation of 6.17 mg g⁻¹ Cr by SFL strain was found similar to one of the highest cellular Cr accumulation values of 6.7 mg g⁻¹ reported in yeast *Pichia guilliermondii* (Kaszycki et al., 2004), however, it would be difficult to directly compare these data as the author have used different experimental conditions including rich optimal growth medium and a different Cr (VI) concentration ranging between 0.1-0.5 mM. Differences in Cr the uptake mechanism exhibited by two strains was observed whereby the less tolerant A1120 showed significantly higher total Cr biosorption (passive uptake) whereas the tolerant SFL strain internalized significantly more Cr into its cytoplasm (active uptake). In literature it is well documented that metal resistant strains show reduced uptake of toxic metal into the cell (Gadd and White 1989). But, in *S. cerevisiae* resistant to Co²⁺ a higher cytosolic concentration of Co²⁺ has been reported compared to the non-resistant parent strain (White and Gadd 1986) which is consistent with the present study. This might be attributed to vacuolar compartmentalisation of metal. Metal transport across cell membranes is an energy-dependent process leading to storage in intracellular organelles like vacuoles, or binding to cysteine-rich small proteins such as metallothioneins (Ahalya et al., 2003). Such a process would take place only within viable cells. Only the SFL strain continued to grow in Cr-rich supplement and the growth of A1120 strain was impaired with the increase in Cr concentrations in the medium. The SFL strain may be metabolically more active and may have intrinsic mechanisms to neutralize the toxic effects of chromate and thus able to tolerate high Cr (VI) concentration and accumulate more Cr inside the cell compared to the A1120 strain.

To further confirm this hypothesis, Cr uptake was studied in the presence of different metabolic inhibitors and as expected, the intracellular accumulation was greatly reduced in SFL than in A1120 strain. The uncouplers of oxidative phosphorylation (OP) blocks the coupling between electron transport and OP reactions in mitochondria and thus prevents ATP synthesis without influencing respiratory chain and H(+)-ATPase (Terada, 1990). The inhibitory effect of 2, 4 DNP in the chromium uptake process indicates the requirement of energy generated by ATP synthesis during OP. DCCD is a proton-translocation inhibitor that blocks the translocation of H⁺ in F_o subunit of F_oF₁-ATP synthase. F_oF₁-ATP synthase is a proton translocating P- type ATPase that catalyse ATP synthesis by using proton motive force generated across the plasma membrane during OP (Toei and Noji, 2013, Das et al., 2009) . This suggested that the transport of chromium into the cell cytoplasm might be driven by H⁺ATPases (Toei and Noji, 2013, Das et al., 2009). In the presence of azide ion (N³) both electron transport and OP are inhibited. The OP is inhibited by blocking the electron transport cascade, particularly via inhibition of cytochrome oxidase *a3* (Thompson et al., 2000).

Taken together, these observations suggest that Cr uptake into the fungal cells is an energy dependent process that takes place via specific transport system. However, a significantly different degree (P<0.001) of Cr uptake inhibition between the two strain (higher Cr uptake inhibition in SFL and lower inhibition in A1120) is indicative of a different nature of energy coupling and different metabolic responses by these fungi during the Cr accumulation. Inhibition of Cr uptake in the range of 25-35% using these metabolic inhibitors, has been reported in *Termitomyces clypeatus* (Das et al., 2009).

Proteomic analysis showed differential expression of proteins in A1120 and SFL strain in response to 50 mg L⁻¹ and 100 mg L⁻¹ Cr (VI) which may indicate

different cellular response by these fungi in the presence of Cr. A ~25kDa, and a ~29kDa protein was induced upon Cr treatment in SFL. This could correspond to a chromate reductase enzyme from *Pseudomonas ambigua*, known to reduce Cr (VI) to Cr (III), which has a similar molecular weight of 25kDa (Suzuki et al., 1992). A protein of molecular weight 20kDa has been purified and characterised as chromate reductase in *Pseudomonas putida* MK1 (Park et al., 2000). Other studies have reported the induction of a 30kDa protein in the presence of Cr in *P. aeruginosa* (Ganguli and Tripathi, 2002), in *Ochrobactrum sp.* (Thacker and Madamwar, 2005). Therefore it can be predicted that chromate reductases might be involved in the reduction of Cr (VI) to Cr (III) in *A. flavus* strains. The differential expression of a ~35 kDa in SFL and A1120 could be attributed to play a significant role in Cr tolerance as this protein was present in low quantity in untreated Cr tolerant SFL and its expression was induced under Cr stress. On the other hand, this protein was strongly expressed in untreated A1120 which was reduced after Cr treatment. Similar to this observation in *Pseudomonas aeruginosa*, a 35.6 kDa glutathione synthetase protein was overexpressed under Cr stress (Kılıç et al., 2010). Glutathione plays a central role in protection against oxidative stress induced by toxic metals by detoxification of the free radicals generated upon metal toxic metal exposure (Jozefczak et al., 2012, Kılıç et al., 2010). Cr (VI) is also known to generate reactive oxygen species during Cr (VI) reduction process via formation of intermediate Cr (IV) and Cr (V). Hence, it may be predicted that glutathione synthetase (~35 kDa protein) might have a potential involvement in protecting SFL strain against Cr (VI) toxicity as indicated by its induction after Cr treatment whereas the downregulation of this protein indicates Cr (VI) induced oxidative damage in A1120. Nevertheless, identification and characterisation of these proteins would provide confirmatory results. Others proteins of 45 kDa, 51 kDa, 62 kDa and

80 kDa molecular weight found in this study, might have a potential role in Cr tolerance as indicated by increased expression in Cr treated SFL compared to A1120.

A consolidative analysis of the above studies demonstrated high Cr tolerance by SFL strain, higher Cr (VI) reduction capacity along with Cr accumulation inside the cell via active transport system utilizing the energy generated during ATP synthesis.

On a proteomic level as well, both the strains responded differently to Cr exposure as depicted through differential expression of certain proteins. Approximately 25kDa, 29kDa, 35 kDa proteins were found to have potential role in such interaction. However, the identification of these proteins remains to be elucidated.

Overall a considerable difference in the mechanism of Cr (VI) tolerance by *Aspergillus flavus* strains A1120 and SFL is established.

CHAPTER 5

Topographical characterisation, *in situ* localization, and speciation of chromium in *A.* *flavus*

5.1 Introduction:

Owing to its toxicity, interaction of Cr (VI) with fungi primarily relies on a detoxification process that includes cell wall binding, intracellular transport and reduction of Cr (VI) to its less toxic form Cr (III). The kinetic mechanisms of these detoxification processes using different fungi including *A. flavus* are well established (Singh et al., 2016, Sharma and Malviya, 2016, Singh and Bishnoi, 2015, Shugaba et al., 2012, Ahluwalia and Goyal, 2010, Deepa et al., 2006). With the emergence of different surface characterisation techniques including spectroscopic and microscopic analysis, it became possible to understand the characteristic physical and chemical interactions occurring between the metal ion and the microbial biomass (Das et al., 2009). Studies have been carried out on the surface characterisation of fungal biomass in relation to Cr (VI) biosorption and biotransformation of Cr (VI) to Cr (III), and the relevant mechanisms have been elucidated, as reported in a chemically pre-treated biomass of *Termitomyces clypeatus* using Fourier transform infrared spectroscopy (FTIR) and scanning electron microscopy (SEM) (Ramrakhiani et al., 2011), in brown seaweed *Ecklonia* using X-ray photoelectron spectroscopy (XPS) and X-ray absorption spectroscopy (XAS) (Park et al., 2007), in *Aspergillus versicolor* using SEM-energy dispersive X-ray analysis (SEM- EDX), attenuated total reflection infrared (ATR-IR), and atomic

force microscopy (AFM) probing (Das et al., 2008). Several reduction mechanisms have also been proposed including direct Cr (VI) reduction, anionic adsorption and/or adsorption coupled reduction, described in *Coriolus versicolor* on the basis of FTIR and SEM- EDX (Sanghi et al., 2009), *Aspergillus niger* SEM, FTIR, transmission electron microscopy-EDX (TEM-EDX) and Raman spectroscopy (Gu et al., 2015, Alonso et al., 2014). Cr accumulation into the cytoplasm and its respective localisation has been described in *Termitomyces clypeatus* using TEM-EDX analysis (Das et al., 2009).

The cell surface of microorganisms acts as the first site of communication with the extracellular environment and hence plays a vital role in metal-microbe interaction (Poljsak et al., 2010). The fungal cell wall is complex in nature comprising of different polysaccharides including chitin, chitosan, 1, 3- β glucan- and 1,6- β glucan, mannan, glycoproteins, and lipids (Adams, 2004, Pessoni et al., 2005, Bowman and Free, 2006, Das et al., 2008). The large surface area and electronegative charge on the fungal cell provides an excellent site for metal binding (Srivastava and Thakur, 2006). Therefore, it is important to understand the interactions and complex formation between Cr and various supramolecular structures present within the fungal biomass (Park et al., 2005) which may facilitate Cr binding. However, little has been reported on Cr interactions with *A. flavus*. There are certain questions that remained unanswered such as: 1) in which form of Cr is taken up by the fungal cells? 2) What is the precise localisation of Cr into the cell? 3) Are there any metal-protein complexes formed by fungi?

To fill these knowledge gaps, topographical characterisation, speciation analysis and *insitu* localisation of Cr were carried out in A1120 and SFL strains of filamentous fungi *A. flavus*. At first, Cr localisation studies were done using Scanning Electron Microscopy (SEM) and Transmission Electron Microscopy

(TEM). Functional groups involved in Cr binding to cell wall were identified by Fourier Transform Infrared Spectroscopy (FTIR). Cr speciation analysis was done using X-ray photoelectron spectroscopy (XPS).

5.2 Results

5.2.1 Localisation of Cr on the cell surface

Scanning electron microscopy (SEM) was carried out to localise the cell surface bound Cr. Fungi grown in broth media without Cr showed no differences in surface morphology between the A1120 (Figure 5.1a) and the SFL strain (Figure 5.1b). The hyphae of both fungi had a smooth surface. The fungal biomass exposed to 100 mg L⁻¹ Cr (VI) was prominently different with irregular deposits on the hyphal surfaces. Particulate aggregates were observed along the subapical and mature regions of the hyphae (Figure 5.1c-f). These were seen at 24 h as individual submicronic particles (Figure 5.1c, d) and later as aggregates (Figure 5.1e, f) in both A1120 and SFL respectively. The tip of the hyphae remained smooth, and particles did not accumulate on surfaces closer than 40µm to the hyphal tip. To confirm the presence of Cr on the hyphae energy dispersive X-ray spectroscopy (EDX) analysis was done. As expected, EDX analysis did not detect Cr on either of the A1120 or SFL fungal surfaces from the untreated biomass (Figure 5.1g). The mature zone with the deposition of aggregates was found rich in Cr when analysed with EDX, indicated by appearance of clear peaks of Cr in the EDX spectrum (Figure 5.1h).

5.2.2 Sub cellular localization of Cr

The intracellular localization of Cr was carried out by transmission electron microscopy (TEM). Micrographs of thin sections of untreated and Cr (VI) treated cells were examined. In the untreated *A. flavus* cells septate hypha was seen along

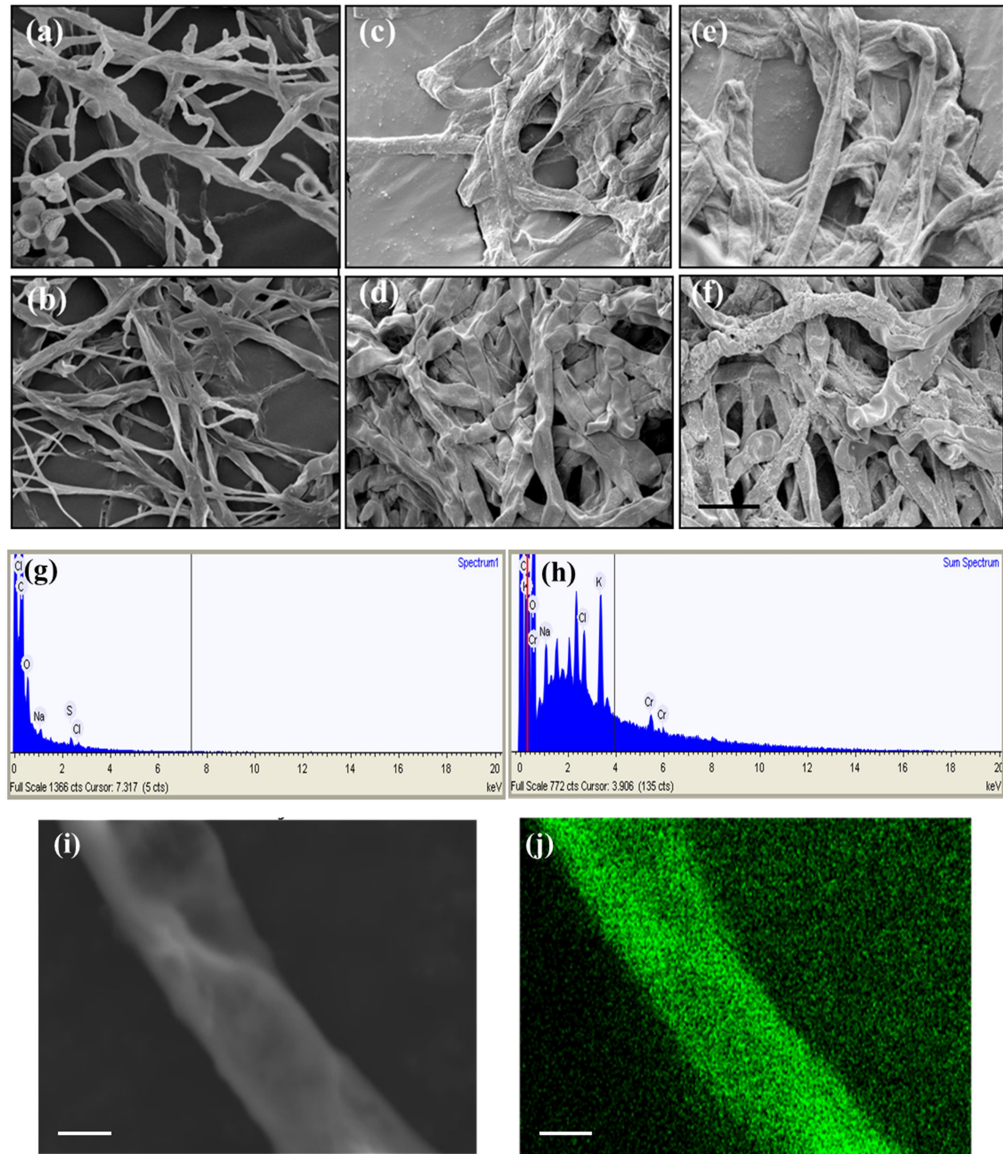


Figure 5.1 SEM EDX analysis of *A. flavus* mycelia grown in broth media with or without 100 mg L^{-1} Cr (VI) supplement. (a, b) micrograph of untreated A1120 and SFL strain resp., after 24 h showing smooth hyphal surface, (c, d) micrographs of treated A1120 and SFL strain resp., after 24 h showing submicronic particles on the hyphal surface, (e, f) micrographs of treated A1120 strain and SFL strain resp., after 96 h showing particle aggregation on the hyphal surface. Scale bar denotes $10 \mu\text{m}$, (g) representative EDX spectra of untreated mature hyphae in which no Cr was detected (h) representative EDX spectra of Cr treated mature hyphae showing Cr peaks (i) representative SEM micrograph of mature hypha used for elemental scanning (j) elemental area map from the same hypha shown in (i) showing uniform distribution of Cr denoted by green coloured Cr-K energy line. Scale bar denotes $2.5 \mu\text{m}$. Further, the elemental mapping acquired from the Cr-treated fungal mycelia confirmed the distribution of Cr along the sub-apical and mature surfaces of the hyphae (Figure 5.1i, j).

with the presence of vacuolar structures and small vesicles in the cytoplasm. The cell wall appeared clear and smooth without the deposition of dense granules in both A1120 (Figure 5.2a) and SFL strain (Figure 5.2b). Electron micrographs of cells treated with 100 mg L^{-1} Cr (VI) for 96 h showed the presence of black dense clumps (indicated by circles) on the cell wall as well as in the cytoplasm in both A1120 (Figure 5.2c) and SFL (Figure 5.2d). Micrographs at higher magnification also showed the presence of dense granules in the internal structures of cell (Figure 5.3e, f) possibly nucleus, mitochondria and outer membrane of the vacuole along with the cell wall. The EDX spectra acquired from the section showed the presence of Cr peak in both the fungi (Figure 5.2g, h) but it could not be confirmed that these clumps are made of Cr. To establish this, point EDX was done in SFL strain at different points (1, 2 and 3) as indicated by red circles in the micrographs (Figure 5.3a) which localised Cr in the cytoplasmic region (EDX spectra of spot1) as well as on the cell wall (EDX spectra of spot 3) and confirmed that the dense clumps are composed of Cr. In the region just outside the cytoplasm no Cr was detected (EDX spectra of spot 2). In addition, point EDX was taken from three different points (1, 2 and 3) inside the cytoplasm. The appearance of Cr peak at these points confirmed Cr sequestration in the membrane bound organelles (Figure 5.3d). Furthermore, line EDX spectra were recorded to support the above observations (Figure 5.3 b, c, e, and f). Line EDX was taken from inside to the outside of the cell (from left to right) and indicated by red line in the micrograph (Figure 5.3b). The spectra showed Cr peaks in the region where dark clumps are present approximately at $0\text{-}0.2 \mu\text{m}$, a higher peak at $\sim 1.3\text{-}1.7 \mu\text{m}$. The peak dropped down at $\sim 1.8\text{-}2.2 \mu\text{m}$ in the periplasmic space and again went up at $2.5 \mu\text{m}$ at the cell wall and disappeared outside the cell at $\sim 2.6\text{-}3.2 \mu\text{m}$ (Figure 5.3c). Line EDX of the cytoplasmic region, taken from top to bottom as indicated by orange line in the micrograph (Figure 5.3e)

showed higher amount of Cr perhaps in the nuclear region especially around the nuclear membrane (0-0.15 μm) in comparison to the cytoplasmic region (0.12- 0.22 μm). Cr peak was further increased around the vacuole membrane which then disappeared inside the vacuole (Figure 5.3f).

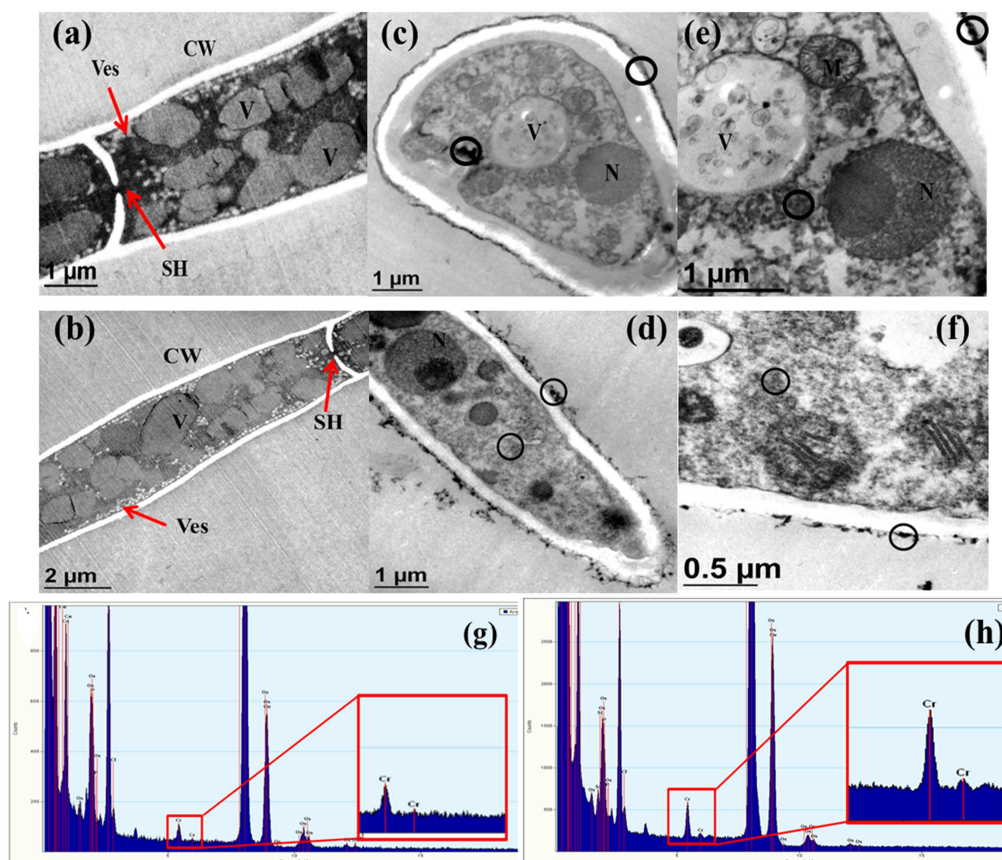


Figure 5.2 TEM EDX analysis of *A. flavus* mycelia grown in broth media for 96 h with or without $100 \text{ mg L}^{-1}\text{Cr}$ (VI) supplement (a, b) micrographs of untreated A1120 and SFL strain respectively, showing clear wall (CW), septate hypha (SH), vesicles (Ves), vacuoles (V) shown by red arrow, (c, d) micrographs of Cr treated A1120 and SFL strains resp., showing the ultrastructure of fungal cells (V=vacuoles, M=mitochondria, N=nucleus) where black dense clumps were observed on the cell surface and cytoplasmic region (indicated by black circle), (e, f) micrographs at Cr treated A1120 and SFL strains resp., at higher magnification where the black dense clumps observed on the cell surface and cytoplasmic region are indicated by black circle (g, h) EDX spectra of Cr treated A1120 strain and SFL strain resp., showing Cr peaks (indicated by red squares).

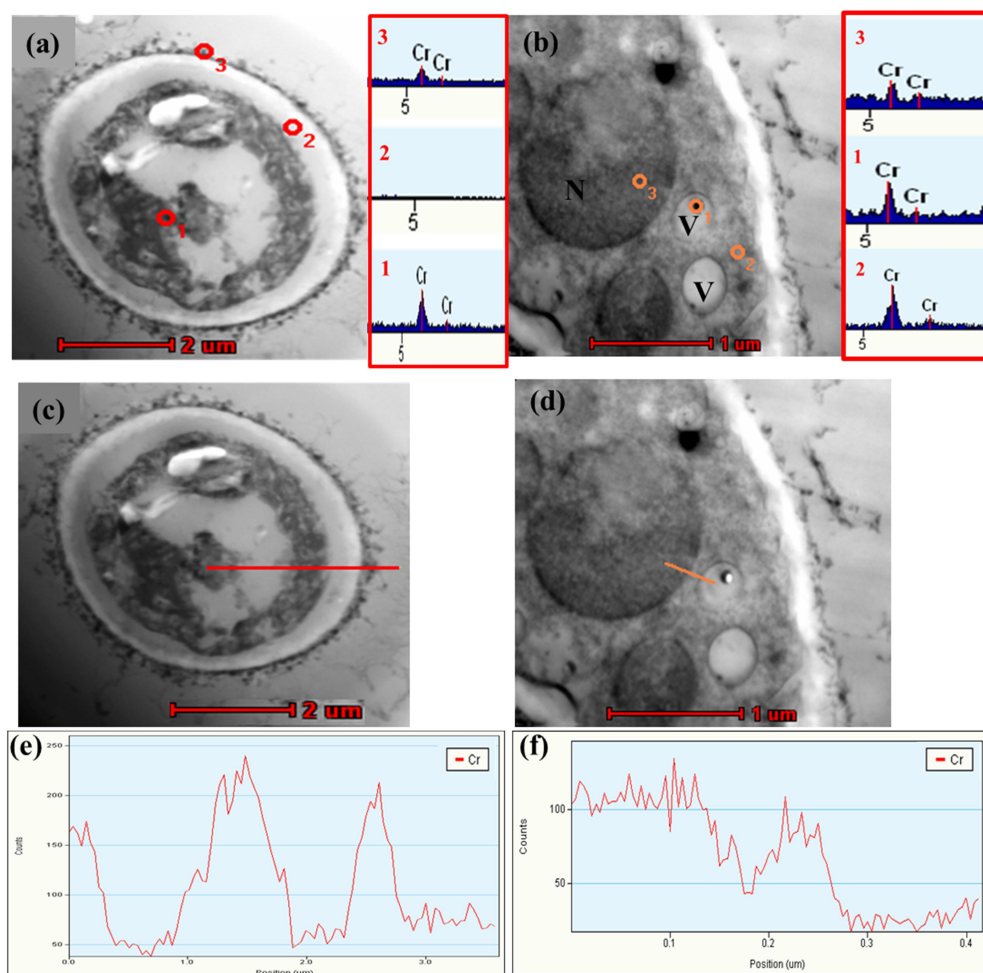


Figure 5.3 Point and Line EDX analysis of *A. flavus* cells treated with $100 \text{ mg L}^{-1} \text{Cr(VI)}$ (a, b) STEM micrographs showing three spots (1, 2, 3) at which EDX spectra were recorded. EDX spectra of the same spots are on the right side of the respective image (red inset), showing the presence of Cr on the cell surface, cytoplasm and vacuoles (V) except for point 2 right outside the cytoplasmic region [EDX spectra of spot 2 in (a)], (c, d) STEM micrographs showing the region at which line EDX scan as done (shown by red and orange line), the respective EDX spectra (e, f) confirmed the presence of Cr in the intracellular region of the cell.

5.2.3 Identification of functional groups involved in Cr binding:

The functional groups likely to be involved in chromium adsorption to the fungal cell wall were identified by Fourier transform infrared spectroscopy (FTIR). The FTIR spectra were recorded for untreated and $100 \text{ mg L}^{-1} \text{Cr(VI)}$ treated biomass at 48 h and 96 h. FTIR spectral analysis showed a number of absorption peaks in the

untreated and Cr (VI) treated fungal biomass. The observed peaks were in the range 3500-3200, 3000-2800, 1760-1665, 1200-1000 cm^{-1} (Figure 5.4). The broad peak appearing in the region 3500-3200 cm^{-1} is attributed to -OH and -NH stretching. Two medium intensity peaks at around 2921.34 cm^{-1} (SFL), 2922.47 cm^{-1} (A1120) and 2851.76 cm^{-1} (SFL), 2852.81 cm^{-1} (A1120) indicative of -CH asymmetric and symmetric stretching vibrations of methylene hydrogen. A medium intensity peak at 1744.37 cm^{-1} (SFL) and 1743.59 cm^{-1} (A1120) represents C=O stretching band of carboxylic group. The appearance of bands in the range of 1650-1500 cm^{-1} is representative of primary and secondary amines. A sharp peak at 1637.34 cm^{-1} (SFL) and 1639.57 cm^{-1} (A1120) is attributed to amide I band mainly in C=O stretching mode. The peak at 1588.38 cm^{-1} (SFL) and 1543.85 cm^{-1} (A1120) represents amide II band chiefly in O=C-N-H bending mode of chitin and chitosan present on the fungal cell wall (Sanghi et al., 2009). A small peak appeared at 1376.17 cm^{-1} (SFL) and 1375.61 cm^{-1} (A1120) represents -CH₃ wagging (umbrella deformation; a type of structural deformation in an umbrella closing manner) (Sanghi and Srivastava, 2010). The region 1300-1200 cm^{-1} is characteristic of more intricate amide III region. A number of peaks were found in this region denoting a large amount of structural proteins constituting the fungal biomass. The small peak emerging at corresponds to C-H stretching in amide III and C-O stretching. A strong and 1238.39 cm^{-1} (SFL) and 1234.01 cm^{-1} sharp peak at 1025.59 cm^{-1} (SFL) and 1023.21 cm^{-1} (A1120) denotes C-OH stretching. Two weak intensity peaks in the region 1200-1000 cm^{-1} approx. are the characteristic adsorption peaks of phosphate groups. The peaks occurring in the region 700-400 cm^{-1} are attributed to the presence of nitro compounds and disulphide groups (Ramrakhiani et al., 2011). The spectra of Cr-laden biomass showed notable differences when compared with the spectra of the untreated biomass of both A1120 and SFL strain as evident by the

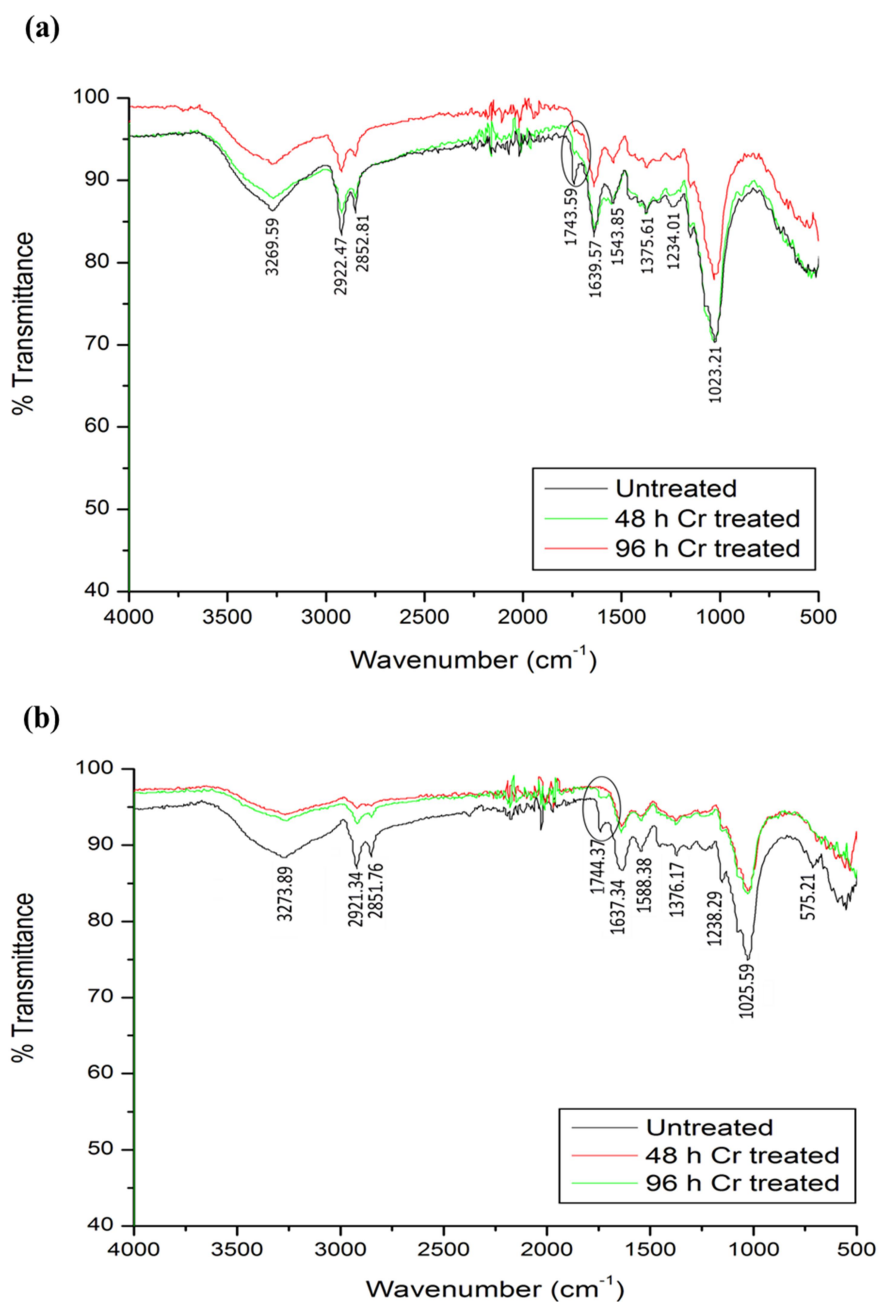


Figure 5.4 FTIR spectra for 100 mg L⁻¹Cr (VI) treated *A. flavus* biomass showing differences in the untreated and Cr treated mycelia observed by stronger peaks in the untreated mycelia. Black circle indicates complete disappearance of peak at ~1744 cm⁻¹ after 96 h of Cr treatment (a) A1120, significant difference in the peak intensity was observed at 96 h (b) SFL, difference in the peak intensity was observed at both 48 h and 96 h.

changes in peak intensity (Figure 5.4) where stronger peaks were observed in the spectra of untreated biomass. In A1120, there was not much difference in the peak intensity between the untreated and 48 h treated biomass but the peaks were significantly different after 96 h of treatment (Figure 5.4a). In SFL, a difference in the peak intensity was observed within 48 h (Figure 5.4b). The details of peak positions are given in Table 5.1. Apart from this, the two most remarkable differences observed were the complete disappearance of the peak at 1743.59 cm^{-1} and 1744.37 cm^{-1} (indicated by circle) after Cr treatment in both A1120 (Figure 5.4a) and SFL strain (Figure 5.4b) and narrowing of the peaks appeared in the region $3500\text{-}3200\text{ cm}^{-1}$.

5.2.4 Determination of Cr speciation by using X-ray photoelectron spectroscopy:

X-ray photoelectron spectroscopy (XPS) was done to determine the change in oxidation state of Cr during the biosorption process. The fungal biomass was treated with 100 mg L^{-1} Cr (VI) up to 96 h. XPS spectra were recorded Cr treated A1120 and SFL biomass at 48 h and 96 h and detailed analysis of photoelectron spectrum was done. High resolution spectra collected from Cr2p core region of Cr treated biomass were collected. In the XPS spectra of A1120 strain treated with Cr (VI), the main Cr2p peak at 576.9 eV was observed (Figure 5.5a) and in the spectra of SFL strain the main peak was observed at around 577.1eV (Table 5.2) binding energy (Figure 5.5b). The peak observed corresponds to Cr (III) in hydroxide form. The Cr 2p peak consists of a doublet (Cr $2p_{3/2}$ and Cr $2p_{1/2}$). Doublets were normally both fit to get peak positions, however for Cr the secondary peak is complicated with satellite peaks, so only the larger (Cr $2p_{3/2}$) peak was fitted. The $2p_{1/2}$ peaks were

FTIR Peak s	A1120 Control	A1120 48 h	A1120 96 h	SFL Control	SFL 48 h	SFL 96 h	Representative of functional groups
3500-3200 cm ⁻¹	3272.96	3268.86	3274.45	3276.71	3269.44	3258.74	-OH group, -NH stretching and the acetamide group of the chitin fraction.
3000-2800 cm ⁻¹	2921.15 2851.72	2920.04 2851.10	2921.2851.73	2920.79 2851.70	2918.75	2917.61 2847.49	CH asymmetric and symmetric stretching vibrations of methylene hydrogen.
1650-1500 cm ⁻¹	1638.95 1543.57	1638.03 1553.02	1639.21 1542.91	1635.23 1544.35	1638.14 1548.54	1639.08 1540.77	Amide I band primarily in C=O stretching mode O=C-N-H bending of amide II bands present in both chitin and chitosan on the cell wall.
1760-1665 cm ⁻¹	1741.81	-	-	1740.95	-	-	C=O stretching band of carboxyl groups.
1400-1000 cm ⁻¹	1375.67	1376.25	1370.14	1373.53	1375.97	1376.01	C-N stretching, in-plane O-H bending, sulphur and phosphorus compound
1200-1000 cm ⁻¹	1244.16	-	-	1233.80	-	-	C-H stretching in amide III and C-O stretching

Table 5.1: Peak positions and allocation of FTIR bands in untreated (control) and Cr treated A1120 and SFL strain.

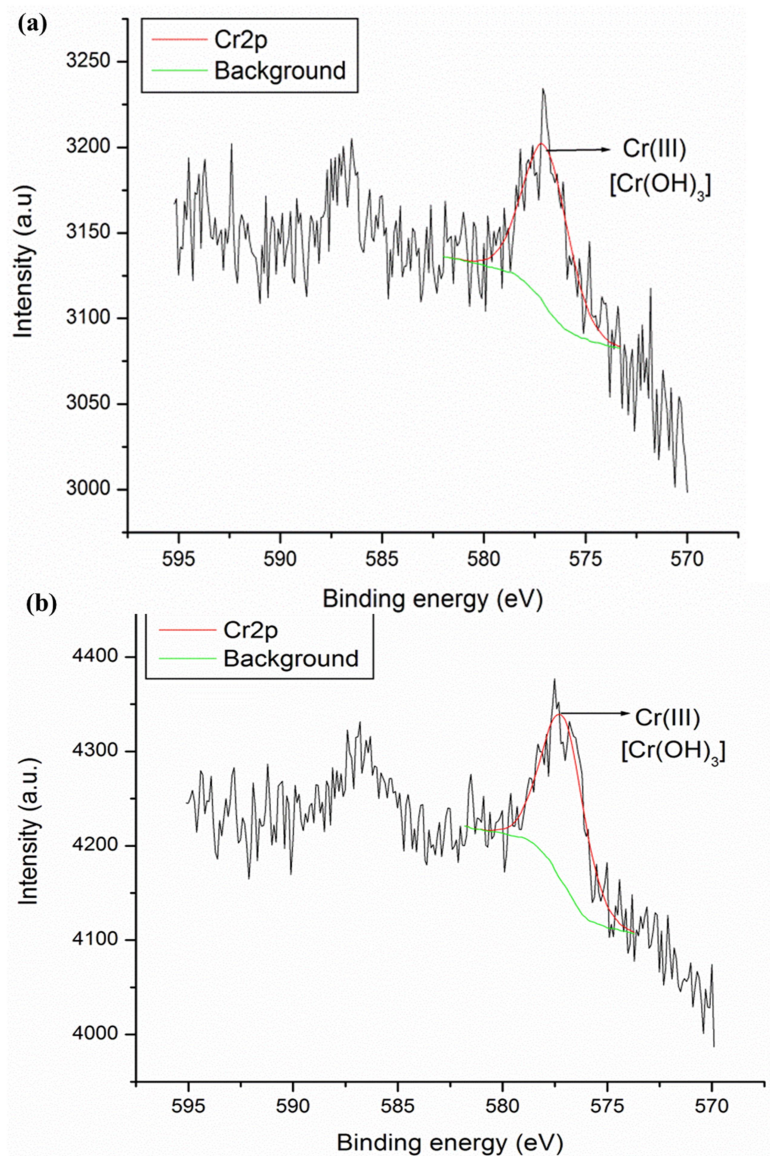


Figure 5.5 High resolution Cr_{2p} spectra recorded after treating *A. flavus* biomass treated with 100 mg L⁻¹Cr (VI) showing a single peak around 577.1eV corresponding to Cr (III) in hydroxide form. The second peak at 586.5eV does not correspond to any other form of Cr (a) A1120 (b) SFL

Table 5.2 Peak position obtained in Cr_{2p} spectra

Treatment time	Cr 2p _{3/2} Peak position (eV)	
	A1120	SFL
48 h	577.0	577.2
96 h	576.9	577.1

of Cr was identified on the fungal cell surface. The XPS spectra of cytoplasmic extracts of Cr (VI) treated cells were also recorded however, no peaks were detected (Figure not shown) perhaps Cr was present in very low concentration.

5.3 Discussion:

Previous studies have attempted to characterise the mechanism of Cr (VI) uptake as well as reduction to Cr (III) in different filamentous fungi by employing different types of instrumental analysis. However, in *A. flavus* a detailed physiochemical investigation of Cr interaction with the fungal cells has not previously been reported. In the present study, topographical characterisation, subcellular localisation and speciation analysis of Cr was carried out in A1120 and SFL strain of *A. flavus*.

SEM analysis showed deposition of irregular aggregates on the surface of Cr (VI) treated mycelia in both A1120 and SFL fungi, while the untreated mycelia had a smooth surface. These aggregates were majorly found on the maturing region of hyphae. This is likely due to the differences between the apical, subapical, and mature zones of the hyphae. The apical zone is the actively growing region predominantly richer in chitin, and relatively lower in proteins than mature hyphae. The mature zone is the cytoplasmically more active zone, highly vacuolated and loaded with enzymes involved in metal homeostasis (Lee et al., 2010, Gow and Gadd, 1995). There was no significant difference observed in the surface morphology between A1120 and SFL strain with respect to Cr exposure. EDX analysis confirmed the presence of Cr on the hyphal surface in both A1120 and SFL fungi. Thus, a combined SEM EDX observation suggested that the fungal strains had Cr particles deposited across the maturing hyphal surface as a result of Cr adsorption to the cell wall. Similar to our observations, a uniform distribution of Cr on the fungal hyphae along with the formation of aggregates was reported in *A.*

niger (Gu et al., 2015, Khambhaty et al., 2009, Srivastava and Thakur, 2006), in *A. versicolor* nearly uniform distribution of mercury (Hg) together with the formation of nanostructures on the cell surface (Das et al., 2007). These findings strongly suggest that fungal cell surface modifications are a consequence of metal adsorption however no substantial difference was observed between A1120 and SFL strain. The limitations of SEM- EDS are that it does not differentiate between Cr (VI) and Cr (III), nor internal versus surface bound Cr. Thus, further characterization of the fungal surface in response to Cr (VI) was performed.

TEM-EDX study that Cr [either Cr (VI) and/or Cr (III)] was uniformly adsorbed to the cell surface in both A1120 and SFL strain, indicating the first site of fungal–metal interaction is the cell wall during the Cr uptake process. The Cr binding to the cell wall could be due to the electrostatic interaction between the metal ion and the various functional groups present on the cell surface (Das et al., 2009). Further, subcellular localisation of Cr was confirmed by point EDX and line EDX analysis. The appearance of Cr peak in the cellular structures confirmed the internalization of Cr into the cell and the membrane bound cellular organelles but not in the periplasmic space. This study reports for the first time the localization of chromium in the internal membrane bound cell structures. No significant difference was observed between the two fungal strains. TEM-EDX analysis suggested the mechanism of Cr biosorption adopted by this fungus, that involves initial Cr binding to the cell wall followed by Cr transportation into the cell and compartmentalization into the membrane bound organelles. The TEM study could not differentiate between the oxidation states of Cr however, since Cr (III) due to its limited solubility, is highly impermeable to biological membranes (Chang et al., 2016, Chourey et al., 2006), it can be assumed that Cr in hexavalent form is transported into the cell. Similar observations of intracellular accumulation of Cr following

initial Cr adsorption to cell wall has also been reported in *A. niger var tubigenis* Ed8 (Alonso et al., 2014) and *Termitomyces clypeatus* (Das et al., 2009). They described the presence of electron dense granules of chromium on the cell wall, periplasmic space, cytoplasmic membrane and within the cytoplasm of the fungal cell. In contrast, in another study, the appearance of an electron dense layer throughout the cell wall of *A. versicolor* mycelia without any intracellular accumulation was reported suggesting the role of cell wall components as major chromium binding site whereas the process of transportation of chromium inside the cytoplasm was found to be insignificant (Das et. al, 2008). A further in-depth understanding of the cell surface phenomena and the information about the different valence states of chromium is needed to describe in detail the Cr biosorption mechanism.

The characterisation of Cr adsorption to the cell wall was done by FTIR analysis. The complex nature of fungal cell wall was indicated by the presence of number of absorption peaks obtained in the FTIR spectral analysis (Ahluwalia and Goyal, 2010). Prominent differences observed in the FTIR spectra of untreated and chromium treated biomass indicated chemical interaction between the metal ion and the functional groups present on the cell wall. Interestingly, differences in the peak intensities were observed with the increase in Cr treatment time. In A1120 there was a minute difference observed in the spectral peak intensity between untreated and 48 h treated biomass whereas the peaks were considerably weaker after 96 h. In contrast, significantly weaker peaks were observed within 48 h of Cr treatment in SFL strain. This may be due to the resistant nature of SFL strain in which the interaction and subsequent complexation of Cr with the biomass may occur earlier than A1120. The FTIR study identified that the functional groups that provide chromium binding sites on the fungal cell walls in both A1120 and SFL strain were

predominantly amines and hydroxides (3269 cm^{-1} , 3273 cm^{-1}), phospholipids (2921 cm^{-1} and 2851 cm^{-1}), carboxyl (1744.30 cm^{-1}), amides (1637.34 cm^{-1} , 1639.57 cm^{-1} , 1588.38 cm^{-1} , 1543.85 cm^{-1} , 1238.39 cm^{-1} , 1234.01 cm^{-1}), proteins (1376.17 cm^{-1} and 1375.61 cm^{-1}), carbohydrates (1025.59 cm^{-1} , 1023.21 cm^{-1}). Similar observations have been reported in various other fungal organisms as well such as *A. niger* (Gu et al., 2015), *Termitomyces clypeatus* (Das et al., 2009, Ramrakhiani et al., 2011), *Coriolus versicolor* (Sanghi et al., 2009), *Trichoderma*, *C. resiniae*, *P. chrysosporium* (Ahluwalia and Goyal, 2010), *A. Versicolor* mycelia (Das et al., 2008).

XPS study revealed the information regarding the changes in the valence state of Cr during the biosorption process. The observed peaks in the XPS spectra at 576.9 eV (A1120) and 577.1 eV (SFL) were consistent with Cr (III) in hydroxide form (Biesinger et al., 2011) suggesting only Cr (III) is adsorbed by the *A. flavus* biomass. This indicates Cr (VI) is reduced to Cr (III) in the extracellular medium prior to its aggregation on the cell wall, well supported by the findings of the preceding CHAPTER. Previous studies showed only Cr (III) existed on the surface of Cr- laden biomass of brown seaweed *Ecklonia* (Park et al., 2008) as a result of redox reactions occurring on the surface of biomass. In bacterium *Shewanella oneidensis*, XPS studies showed the presence of only trivalent chromium on the cell surface as a result of enzymatic reduction of Cr (VI) (Neal et al., 2002). In contrast to the findings of this study, presence of both Cr (VI) and Cr (III) on *A. versicolor* cell surface was reported (Das et al., 2008). XPS study did not reveal any differences between A1120 and SFL strain.

To summarise, this qualitative analysis revealed that both A1120 and SFL strain exhibited similar physical and chemical interaction with Cr taking place at topographical and subcellular level, indicated by SEM, TEM, FTIR and XPS

analysis. In terms of mechanism, only Cr (III) was adsorbed to the cell surface and Cr (VI) is transported into the cell. Proteins, lipids and carbohydrates acted as the major Cr binding sites. Further genomic study is required to decode the mechanism on a molecular level.

CHAPTER 6

Structural and functional characterisation of genes involved in chromium transport in *Aspergillus flavus*: Bioinformatics and gene expression study

6.1 Introduction:

The harmful effects are mainly associated with the intracellular uptake of chromate ions (Chourey et al., 2006). Once inside the cell, Cr (VI) undergoes a series of enzymatic reduction reactions and produces unstable Cr (IV) and Cr (V) intermediates that can cause genotoxicity (Viti et al., 2014). Metal transport proteins that play a crucial role in preventing Cr toxicity by sequestration of metal ions (Clemens S., 2001, Williams and Hall, 2000) in different organelles, trafficking, storage, active extrusion and the capability to regulate intracellular concentrations of these metal ions (Slocik et al., 2004, Festa and Thiele, 2011).

In several bacteria including *Pseudomonas aeruginosa* (Cervantes et al., 1990), *Cupriavidus metallidurans* formerly *Alcaligenes eutrophus* and *Ralstonia metallidurans* (Nies et al., 1990) a molecular mechanism of resistance to chromate has been described (Ramírez-Díaz MI et al., 2008, Viti et al., 2014). One of the best characterised mechanism is efflux of chromate ion mediated via the ChrA transporter, a hydrophobic protein with 12 proposed transmembrane-spanning domains (Cervantes et al., 2001, Cervantes et al., 1990, Nies et al., 1990), belonging to chromate ion transporter (CHR) superfamily that transport chromate out of the cell (Alvarez et al., 1999). Chromate uptake and resistance is also reported to be

mediated by the sulphate transport system due to the structural similarity between the tetrahedral chromate anion (CrO_4^{2-}) and the sulphate anion (SO_4^{2-}). In a wide range of cell types including, bacteria, fungi, yeast, plants, uptake of Cr via sulphate uptake pathway has been demonstrated (Ohtake et al., 1987, Ohta et al., 1971, Ramirez-Diaz et al., 2008, Das et al., 2009, Piłsyk and Paszewski, 2009). Involvement of genes encoding several other transporters such as PDR-like ABC transporter, multidrug resistance protein 4 and glutathione S-transferase GSTU6 under Cr stress has also been demonstrated in rice (Dubey et al., 2010). The molecular mechanisms that confer resistance to Cr (VI) in microorganism, in particular fungi are poorly understood.

So far, there is no report on systematic identification and characterization of critical genes involved in Cr-responsiveness, uptake, transportation and sequestration in *Aspergillus flavus*. This led to the hypothesis that, changes in the expression of genes encoding metal transporters may assist in unravelling the molecular mechanism of Cr resistance and/or tolerance in *A. flavus*. This hypothesis was tested by identification and structural and functional characterization of putative Cr transporter genes expressed under Cr toxicity in A1120 and SFL strain of *A. flavus*. Comparative genomics was used to identify four putative Cr transporter genes. In addition, computational analysis was executed for the functional inference of these proteins. Sequence analysis was done to establish relationships with well-characterised homologues that are experimentally characterised, using sequence based search such as BLAST (Altschul et al., 1990). Multiple sequence alignment were generated to identify the conserved regions using Clustal Omega programme (Sievers et al., 2011) and putative metal binding sites were predicted using Multiple Em for Motif Elicitation (MEME), Version 4.11.1. MEGA version 6 was employed to construct the Phylogenetic tree. The physiochemical properties of proteins were

determined by Expasy's ProtParam server and structural prediction of the identified Cr transport proteins were carried out using Phyre2 web portal for protein modelling, prediction and analysis. Further, quantitative real time PCR (qRT PCR) analysis was executed to determine the transcripts level and establish the responsiveness of genes to Cr (VI).

Overall, a comprehensive comparative investigation was done to determine functional similarities and differences between the reference (A1120) and the Cr tolerant (SFL) strain on a molecular level in response to Cr stress which led to delineate the mechanism of Cr resistance in *A. flavus*.

6.2 Results:

6.2.1 Identification of putative chromium transporter genes:

Employing the comparative genomics approach, putative Cr transport proteins were identified in Cr tolerant SFL strain of *A. flavus*. Amino acid sequences encoding metal ion transporters were retrieved from the sequenced genome of reference strain *Aspergillus flavus* (NCBI Accession number; AAIH00000000.2) obtained from NCBI genome database. Four putative Cr uptake and efflux genes were identified based on a literature search. The putative Cr transport genes included:

1. Putative sulphate transporter (Accession number: XP_002374529.1),
2. Putative ABC iron exporter, Atm1 (Accession number: XP_002374920.1),
3. Putative vacuolar ABC heavy metal transporter, Hmt1 (Accession number: XP_002379308.1),
4. Putative ABC efflux transporter (Accession number: XP_002373430.1).

Whole genome sequencing of the SFL strain has been carried out by TERI (The Energy and Resources Institute) researchers and the sequence has been putatively annotated (unpublished). This data was used for the study. The four identified

transporter gene sequences from reference strain A1120 were used as bait for fishing out the putative Cr transporter genes in the sequenced genome of SFL strain. Sequences with maximum identity were selected as putative Cr transporters in SFL strain, namely, scaffold_9G379 (putative sulphate transporter), scaffold_12G096 (putative Atm1), scaffold_4G491 (putative Hmt1) and scaffold_8G356 (putative ABC efflux transporter). Since, A1120 and SFL exhibited different degree of tolerance as well as different protein expression profiles, it is likely that besides the four studied proteins other proteins might not be expressed in A1120 are responsible for the differential tolerance observed in the two strains.

For putative sulphate uptake transporter from A1120, query coverage of 74% showed 99% identity with sulphate permease 2 (scaffold_9G379) from SFL (Figure: 6.1a). A query coverage of 98% of putative ABC iron exporter, Atm1, from A1120 showed 96% identity with iron sulphur cluster transporter, Atm1 (scaffold_12G096) from SFL (Figure 6.1b). In case of putative vacuolar heavy metal transporter (Hmt1) from A1120, a query coverage of 63% showed 100% identity with ABC transporter (scaffold_13G402) from SFL (Figure: 6.1c). With query coverage of ninety percent, the ABC efflux transporter from A1120 showed 100% identity with pleotropic drug resistant protein (scaffold_8G356) from SFL (Figure 6.1d).

6.2.2 Sequence homology analysis of Cr genes in A1120 and SFL strains, and *insilico* identification of putative metal binding sites:

BLAST searches against NCBI non-redundant protein database were performed to identify the metal transporters genes, homologous to putative Cr transporters, in other eukaryotic organisms including *Aspergillus species*, *Penicillium species*, *Talaromyces species*, as the genome of these fungal species are fully sequenced, and two well studied reference species, *Saccharomyces cerevisiae* and *Arabidopsis*

```

XP_002374529.1      MPGDLKTRIG HGAAKALGIK IPYRDPLGVH ADPVTIRGESH FSVGTIDTYS YLEPEPTPAE WLKEVCPSPWH QVGRIFYNLF PFLSWITRYN 90
scaffold_9G379      -----
Clustal Consensus  1
XP_002374529.1      LQWLLGDMIA GVTVGAVVVP QGMAYAKLAN LPVEISPLVI FVQPVAVMS TLTGHVIASC LAIICGAVVC AMGLLRLGFI VDFIPLPAIS 180
scaffold_9G379      -----
Clustal Consensus  ***** 19
XP_002374529.1      AFMTGSAINI CSQGQKMDLG ETADPSTKDS TYLVIINTLK HLPsAKIDAA MGVSALAMLY IIRSGCNYGA KKFPRIHAKVW FVSTLRTVTF 270
scaffold_9G379      AFMTGSAINI CSQGQKMDLG ETADPSTKDS TYLVIINTLK HLPsAKIDAA MGVSALAMLY IIRSGCNYGA KKFPRIHAKVW FVSTLRTVTF 109
Clustal Consensus  ***** 109
XP_002374529.1      VILFYTMISA AVNLHRRSNP RFKLLGKVRP GFQHAAPVQV NSRIISAFAS ELPASIVLL IEHIAISKSF GRVNNYIDP SQELVAIGVS 360
scaffold_9G379      VILFYTMISA AVNLHRRSNP RFKLLGKVRP GFQHAAPVQV NSRIISAFAS ELPASIVLL IEHIAISKSF GRVNNYIDP SQELVAIGVS 199
Clustal Consensus  ***** 199
XP_002374529.1      NLLGPFLGGY PATGFSRSTA IKSAGVTRP LAGVITAVVV LLAIYALPAV FFYIPKASLA GVIIHAVGDL ITPPNIVYQF WRVSPDLDAI 450
scaffold_9G379      NLLGPFLGGY PATGFSRSTA IKSAGVTRP LAGVITAVVV LLAIYALPAV FFYIPKASLA GVIIHAVGDL ITPPNIVYQF WRVSPDLDAI 289
Clustal Consensus  ***** 289
XP_002374529.1      FFIGVIVTVF TTIEIGIYCT VCVSVAILLF RVAKARGQFL GRVTIHSVIG DHLVQDDGKY GSANSPNAAS DDKDELSRSI FLPINHDTGS 540
scaffold_9G379      FFIGVIVTVF TTIEIGIYCT VCVSVAILLF RVAKARGQFL GRVTIHSVIG DHLVQDDGKY GSANSPNAAS DDKDELSRSI FLPINHDTGS 379
Clustal Consensus  ***** 379
XP_002374529.1      NPDEVVQQPY PGIPIYRFSE GFNYPNANHY TDYLVQTIQK HTRRTNPFYS GKPGDRPWNN PGPGRKSED DESHLLPLQA VILDFSSVNN 630
scaffold_9G379      NPDEVVQQPY PGIPIYRFSE GFNYPNANHY TDYLVQTIQK HTRRTNPFYS GKPGDRPWNN PGPGRKSED DESHLLPLQA VILDFSSVNN 469
Clustal Consensus  ***** 469
XP_002374529.1      VDVTsvQnLI DVrNQLDLYA S----PKTV QWHFAHINNR WTKRALAAG PGPSPDSDE GFQRWKPIFS VAEIEGSASA AAHAEMVWNR 715
scaffold_9G379      VDVTsvQnLI DVrNQLDLYA SPKTYRQKTV QWHFAHINNR WTKRALAAG PGPSPDSDE GFQRWKPIFS VAEIEGSASA AAHAEMVWNR 559
Clustal Consensus  ***** * 554
XP_002374529.1      HTQHNIKSED LEHGLKHDSE TTERETHGIE ESSDASSTRE DKLQDLKDS KAYRSRRRVA MVQGLNRPPF HIDLTSALQS ALANAGEQPD 805
scaffold_9G379      HTQHNIKSED LEHGLKHDSE TTERETHGIE ESSDASSTRE DSCNGT-----
Clustal Consensus  ***** * : 596
XP_002374529.1      PRMNVLDA 813
scaffold_9G379      ----- 605
Clustal Consensus  ***** 596

```

Figure 6.1a: Sequence alignment of putative sulfate transporter from A1120 (XP_002374529.1) with amino acid sequence of putative sulphate permease 2 from SFL (scaffold_9G379) showing identical and partially conserved residues. Identical residues are denoted by asterisk (*). Partially conserved residues are denoted by either dot (.) or semi colon (:), where dot indicates the residues are more or less similar and semi-colon indicates the residues at that position are highly similar.

thaliana. The name of the identified species and corresponding transporter type is given in **Table 6.1**. Multiple sequence alignment of representative homologous transporter protein from different species was produced, using sequence alignment tool Clustal omega, to obtain structurally/functionally important regions. These functional and/or structural regions, called domains, are highly conserved across species. NCBI conserved domains database search (Marchler-Bauer A et al., 2015), was used for the functional annotation of these conserved domains. Identification of putative metal binding sites is an important step for the function prediction of proteins. This was done by prediction of structural motifs. Motifs are a particular

```

XP_002374920.1 ----- 1
scaffold_12G096 MLPRARPPC LRVPGDFHR GPAVPRSTR ISTRHSIQFR VFTSKGLLN KNATSEPKTP IGSPLAQS ADQKTKNAQN AAGTPKRDL 90
Clustal Consensus ----- 1

XP_002374920.1 ----- 31
scaffold_12G096 SETMVGKQEQ RKADWAIMKE MAKYLWPKIL NVNVFFYFKS IVDSMNVDF AIGGTAYTVA GSMIIAYT --- --GVTRIGAT 180
Clustal Consensus ***** ***** ***** ***** ***** ***** ***** ***** ***** ***** ***** 30

XP_002374920.1 LFQELRNAVF ASVAQKARR VARNVFEHLL RLDLNFHLSR QTGGLTRAI D RGTKGISFLL TSMVFHVVPT ALEISLVCGI LTYQGAQFA 121
scaffold_12G096 LFQELRNAVF ASVAQKARR VARNVFEHLL RLDLNFHLSR QTGGLTRAI D RGTKGISFLL TSMVFHVVPT ALEISLVCGI LTYQGAQFA 265
Clustal Consensus ***** ***** ***** ***** ***** ***** ***** ***** ***** ***** ***** 115

XP_002374920.1 AITAATMVAY SAFTITTTAW RTKFRKQANA ADNRGATVAV D SLINYEAVK YFNNEKFEVA RYDKALKAYE DASIKVTTSL AFLNNGQNM 211
scaffold_12G096 AITAATMVAY SAFTITTTAW RTKFRKQANA ADNRGATVAV D SLINYEAVK YFNNEKFEVA RYDKALKAYE DASIKVTTSL AFLNNGQNM 355
Clustal Consensus ***** ***** ***** ***** ***** ***** ***** ***** ***** ***** ***** 205

XP_002374920.1 FSSALAGMMY LAANGVASGS LTVGDLVMVN QLVFQLSVPL NFGSSVYREL RQSLDME TL FNLQKVNVI TEKPNAKPLQ LHRGGEIKFE 301
scaffold_12G096 FSSALAGMMY LAANGVASGS LTVGDLVMVN QLVFQLSVPL NFGSSVYREL RQSLDME TL FNLQKVNVI TEKPNAKPLQ LHRGGEIKFE 445
Clustal Consensus ***** ***** ***** ***** ***** ***** ***** ***** ***** ***** ***** 295

XP_002374920.1 NVTFGYHPR PILKNASFTI PAGQKFAIVG PSGCGKSTIL RLLFRYDVQ EGRILVDGQD VRDVTLES LR KAIGVVPQDT PLFNDSIAHN 391
scaffold_12G096 NVTFGYHPR PILKNASFTI PAGQKFAIVG PSGCGKSTIL RLLFRYDVQ EGRILVDGQD VRDVTLES LR KAIGVVPQDT PLFNDSIAHN 535
Clustal Consensus ***** ***** ***** ***** ***** ***** ***** ***** ***** ***** ***** 385

XP_002374920.1 IRYGRIDATD EVRKAQRA HIHELIEKLP EGYKTVGER GMMISGGEKQ RLAI SRLIK DPPELLFFDEA TSALDITYEQ ALLQINISVL 481
scaffold_12G096 IRYGRIDATD EVRKAQRA HIHELIEKLP EGYKTVGER GMMISGGEKQ RLAI SRLIK DPPELLFFDEA TSALDITYEQ ALLQINISVL 625
Clustal Consensus ***** ***** ***** ***** ***** ***** ***** ***** ***** ***** ***** 475

XP_002374920.1 KDKARTSVFV AHRLRITCDS DQILVLKEGR VAETGSHREL LELDCIYAE L WNCQEPVCL CLVY----- ----- 545
scaffold_12G096 KDKARTSVFV AHRLRITCDS DQILVLKEGR VAETGSHREL LELDCIYAE L WNAQEMSAQ DPESQNAEL BEGAGQEVLP DSRQK 710
Clustal Consensus ***** ***** ***** ***** ***** ***** ***** ***** ***** ***** ***** 529

```

Figure 6.1b: Sequence alignment of putative ABC iron exporter, Atm1 from A1120 (XP_002374920.1) with amino acid sequence of iron sulphur cluster transporter, Atm1 SFL (scaffold_12G096) showing identical and partially conserved residues. Identical residues are denoted by asterisk (*). Partially conserved residues are denoted by either dot (.) or semi colon (:), where dot indicates the residues are more or less similar and semi-colon indicates the residues at that position are highly similar.

```

XP_002379308.1 MDSHHATRQL LEYLRTGYPI LLLLVFISAF VANSVLAARN ANNSTTAAQT GPGGRPLPKR SRSTMAIMKN PQRKSNQTRS WFRWLSVGIL 90
scaffold_13G402 ----- 1
Clustal Consensus ----- 1

XP_002379308.1 LTLIGDAAVN VAHVMSRSE QNWCGQSVVI YVGSFFVYS IILVSLD TD PSPTFQFVP WLVAVPIELA ILGISSSINA GNHHEPVVGD 180
scaffold_13G402 ----- 1
Clustal Consensus ----- 1

XP_002379308.1 PTGGRLQKGV TSWELLELIC NCVRVLISI LVALYVFSSI RMHSSSRKAP RAYANGASET TGLLDPSHAE NGNAYGSTPA NQQPTKPADA 270
scaffold_13G402 ----- 1
Clustal Consensus ----- 1

XP_002379308.1 WVRPTTVPST SWWEYLSGYS LFFPYLWPSK SRRLQIVVVI CFIILVLRV VNVLVLQVG VITRKLTKG DDFVDPVFDI CLYILFRWLQ 360
scaffold_13G402 ----- 1
Clustal Consensus ----- 1

XP_002379308.1 GNQGLIGSLR SSLWIPVSQY SYMELSTA AF EHVHSLSLDF HLGKKTGEVL SALS KGSIN TFEQVTFQV VPMLVDLCVA IVYELIALDA 450
scaffold_13G402 ----- --MELSTA AF EHVHSLSLDF HLGKKTGEVL SALS KGSIN TFEQVTFQV VPMLVDLCVA IVYELIALDA 68
Clustal Consensus ***** ***** ***** ***** ***** ***** ***** ***** ***** ***** ***** 68

XP_002379308.1 YYALVVTIVT FCYLVIVRM AQWRAEIRQ MVNASRQEDA VKND SMVSYE TVKYFNAEDY EEDRYGAVS DFORAEYHVL FSLNLMNTSQ 540
scaffold_13G402 YYALVVTIVT FCYLVIVRM AQWRAEIRQ MVNASRQEDA VKND SMVSYE TVKYFNAEDY EEDRYGAVS DFORAEYHVL FSLNLMNTSQ 158
Clustal Consensus ***** ***** ***** ***** ***** ***** ***** ***** ***** ***** ***** 158

XP_002379308.1 NTVFMLGLLI ACFIAAYQVS LGQRDVGEFV SLLTYMAQLQ GPLNFFGTFY RSIQSALINS ERLLLEFRQ PTVVDMPSAT PLPCKGDIA 630
scaffold_13G402 NTVFMLGLLI ACFIAAYQVS LGQRDVGEFV SLLTYMAQLQ GPLNFFGTFY RSIQSALINS ERLLLEFRQ PTVVDMPSAT PLPCKGDIA 248
Clustal Consensus ***** ***** ***** ***** ***** ***** ***** ***** ***** ***** ***** 248

XP_002379308.1 FENVKESYDS RKPALNGLTF RCEPGTTAL VGESGGKST VFRLLFRFYN SEWGRILIDG HDVKNTTIDS LRKHIGVVPQ DTVLNEEELM 720
scaffold_13G402 FENVKESYDS RKPALNGLTF RCEPGTTAL VGESGGKST VFRLLFRFYN SEWGRILIDG HDVKNTTIDS LRKHIGVVPQ DTVLNEEELM 338
Clustal Consensus ***** ***** ***** ***** ***** ***** ***** ***** ***** ***** ***** 338

XP_002379308.1 YNLKYANQNA TDEDVYEACK AASIHDKIMS FPDKYNKVG ERGLRLSGGE KQVAIARTI LKNPRILLD EATAALDTET EEHIQCALST 810
scaffold_13G402 YNLKYANQNA TDEDVYEACK AASIHDKIMS FPDKYNKVG ERGLRLSGGE KQVAIARTI LKNPRILLD EATAALDTET EEHIQCALST 428
Clustal Consensus ***** ***** ***** ***** ***** ***** ***** ***** ***** ***** ***** 428

XP_002379308.1 LSRGRMLIVI AHRLSITTTA DRILVLHEGK VAESCTHDQL LAMKGRVASM WRKQIRAORA AEAQVLQDR AQRLRSASTS GAVGDDSSSQ 900
scaffold_13G402 LSRGRMLIVI AHRLSITTTA DRILVLHEGK VAESCTHDQL LAMKGRVASM WRKQIRAORA AEAQVLQDR AQRLRSASTS GAVGDDSSSQ 518
Clustal Consensus ***** ***** ***** ***** ***** ***** ***** ***** ***** ***** ***** 518

XP_002379308.1 SDEDRNGNTH ASAVRQTQGH HWPAMDQKA 929
scaffold_13G402 SDEDRNGNTH ASAVRQTQGH HWPAMDQKA 547
Clustal Consensus ***** ***** ***** ***** ***** ***** ***** ***** ***** ***** ***** 547

```

Figure 6.1c: Sequence alignment of putative vacuolar heavy metal transporter, Hmt1 from A1120 (XP_002379308.1) with amino acid sequence of putative ABC transporter from SFL (scaffold_13G402) showing identical and partially conserved residues. Identical residues are denoted by asterisk (*).

Gene		Species					
		<i>Aspergillus parasiticus</i> SU-1 (taxid:1403190)	<i>Aspergillus oryzae</i> RIB40 (taxid:510516)	<i>Talaromyces marneffei</i> (taxid:37727)	<i>Penicillium italicum</i> (taxid:40296)	<i>Saccharomyces cerevisiae</i> (taxid:4932)	<i>Arabidopsis thaliana</i> (taxid:3702)
Sulphate uptake	Description	SUL1 like protein	sulfate permease 2	sulfate transporter, putative	sulfate anion transporter	Sul1p	sulfate transporter 2;2
	Accession	KJK65149.1	XP_001819936.1	XP_002150182.1	KGO75420.1	AJP85721.1	NP_565165.2
Atm1	Description	ATM1 like protein	iron-sulfur clusters transporter atm1	Iron-sulfur clusters transporter atm1, mitochondrial	ABC transporter, integral membrane type 1	Atm1p	ABC transporter of the mitochondrion 3
	Accession	KJK64780.1	XP_001819593.1	KFX43873.1	KGO73433.1	AJS97061.1	NP_200635.1
Hmt1	Description	Hypothetical Protein AOR_1_1188014	ATM1 like protein	vacuolar ABC heavy metal transporter (Hmt1), putative	ABC transporter, integral membrane type 1	ATM1	ABC transporter of the mitochondrion 3
	Accession	XP_001822080.2	KJK60295.1	XP_002150389.1	KGO71896.1	CAA57938.1	NP_200635.1
ABC efflux	Description	Pleiotropic Drug Resistance PDR Family protein	unnamed protein product	ABC efflux transporter, putative	ABC-2 type transporter	hypothetical protein H635_YJM1083_O00069	ABC transporter G family member 37
	Accession	KJK62758.1	BAE56219.1	XP_002143557.1	KGO70414.1	AJT87060.1	NP_190916.1

Table 6.1 Genes used for multiple sequence alignment. The name of the gene from *A. flavus* is given in the leftmost column (Gene). Description of each gene and the corresponding accession number is given in next to leftmost column (Description and accession). Across the top, name of the species used for multiple sequence alignment were listed.

similarity with sulphate permease 2 from *A. oryzae* RIB40 and least similarity with high affinity sulphate transporter 2;2 from *A. thaliana* (27%). Two putative conserved domains were detected shown by red and green bars (Figure 6.2). Further investigations of the conserved domains revealed potential binding sites called motifs (Figure 6.3) which may contain active sites for chromate binding. Of the five motifs discovered, motif 1 (Figure 6.3a) was found within STAS SulP like sulphate transporter domain at the C terminal of protein which contains highly conserved and motif 2, 3, 4 and 5 (Figure 6.3a) were found on sulphate transporter domain at the N terminal. Further motif location analysis showed motif 3 and 4 were present in all

sequences while motif 1, 2 and 5 were present in all except *S. cerevisiae* (Figure 6.3b).



Figure 6.2: Multiple sequence alignment of alignment of putative sulfate transporter from A1120 (XP_002374529.1) and putative sulphate permease 2 from SFL (scaffold_9G379) with SUL1 like protein of *A. parasiticus* SU-1 (Accession no. KJK65149.1), sulfate permease 2 of *A. oryzae* RIB40 (Accession no., XP_001819936.1, sulfate transporter of *T. marneffei* ATCC 18224 (Accession no. XP_002150182.1, sulfate anion transporter of *P. italicum* (Accession no. KGO75420.1), Sul1p of *S. cerevisiae* YJM1444 (Accession no. AJP85721.1) and sulfate transporter 2;2 of *A. thaliana* (Accession no. NP_565165.2) showing conserved regions. Identical residues are denoted by asterisk (*). Partially conserved residues are denoted by either dot (.) or semi colon (:), where dot indicates the residues are more or less similar and semi-colon indicates the residues at that position are highly similar. Red and green bars indicate conserved functional domains.

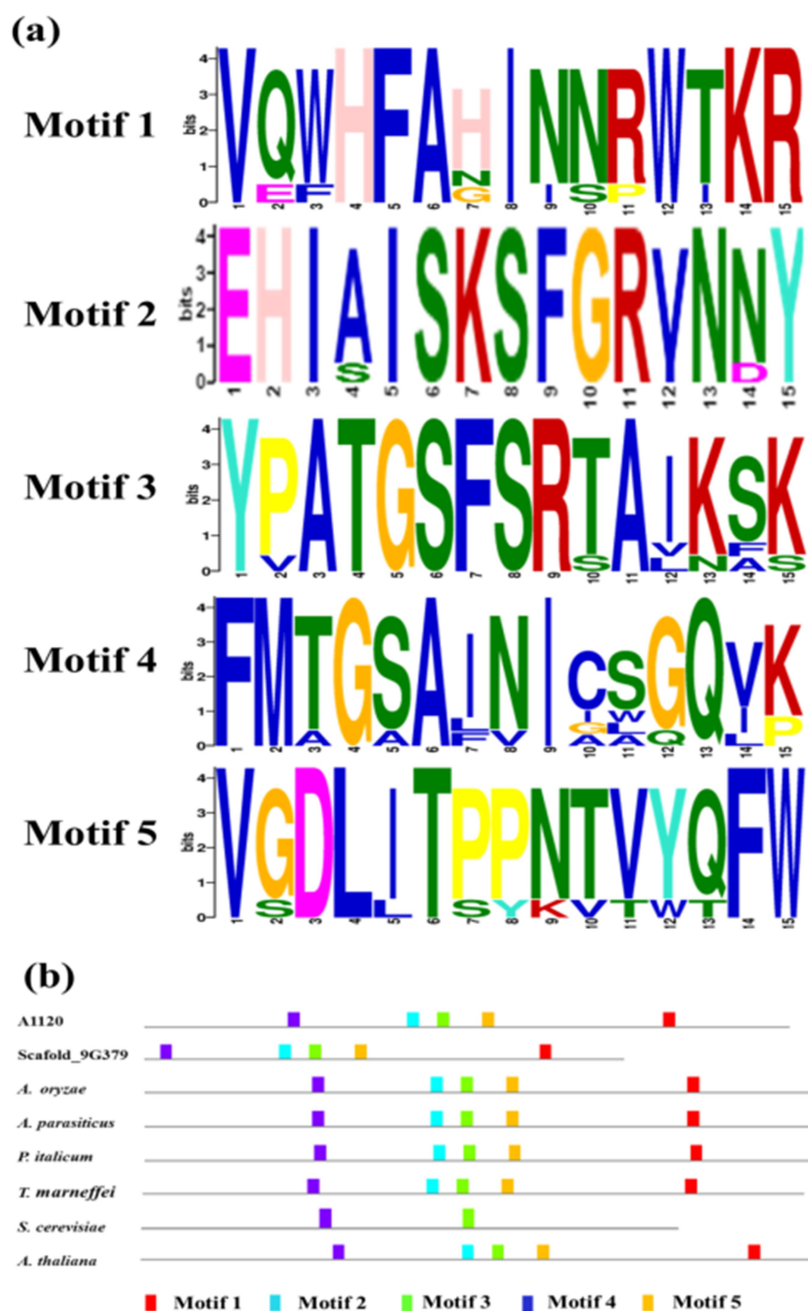


Figure 6.3 Conserved motif analysis of sulfate uptake transporter (a) sequence logo of most conserved five motifs in putative sulphate uptake transporter (b) distribution of conserved motifs in ABC efflux transporter in A1120, SFL, *A. oryzae*, *A. parasiticus*, *P. italicum*, *T. marneffei*, *S. cerevisiae*, *A. thaliana*.

6.2.2.2 ABC iron exporter, *Atm1*:

Sequence alignment of putative *Atm1* transporter in A1120 indicated 98% similarity with ATM1 like protein from *Aspergillus parasiticus* SU-1 and iron-sulphur clusters

transporter atm1 from *Aspergillus oryzae* RIB40 and the least similar sequence was ABC transporter of the mitochondrion 3 (59%). In SFL (scaffold_12G096), the maximum similarity of 100% was found with iron-sulphur clusters transporter atm1 from *Aspergillus oryzae* RIB40 and the least similar sequence was ABC transporter of the mitochondrion 3 (49%) from *A. thaliana*. Two putative conserved domains were detected indicated by red and green bars. The highly conserved invariant amino acid residues are indicated (Figure 6.4). Within the conserved domains putative binding sites were identified which showed 5 most conserved motifs (Figure 6.5) containing potential metal binding residues. Motif 1 and 5 (Figure 6.5a) were related with found within ABC_membrane, cl00549 (accession no. pfam00664) belonging to ABC_membrane superfamily while motif 2, 4 and 5 (Figure 6.5b) were found in ABCC_ATM1 transporter cl21455 (accession no. cd03253), belonging to P-loop NTPases superfamily. All 5 motifs were found to be present in all sequences (Figure 6.5b).

6.2.2.3 Vacuolar heavy metal transporter, Hmt1:

Multiple sequence alignment of putative vacuolar transporter, Hmt1 from A1120 showed 100 % similarity to unnamed protein product from *A. oryzae*. It is also closely related to ATM1 like protein from *Aspergillus parasiticus* SU-1 99% similarity. The least similarity of 33% was found with ATM1 from *S. cerevisiae*. For SFL strain, putative Hmt1 transporter was found closest to hypothetical protein AOR_1_1188014 from *A. oryzae* as well as ATM1 like protein from *A. parasiticus* SU-1 with 100% similarity. The least similarity of 39% was found with ATM1 from *S. cerevisiae*. Two putative conserved domains detected are shown by red and green bars (Figure 6.6). Identification of potential metal binding sites revealed five motifs (Figure 6.7) containing the most conserved active metal binding residues where



Figure 6.4: Multiple sequence alignment of putative ABC iron exporter, Atm1 from A1120 (XP_002374920.1) and iron sulphur cluster transporter, Atm1 from SFL (scaffold_12G096) with iron-sulfur clusters transporter atm1 of *A. oryzae* RIB40 (Accession no. XP_001819593.1), ATM1 like protein of *A. parasiticus* SU-1 (Accession no. KJK64780.1), Iron-sulphur clusters transporter atm1, mitochondrial of *T. marneffei* PM1 (Accession no. KFX43873.1), ABC transporter, integral membrane type 1 of *P. italicum* (Accession no. KGO73433.1), Atm1p of *S. cerevisiae* YJM1463 (Accession no. AJS97061) and ABC transporter of the mitochondrion 3 of *A. thaliana* (Accession no. NP_200635.1) showing the conserved regions. Identical residues are denoted by asterisk (*). Partially conserved residues are denoted by either dot (.) or semi colon (;) where dot indicates the residues are more or less similar and semi-colon indicates the residues at that position are highly similar. Red and green bars indicate conserved functional domains.

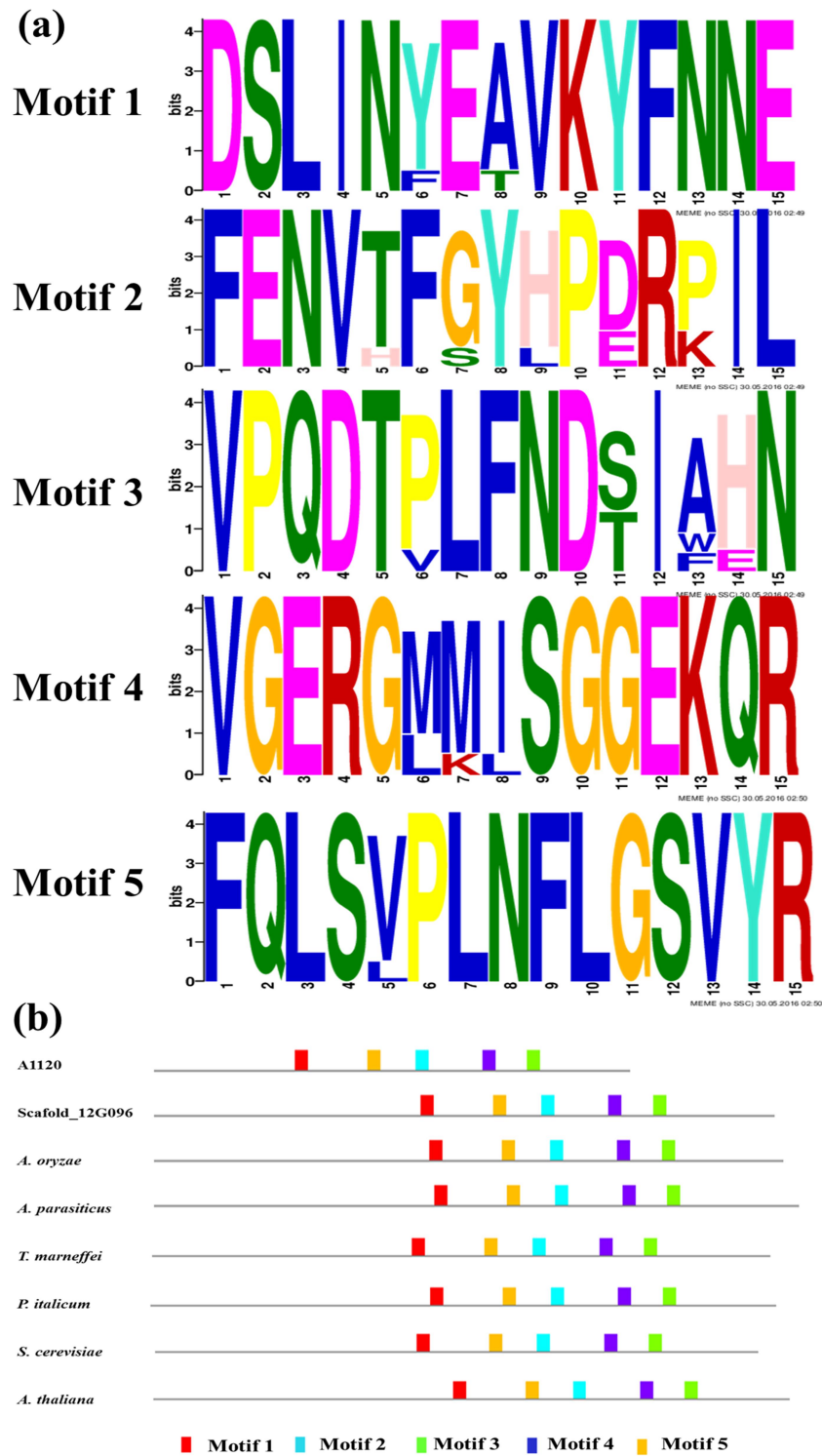


Figure 6.5 Conserved motif analysis of ABC iron exporter ATM1 (a) sequence logo of most conserved five motifs in ATM1 (b) distribution of conserved motifs in ABC efflux transporter in A1120, SFL, *A. oryzae*, *A. parasiticus*, *P. italicum*, *T. marneffei*, *S. cerevisiae*, *A. thaliana*.

motif 1 and 3 (Figure 6.7a) were found in ABCC_ATM1 transporter domain, cl21455 (accession no. cd03253), belonging to P-loop NTPases superfamily and motif 2, 4 and 5 (Figure 6.7a) were found within ABC_membrane domain, cl00549 (accession no. pfam00664) belonging to ABC_membrane superfamily. All 5 motifs were found to be located in all sequences (Figure 6.7b).

6.2.2.4 ABC efflux transporter:

For putative ABC efflux transporter, multiple sequence alignment indicated that ABC efflux transporter of A1120 and SFL (scaffold_8G356) (from here onwards called ABC efflux) are closely related to unnamed protein product from *A. oryzae* with 99% and 100% similarity, respectively. The least similar was ABC transporter G family member 37 from *A. thaliana* having 23 % and 22 % similarity with A1120 and SFL respectively. Two putative conserved domains were found shown by red bars (Figure 6.8). Investigations of putative metal binding sites showed 5 motifs (Figure 6.9) containing the most conserved residues within the conserved domains that act as binding sites where motifs 1, 2 and 5 (Figure 6.9a) were found in P-loop NTPase superfamily domain (accession no. cl21455) and motif 3 (Figure 6.9a) was found in ABC2_membrane superfamily domain cl21474 (accession no. pfam01061) while motif 4 was not a part of either of the two conserved domains. In addition, motif 1, 2 and 5 were present in all sequences, and motif 3 was present in all sequences except *A. thaliana* and motif 4 was present in all sequences except *S. cerevisiae* and *A. thaliana* (Figure 6.9b).

6.2.3 Transmembrane domain (TMD) analysis of putative Cr transporters:

TMMHMM server was used to predict the membrane topology of putative Cr transporters. For putative SUT from A1120, a TMD containing 8 transmembrane

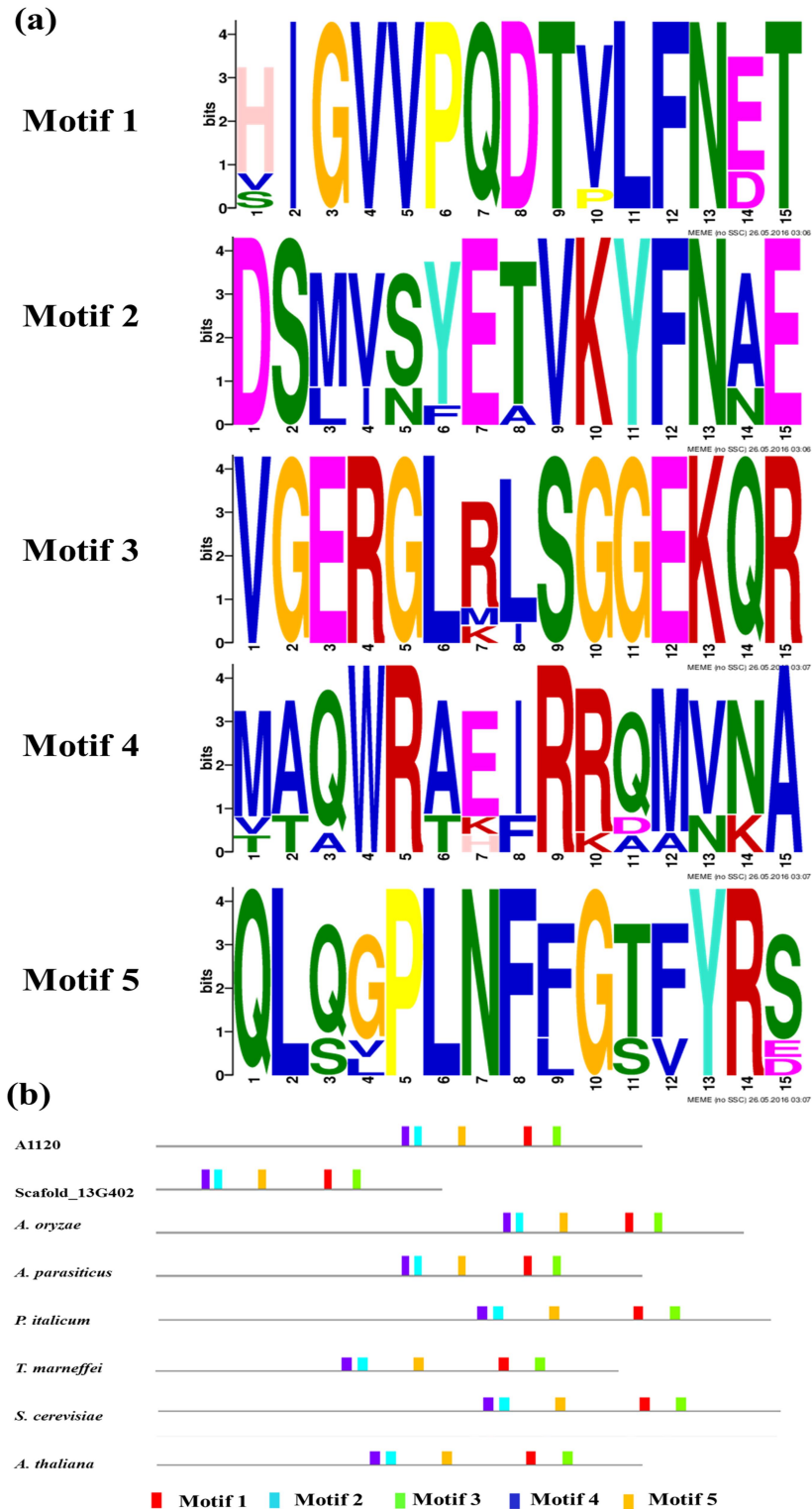


Figure 6.7 Conserved motif analysis of vacuolar heavy metal transporter Hmt1 (a) sequence logo of most conserved five motifs in Hmt1 (b) distribution of conserved motifs in ABC efflux transporter in A1120, SFL, *A. oryzae*, *A. parasiticus*, *P. italicum*, *T. marneffei*, *S. cerevisiae*, and *A. thaliana*.

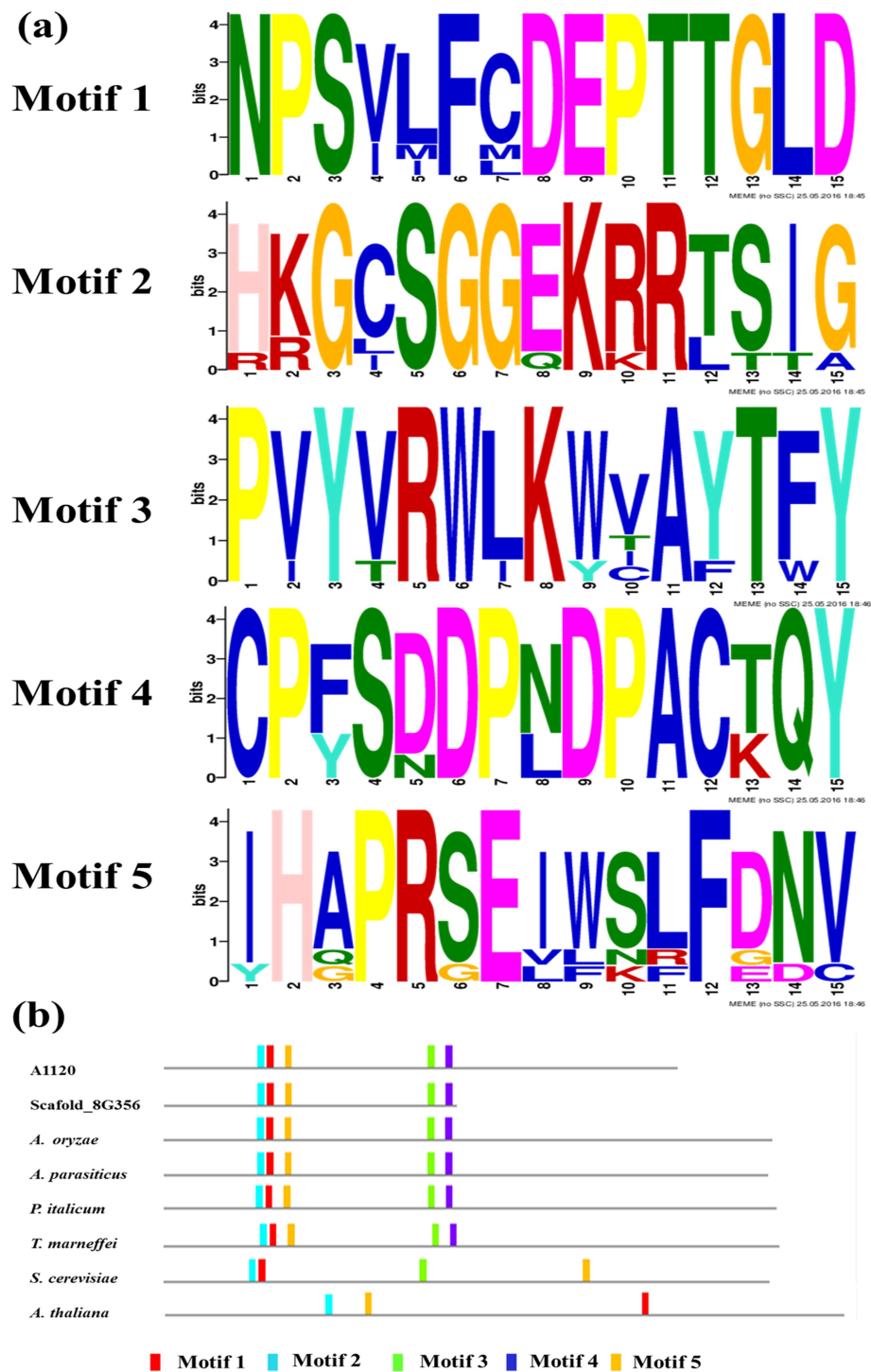


Figure 6.9 Conserved motif analysis of ABC efflux transporter (a) sequence logo of most conserved five motifs in putative ABC efflux transporter (b) distribution of conserved motifs in ABC efflux transporter in A1120, SFL, *A. oryzae*, *A. parasiticus*, *P. italicum*, *T. marneffei*, *S. cerevisiae*, *A. thaliana*.

helices (TMH) with N and C terminus inside the cell was predicted all located within the sulphate transporter domain between 93_{aa}-480_{aa} (Figure 6.10). In SFL, one TMD with 6 TMHs was predicted within the sulphate transporter domain from 7_{aa}-319_{aa} with N and C terminus inside the cell (Figure 6.11).

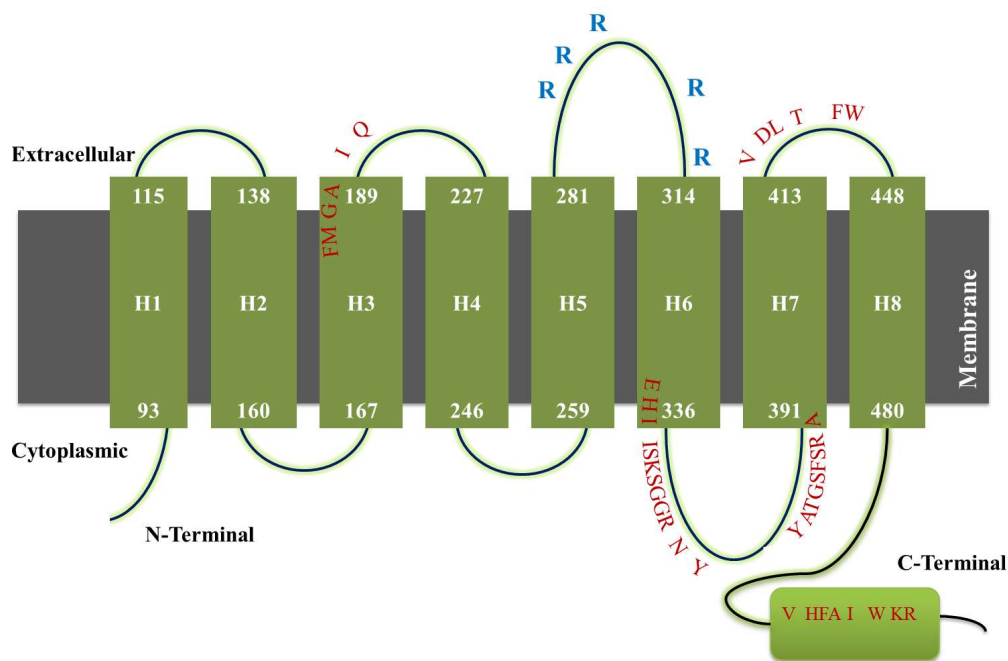


Figure 6.10 Predicted model for transmembrane domain analysis of putative sulfate uptake transporter in A1120 showing 8 transmembrane helix (TMH) with N and C terminals inside. Highly conserved residues identified during motif analysis are marked in red. Approximate positioning of positively charged arginine (R) residue is marked in blue.

For Atm1 transporter, 5 TMH were predicted in A1120 with N terminus outside and C terminal inside the cell (Figure 6.12). All 5 TMH were found within the ABC membrane domain from 20_{aa}-251_{aa}. In SFL, 6 TMH were predicted all within the transmembrane conserved domain from 125_{aa}-395_{aa}, with N and C terminal outside the cell (Figure 6.13). TMH2 (93_{aa}-115_{aa}), TMH3 (119_{aa}-139_{aa}), TMH4 (200_{aa}-223_{aa}), TMH5 (240_{aa}-261_{aa}) of A1120 Atm1 aligned with TMH3 (242_{aa}-260_{aa}), TMH4 (264_{aa}-283_{aa}), TMH5 (344_{aa}-367_{aa}) and TMH6 (384_{aa}-405_{aa}) of SFL Atm1.

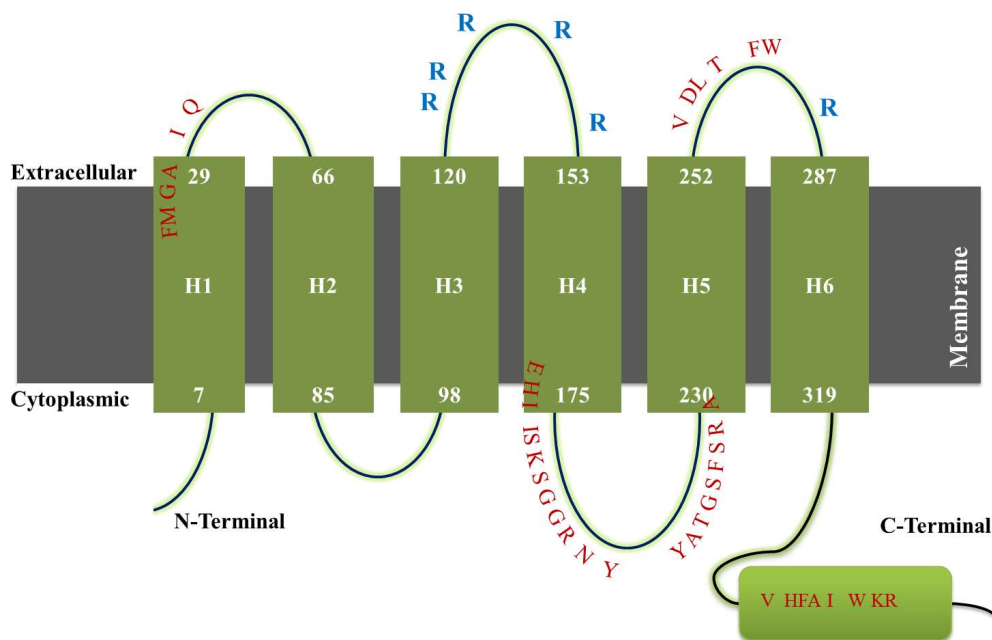


Figure 6.11 Predicted model for transmembrane domain analysis of putative sulfate uptake transporter in SFL showing 6 transmembrane helix (TMH) with N and C terminals inside. Highly conserved residues identified during motif analysis are marked in red. Approximate positioning of positively charged arginine (R) residue is marked in blue.

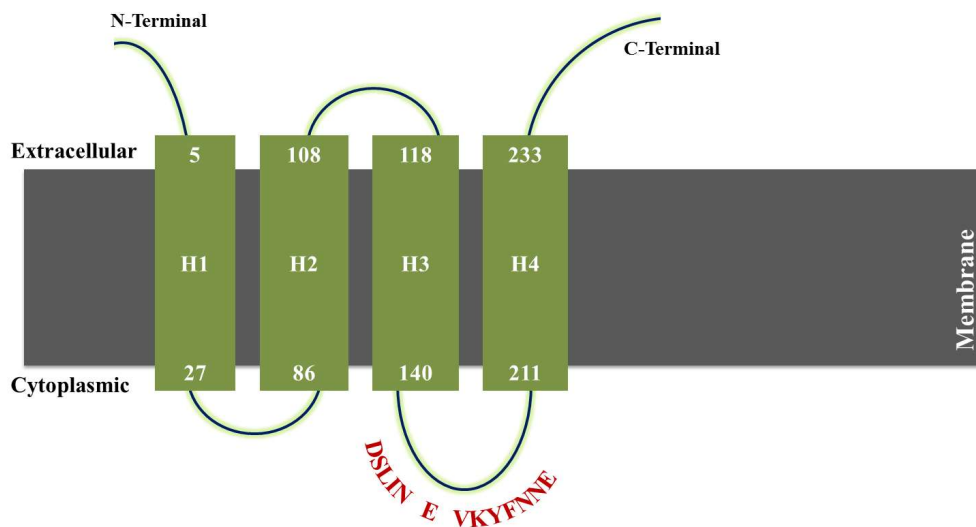


Figure 6.12 Predicted model for transmembrane domain analysis of putative Atm1 transporter in A1120 showing 4 transmembrane helix (TMH) with N and C terminals outside. Highly conserved residues identified during motif analysis are marked in red.

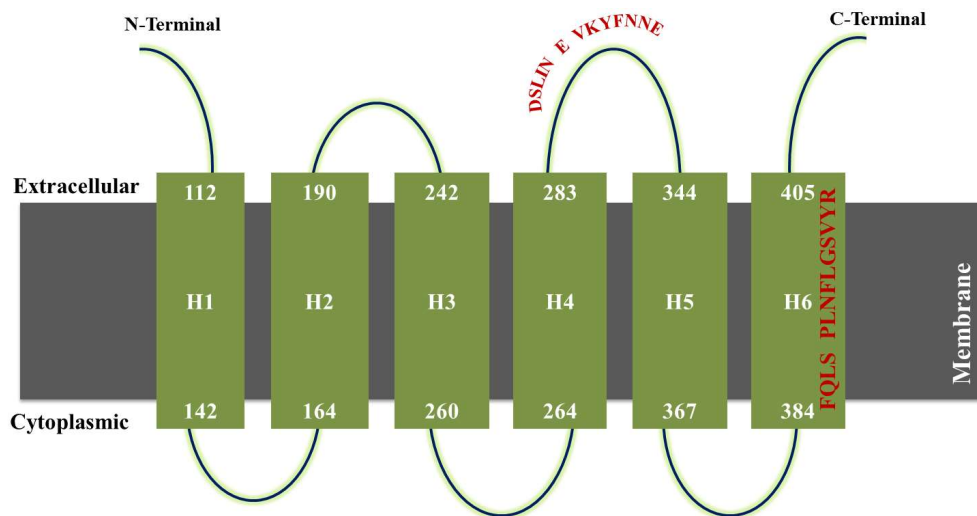


Figure 6.13 Predicted model for transmembrane domain analysis of putative Atm1 transporter in SFL showing 6 transmembrane helix (TMH) with N and C terminals outside. Highly conserved residues identified during motif analysis are marked in red.

For Hmt1, 10 TMH were predicted in A1120 with both N and C terminus outside the cell (Figure 6.14) where TMH5 (305_{aa}-329_{aa}), TMH6 (347_{aa}-374_{aa}), TMH7 (426_{aa}-447_{aa}), TMH8 (451_{aa}-471_{aa}), TMH9 (532_{aa}-555_{aa}), TMH10 (572_{aa}-593_{aa}) were found within the conserved ABC integral membrane domain from (308_{aa}-583_{aa}). In SFL Hmt1 transporter, 4 TMH were predicted with N and C terminal outside the cell (Figure 6.15). All four TMH, TMH1 (44_{aa}-65_{aa}) TMH2 (69_{aa}-89_{aa}), TMH3 (150_{aa}-173_{aa}) and TMH4 (190_{aa}-211_{aa}) aligned with TMH7 to TMH10 from A1120 and were found within the conserved ABC membrane domain from (1_{aa}-201_{aa}). THM1 to TMH6 of A1120 Hmt1 were not found in SFL.

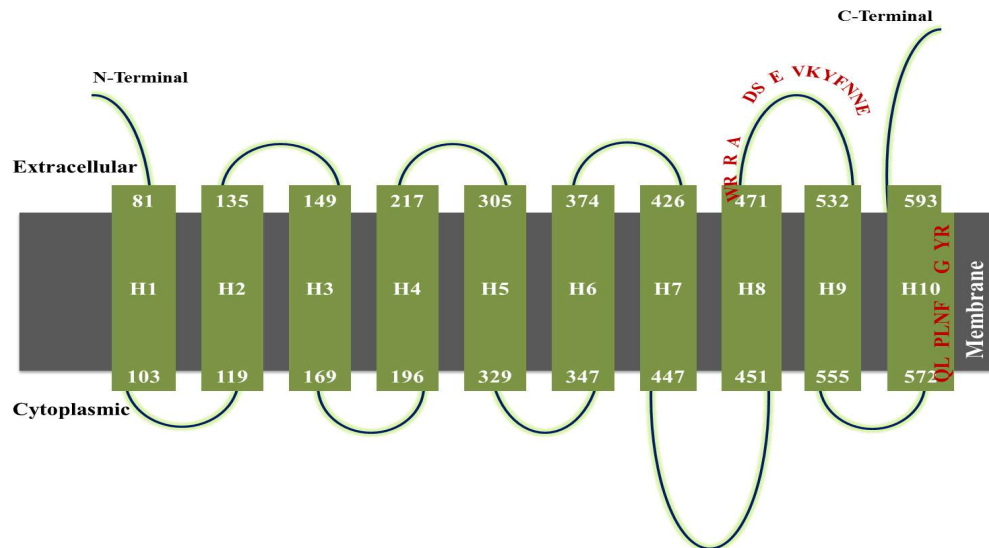


Figure 6.14 Predicted model for transmembrane domain analysis of putative Hmt1 transporter in A1120 showing 10 transmembrane helix (TMH) with N and C terminals outside the cell. Highly conserved residues identified during motif analysis are marked in red.

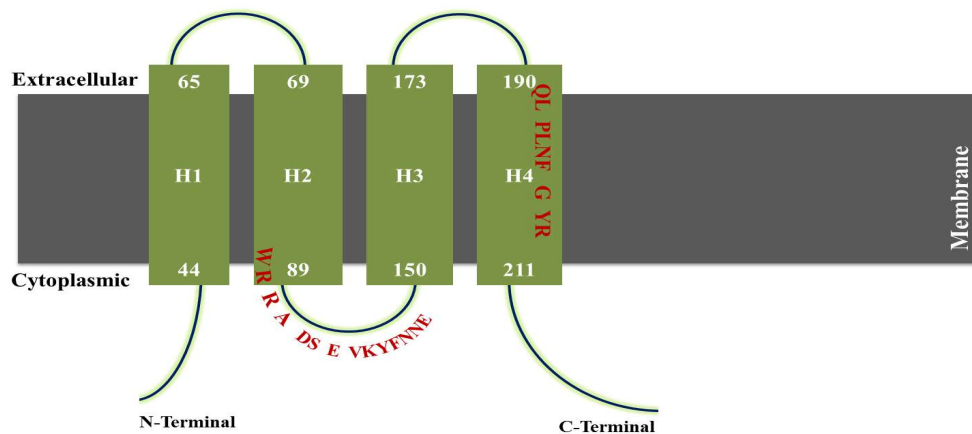


Figure 6.15 Predicted model for transmembrane domain analysis of putative Hmt1 transporter in SFL showing 4 transmembrane helix (TMH) with N and C terminals inside. Highly conserved residues identified during motif analysis are marked in red.

For putative ABC efflux transporter from A1120, 7 TMD were found with N terminus outside and C terminus inside the cell (Figure 6.16) where the first four TMHs, TMH1 (484_{aa}-501_{aa}), TMH2 (508_{aa}-530_{aa}), TMH3 (535_{aa}-557_{aa}), TMH4 (569_{aa}-591_{aa}) were located within the highly conserved ABC2 membrane domain from 376_{aa} -588_{aa}. TMH5 (632_{aa}-654_{aa}) was present outside this domain. The TMH6

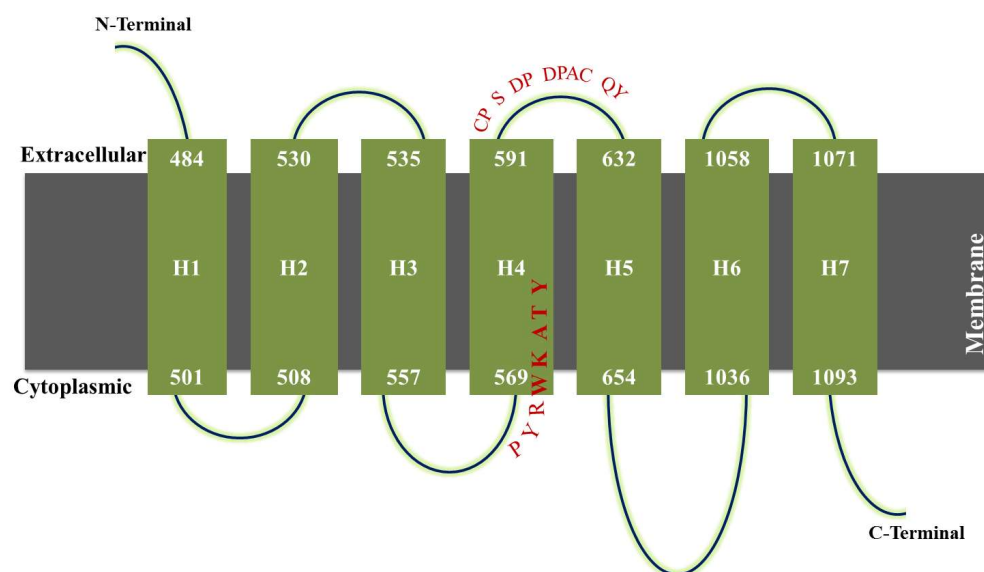


Figure 6.16 Predicted model for transmembrane domain analysis of putative ABC efflux uptake transporter in A1120 showing 7 transmembrane helix (TMH) with N terminal outside and C terminals inside. Highly conserved residues identified during motif analysis are marked in red.

(1036_{aa}-1058_{aa}) and TMH7 (1071-1093_{aa}) were found at C terminal end of protein. On the other hand the predicted topology of SFL ABC efflux transporter (scaffold_8G356) showed the presence of only 4 TMHs (one TMD) from 484_{aa}-591_{aa} right after the NBD from 65_{aa}-285_{aa}, with N and C terminal outside the cell (Figure 6.17). THM 5, 6 and 7 of A1120 transporter were not found in SFL ABC transporter.

6.2.4 Physicochemical properties of putative Cr transporters:

The physico chemical characteristics of putative Cr transport proteins were determined using Expasy's ProtParam tool. A table summarising the general characteristics of each protein including length of amino acids, putative name, and other physicochemical properties such as molecular weight, theoretical Pi, extinction coefficient is given (Table 6.2).

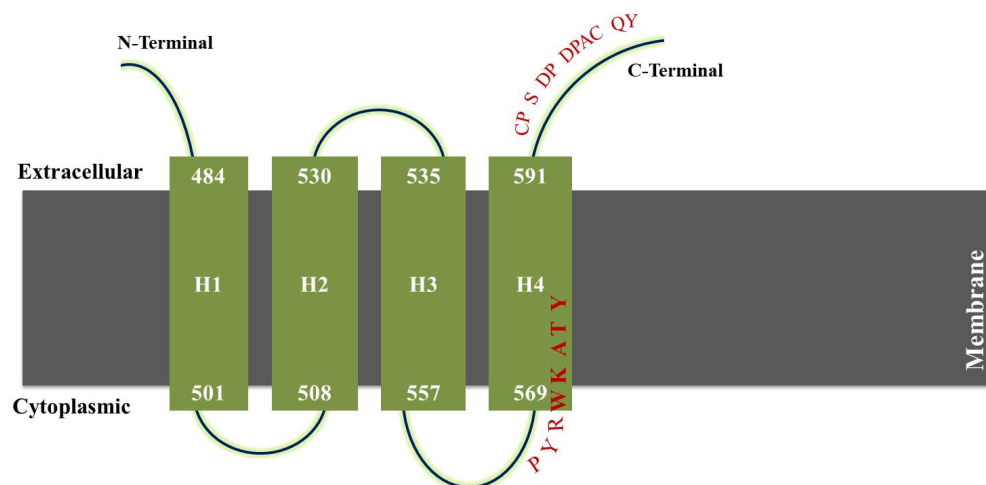


Figure 6.17 Predicted model for transmembrane domain analysis of putative ABC efflux transporter in SFL showing 4 transmembrane helix (TMH) with N and C terminals outside. Highly conserved residues identified during motif analysis are marked in red.

6.2.5 Phylogenetic analysis of putative Cr transporters:

To investigate potential evolutionary relationships, putative Cr transporter sequences were aligned using clustal omega and a phylogenetic tree was constructed using maximum likelihood (ML) method using MEGA version 6 (Tamura et al., 2013). After the analysis, the transporters from *A. flavus* clustered together with other *Aspergillus* species based on the sequence similarity between them (Figure 6.18a-d). In all cases, the transporters from *S. cerevisiae* and *A. thaliana* lay outside the cluster and appeared as outgroups. The value shown next to each branch indicates ML as a percentage (based on 1000 bootstraps) in which the associated taxa clustered together.

6.2.6 Gene expression analysis:

The fungal cells were grown for 48 h in potato dextrose broth. The biomass was then harvested and treated with 50 mg L⁻¹ and 100 mg L⁻¹ Cr (VI) for 1 h, 6 h, and 24 h. Gene expression analysis for all four putative Cr transporter genes was carried out

General Characteristics	Sulphate Uptake	ATM1	Hmt1	ABC efflux
A1120 (Reference strain)				
Putative name	Sulphate uptake transporter	ABC iron exporter	Vacuolar heavy metal transporter	ABC efflux transporter
Number of amino acids	813	545	929	1097
Number of TMD	8	4	10	7
Molecular Weight (Units)	89182.5	60260.4	103512.6	121564.1
Theoretical Pi	8.54	8.73	8.72	8.56
Extinction coefficient	94240	39560	143295	114305
Extinction coefficient *	93740	39310	142670	113680
SFL (Tolerant strain)				
Putative name	Sulphate permease 2	Iron sulphur cluster transporter	Vacuolar ABC transporter	Pleotropic drug resistant protein
Number of amino acids	605	710	547	625
Number of TMD	6	6	4	4
Molecular Weight (Units)	66472.9	78343.5	61216.5	69080.9
Theoretical Pi	8.59	9.14	6.58	6.09
Extinction coefficient	61560	53415	52175	65820
Extinction coefficient *	61310	53290	51800	65320

Table: 6.2 General characteristics of putative Cr transport proteins

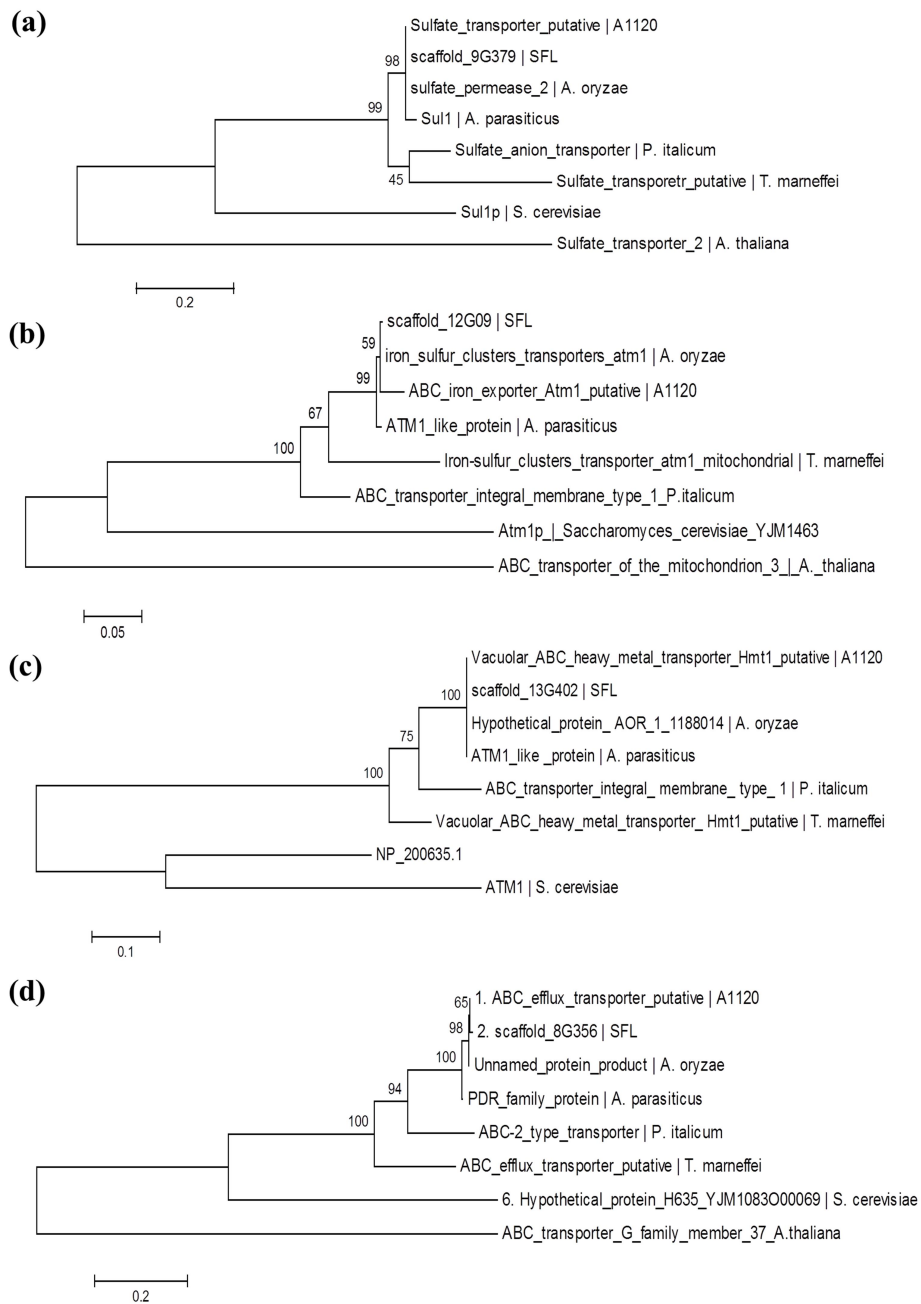


Figure 6.18 Molecular Phylogenetic analysis of putative Cr transporter by Maximum Likelihood method. The evolutionary history was inferred by using the Maximum Likelihood method based on the JTT matrix-based model. The percentage of trees in which the associated taxa clustered together is shown next to the branches. The tree is drawn to scale, with branch lengths measured in the number of substitutions per site. The analysis involved 8 amino acid sequences. All positions containing gaps and missing data were eliminated. Evolutionary analyses were conducted in MEGA6. (a) Phylogenetic tree of putative sulphate uptake transporter (b) phylogenetic tree of putative Atm1 transporter (c) phylogenetic tree of putative Hmt1 transporter (d) phylogenetic tree of putative ABC efflux transporters

using quantitative real time PCR and changes in relative mRNA expression was measured in control (not treated with Cr), SFL and A1120 strain. No template control reactions lacking template cDNA were negative for all analysed samples.

6.2.6.1 Sulphate uptake transporter: The expression of putative sulphate uptake transporter (SUT) was significantly upregulated in both SFL and A1120 strain after 1 h with relative expression of 3.5 and 1.5 folds of their respective controls (Figure 6.19a). After 6 h, the mRNA expression was significantly ($p < 0.05$) reduced to basal level i.e., control in both SFL and A1120 and remained unchanged till 24 h without significant change in expression (Figure 6.19a). With the increase in Cr (VI) concentration to 100 mg L^{-1} the mRNA expression level of SUT increased significantly ($p < 0.05$) by 6.6 folds and 2.6 folds after 1 h in SFL and A1120 strain respectively, compared to control (Figure 6.19b). After 6 h, the mRNA expression significantly ($p < 0.05$) downregulated below to control and remained unchanged and there was no significant change in the gene expression after 24 h in SFL where as in A1120 strain the expression level after reducing significantly below to control went slightly up after 24 h (Figure 6.19b). The expression pattern of putative SUT was similar for both strains at 50 mg L^{-1} and 100 mg L^{-1} Cr concentrations. However, the relative expression of sulphate transporter in SFL was approximately 2 folds (at 50 mg L^{-1}) and 4 folds (at 100 mg L^{-1}) higher than that of A1120 with probability values of: $p < 0.05$ to $p < 0.001$ at three treatment times i.e., 1 h, 6 h and 24 h.

6.2.6.2 ABC iron exporter, Atm1: The transcript level of putative Atm1 transporter in SFL was upregulated significantly ($p < 0.05$ to $p < 0.001$) after 50 mg L^{-1} Cr (VI) treatment, with relative mRNA expression of 1.7 folds, 2.1 folds and 2.7 folds after 1h, 6 h, and 24 h respectively, to that of control (Figure 6.20a). With the increase in

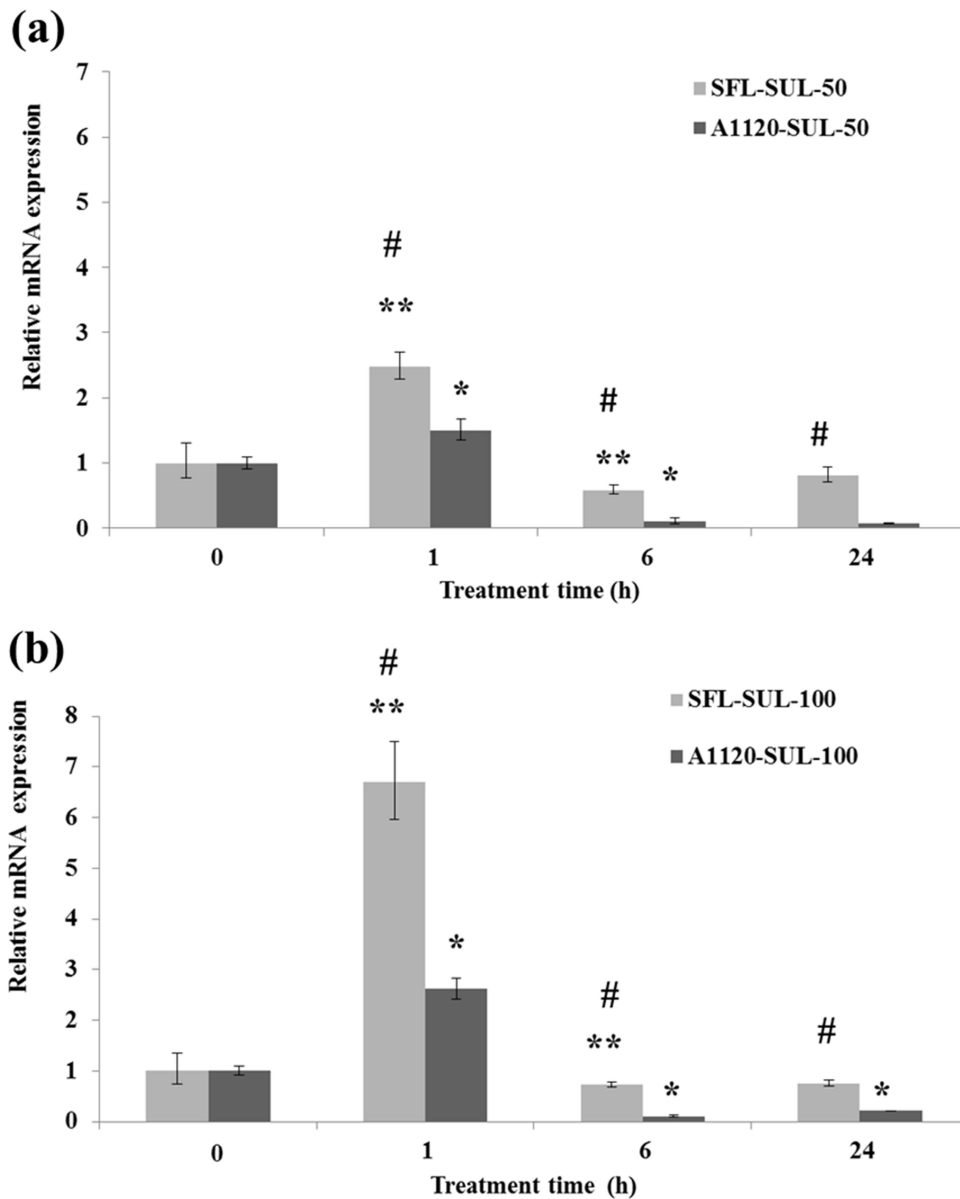


Figure 6.19 Relative mRNA expression levels for putative sulphate uptake transporter gene in response to 50 and 100 mg L⁻¹ Cr at time points of 0, 1, 6 and 24 hours. Real-time qPCR was used to detect differences in expression of the putative Cr transporter gene. Significant values (p<0.05 to p<0.001) for 1, 6 and 24 hour treatments compared with basal level in SFL and A1120 strain are denoted by asterisk (** and *) respectively. Significant differences (p<0.05 to p<0.001) in the relative mRNA expression between SFL and A1120 at each time point are denoted by hashtag (#). After 1 h exposure SUT was significantly (p<0.05) upregulated. After 6 h and 24 h the mRNA expression was significantly (p<0.05) reduced to basal level at both (a) at 50 mg L⁻¹ (b) at 100 mg L⁻¹

Cr (VI) concentration to 100 mg L⁻¹, the transcripts showed 5.57 fold, 6.59 fold and 11.27 fold increase after 1 h, 6 h and 24 h respectively, compared to that of control (Figure 6.20b). In contrast, in A1120, no significant ($p>0.05$) change in the mRNA expression was observed after Cr (VI) treatment at both 50 mg L⁻¹ and 100 mg L⁻¹ as compared to that of control (Figure 6.20a,b). The expression patterns of *Atm1* gene were significantly different in A1120 and SFL strain.

6.2.6.3 Vacuolar heavy metal transporter, *Hmt1*: For *Hmt1*, the mRNA expression level decreased significantly, in both A1120 and SFL, below to that of control ($p\leq 0.005$) after 1 h. After 6 h and the expression of *Hmt1* transporter further decreased significantly ($p<0.05$) and went slightly up but still remaining significantly below to basal level after 24 h in both SFL and A1120 strain at 50 and 100 mg L⁻¹ Cr treatment (Figure 6.21a,b). There was no significant difference in expression of putative *Hmt1* gene between SFL and A1120 strain.

6.2.6.4 ABC efflux transporter: The expression of putative ABC efflux transporter in SFL significantly decreased after 1 h of exposure in comparison to the control i.e., untreated or 0 h treated ($p<0.05$) and remained constant up to 6 h of exposure without any significant change ($p>0.05$) which reverted back to basal level i.e., control after 24 h of exposure (Figure 6.22a). In A1120 strain, the expression of putative ABC efflux transporter significantly decreased within 1 h of exposure ($p=0.007$) and remained unchanged thereafter at 6 h as well as 24 h (Figure 6.22a). There was no significant change in the mRNA expression level between SFL and A1120 strain initially at 1h ($p>0.05$) and 6 h ($p>0.05$) whereas after 24 h the expression of putative ABC efflux transporter was significantly lower in A1120 strain compared to SFL ($p<0.05$). When the Cr concentration was increased to 100

mg L⁻¹, the expression level of putative ABC efflux transporter in SFL strain decreased significantly below the control level after 1 h (p<0.05) and 6 h (p<0.05) (Figure 6.22b). After 24 h of exposure, the expression increased significantly above the control level (p<0.05). In A1120 the mRNA expression levels reduced significantly after 1 h (p<0.05) and 6 h (p<0.05) of Cr exposure as compared to the basal level and remained constant after 24 h (Figure 6.22b). Putative ABC efflux transporter expressed differentially in SFL and A1120. The differences in the expression levels were significant (p<0.05) at each treatment time.

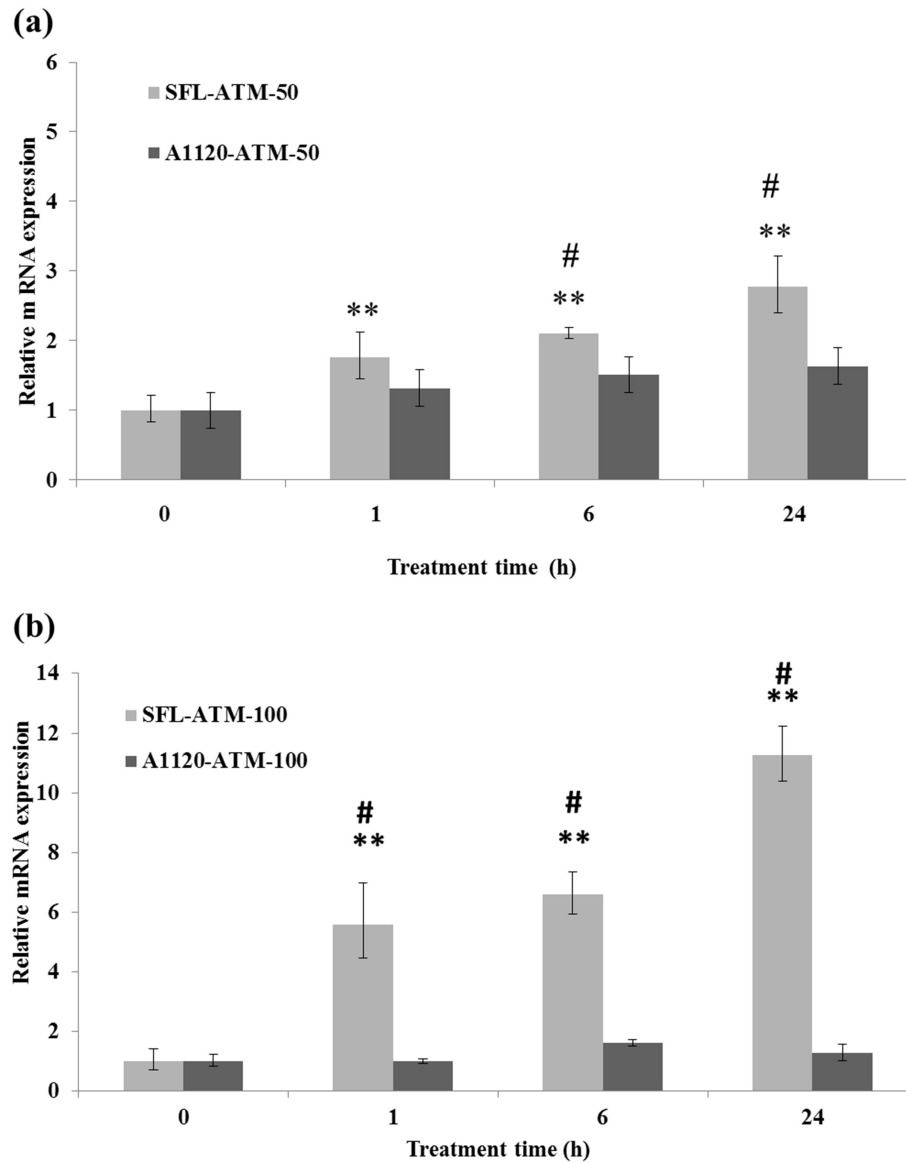


Figure 6.20 Relative mRNA expression levels for putative ABC iron exporter transporter, *Atm1* gene in response to 50 and 100 mg L⁻¹ Cr at time points of 0, 1, 6 and 24 hours. Real-time qPCR was used to detect differences in expression of the putative Cr transporter gene. Significant values ($p < 0.05$ to $p < 0.001$) for 1, 6 and 24 hour treatments compared with control level in SFL strain are denoted by asterisk (**). Significant differences ($p < 0.05$ to $p < 0.001$) in the relative mRNA expression between SFL and A1120 at each time point are denoted by hashtag (#). In SFL, *Atm1* was significantly upregulated after 1 h, 6 h and 24 h of Cr exposure in SFL. In A1120, *Atm1* expression level remained unchanged after Cr exposure (a) at 50 mg L⁻¹ (b) at 100 mg L⁻¹

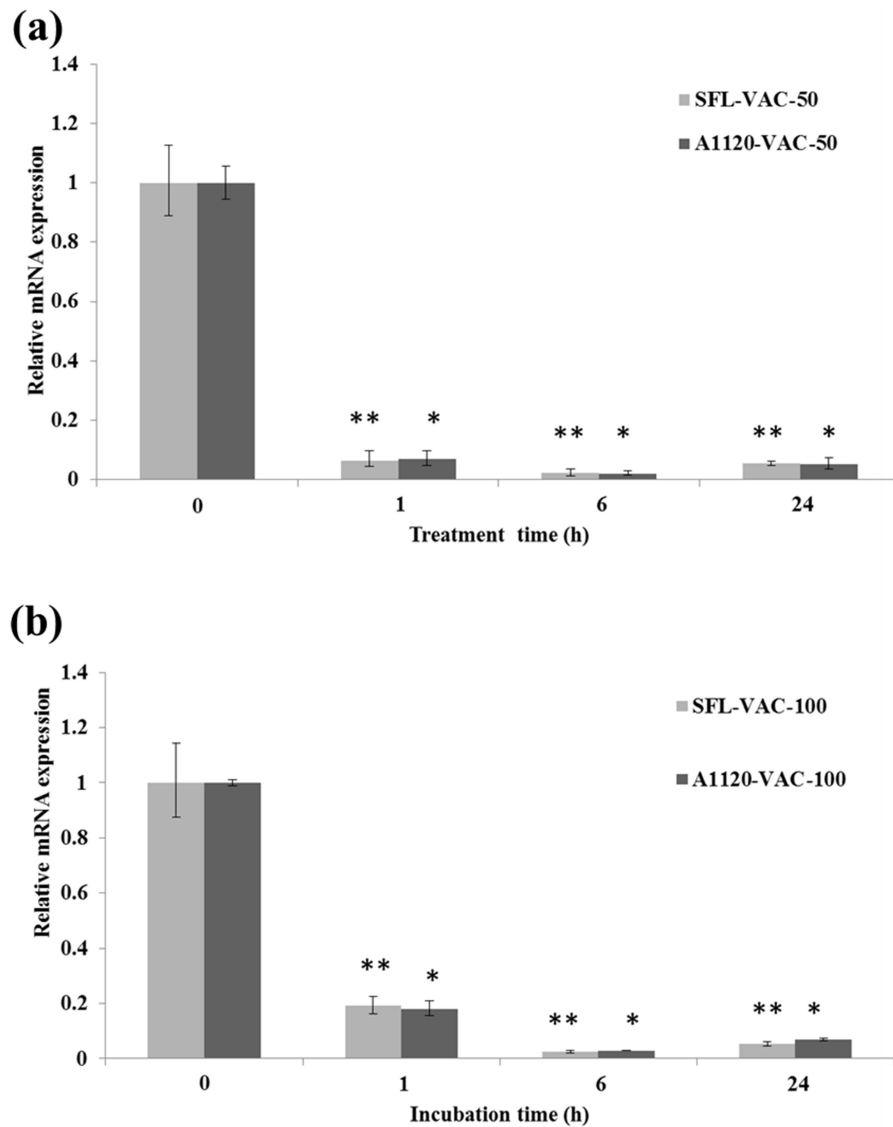


Figure 6.21 Relative mRNA expression levels for putative vacuolar heavy metal transporter, Hmt1 gene in response to 50 and 100 mg L⁻¹ Cr at time points of 0, 1, 6 and 24 hours (a) Real-time qPCR was used to detect differences in expression of the putative Cr transporter gene. Significant values (p<0.05 to p<0.001) for 1, 6 and 24 hour treatments compared with control level in SFL strain are denoted by asterisk (**) and (*) in A1120 strain respectively. Significant differences (p<0.05 to p<0.001) in the relative mRNA expression of putative Hmt1 transporter between A1120 and SFL at each time point are denoted by hashtag (#). The mRNA expression reduced significantly (p<0.05) after 1h, 6 h and 24 h of Cr exposure in both A1120 and SFL strain (a) at 50 mg L⁻¹ (b) at 100 mg L⁻¹

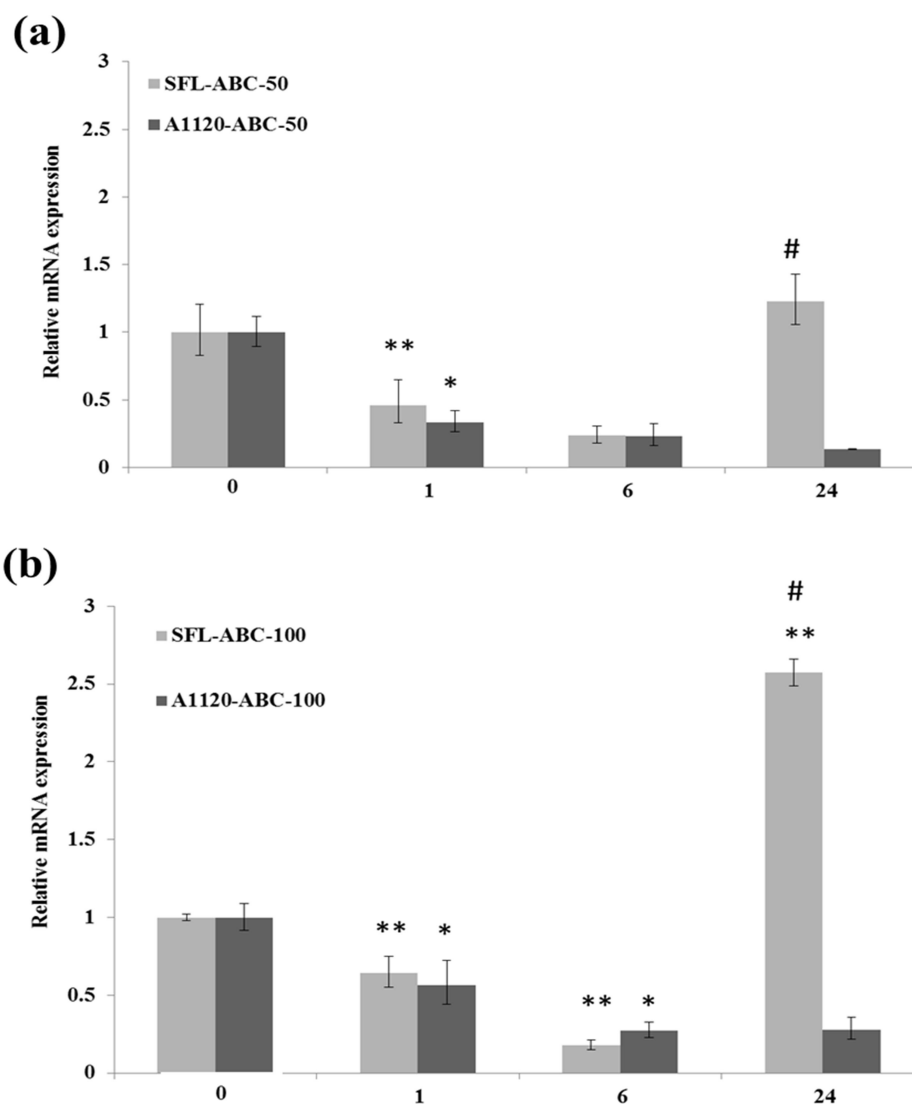


Figure 6.22 Relative mRNA expression levels for putative ABC efflux transporter gene in response to 50 and 100 mg L⁻¹ Cr at time points of 0, 1, 6 and 24 hours (a) Real-time qPCR was used to detect differences in expression of the putative Cr transporter gene. Significant values ($p < 0.05$ to $p < 0.001$) for 1, 6 and 24 hour treatments compared with control level in SFL strain are denoted by asterisk (**), (*) in A1120 strain respectively. Significant differences ($p < 0.05$ to $p < 0.001$) in the relative mRNA expression between SFL and A1120 at each time point are denoted by hashtag (#). In SFL at 50 mg L⁻¹, the expression of ABC efflux transporter decreased significantly ($p < 0.05$) below the basal level after 1 h. After 6 h, there was no significant change ($p > 0.05$) in expression. After 24 h, the mRNA expression significantly increased ($p < 0.05$) from 6 h but reverted back to basal level. In A1120, the mRNA expression decreased significantly ($p < 0.05$) after 1 h. At 100 mg L⁻¹ the mRNA expression was significantly reduced below the basal level after 1 h and 6 h. After 24 h, there was upregulation in gene expression significantly ($p < 0.05$) above the basal level. In A1120 the mRNA expression was significantly ($p < 0.05$) downregulated after Cr exposure at 1 h and 6h with no further change in expression (a) at 50 mg L⁻¹ (b) at 100 mg L⁻¹

6.3 Discussion:

The molecular mechanism of Cr tolerance and Cr transport in filamentous fungi remain unclear. Genes encoding metal uptake and efflux transporters may get expressed during Cr exposure in microorganisms and their differential expression may provide insights into the underlying molecular mechanism of Cr (VI) tolerance. To prove this hypothesis, four putative Cr uptake and efflux genes were identified (though there could be other genes present particularly in SFL strain that may also play a significant role in Cr tolerance), *insilico* analysis were performed for structural characterisation of these genes. The time course regulation of gene expression in *A. flavus* cells in response to exposure to 50 mg L⁻¹ and 100 mg L⁻¹ Cr (VI) was analysed in a non-tolerant and a Cr tolerant strain of *A. flavus*, A1120 and SFL, respectively accounting for their differences in function in relation to Cr toxicity.

Sequence similarity analysis of the putative A1120 and SFL (Scaffold_ 9G379) sulphate uptake transporter (SUT) revealed 99% similarity with sulphate permease 2 from *A. oryzae* RIB40. Two putative highly conserved domains were detected; a sulphate transporter domain belonging to SLC26A/SulP transporter family, transport commission no. 2.A.53 (Shibagaki and Grossman, 2006) towards the N terminal, is the transmembrane domain and a STAS (sulphate transporter and anti-sigma factor antagonist) SulP like sulphate transporter domain belonging to STAS superfamily, at the C-terminal region of SLC26/SulP transporters that extends into the cytoplasmic region of the cell (Shibagaki and Grossman, 2006). Proteins belonging to this large and ubiquitous SLC26A/SulP family are known to function as inorganic anion uptake transporters or anion: anion exchange transporters (Sandal and Marcker, 1994; Smith et al., 1995, Piłsyk and Paszewski, 2009). The STAS domain is a highly conserved region of sulphate transporter across different species from eubacteria to

humans. It has been reported that mutations in the STAS domain lead to several human diseases hinting towards the regulatory role of STAS domain (Babu et al., 2010). Deletion of whole STAS domain completely prohibited sulphate transport activity in *A. thaliana* (Rouached et al., 2005). A1120 is 813 aa (amino acid) long and is predicted to contain 8 TMH which is slightly different from the membrane topology of 10 to 14 TMH of other SulP family transporters (Alper and Sharma, 2013) whereas SFL SUT is 605 aa (amino acid) long predicted to possess 6TMH. TMH1 (93_{aa}-115_{aa}) and TMH2 (138_{aa}-160_{aa}) at the N-terminal end of A1120 sulphate transporter were not found in SFL sulphate transporter. This indicates a difference in membrane topology between SFL and A1120 SUT. The presence of extracellular charged residues might have important functional property in these transporters. The uptake of sulphate was inhibited by an arginine-binding reagent, phenylglyoxal (Clarkson et al., 1992). Hence these basic residues were expected to play a role in sulphate anion binding and channelling (Smith et al., 1995). An extracellular loop rich in positively charged arginine (R) residues was present in both A1120 (between TMH5 and TMH6) and SFL (between TMH3 and TMH4). Therefore it can be assumed that extracellular R^{286aa}, R^{287aa}, R^{291aa}, R^{300aa}, R^{313aa} in A1120 and R^{125aa}, R^{126aa}, R^{130aa}, R^{139aa}, R^{152aa}, R^{217aa}, R^{227aa}, R^{281aa} in SFL might play a role in binding of chromate anions. Further, substitution mutations of several amino acids including valine (V), phenylalanine (F), alanine (A), isoleucine (I), arginine (R) etc. present in the STAS domain were found to affect the transport activity and stability of these transporters in *S. cerevisiae* transformants of *A. thaliana* Sultr 1;2 gene and thus reported to play a critical role in the function and stability of sulphate transporters. In the present study apart from above mentioned (V, A, I, R) residues, histidine (H), tryptophan (W), lysine (K), and arginine (R) were found highly conserved (motif 1) across species in the STAS domain. Other

completely conserved amino acid residues within the transmembrane region were identified however their function with respect to Cr binding is not yet known. Hence it can be hypothesized that these residues might play a similar regulatory role during CrO_4^{2-} uptake in *A. flavus*. Upon exposure to Cr (VI), the expression of sulphate transporter was upregulated by 3.5 and 1.5 folds (at 50 mg L^{-1}) and 6.6 folds and 2.6 folds (at 100 mg L^{-1}) within 1 h in A1120 and SFL strain respectively, compared to the basal level (0 h). Higher expression of sulphate transporter in SFL indicates high Cr accumulation capacity of this strain as also observed in the Cr uptake study. By 6 h the expression is reduced below the basal level and remained unchanged up to 24 h. Thus, an increased expression of sulphate transporter gene in the presence of Cr (VI) results in enhanced Cr accumulation within 1 h of exposure. Reduction in transcript level after 6 h of Cr exposure may indicate activation of other regulatory mechanism to limit the excess accumulation of Cr into the cells. Similarly, upregulation of high-affinity sulphate transporter SHST1 in *Brassica juncea* has been reported to play a role in enhanced Cr uptake (Lindblom et al., 2006). Upregulation of sulphate ABC transporters after chromate exposure has also been reported in bacteria *Shewanella oneidensis* MR-1 (Brown et al., 2006), *Arthrobacter* sp. Strain FB24 (Henne et al., 2009). These observations confirm the hypothesis that chromate may be transported into the cytoplasm via sulphate transport system.

Sequence similarity analysis revealed ABC (ATP Binding Cassette) iron exporter, Atm1 from A1120 and SFL is homologous to iron-sulphur clusters transporter atm1 from *Aspergillus oryzae* RIB40. Sequence alignment showed highly conserved ABC membrane domain and ABCC ATM1 transporter domain (ATP-binding cassette domain of iron-sulphur clusters transporter, subfamily C; ATM1). ABC membrane domain is the transmembrane region (TMD) followed by ABCC ATM1 which is the nucleotide binding domain (NBD) containing the conserved Walker A

(GxxxxGK[S/T] where x is any residue) also known as nucleotide phosphate binding motif, the Walker B motif (hhhh[D/E], where h is a hydrophobic residue), ABC signature motif (LSGGQ) a characteristic feature of this family of transporters (Marchler-Bauer A et al., 2015, Walker et al., 1982, Higgins 1992). This suggests Atm1 is a half size ABC transporter with TMD-NBD configuration that might function as homodimer (Chloupkova et al., 2004). It may also function as heterodimer as described in yeast (Decottignies and Goffeau, 1997). In general, ATP binding cassette transporters constitutes a large group of integral membrane proteins, ubiquitously found in all organisms from bacteria to humans, that are involved in ATP dependent transport of various substrates/ligands including metals, inorganic ions, nutrients, sugars, chemotherapeutic drugs etc., across the cellular membrane (Linton, 2007, Piehler et al., 2012). Atm1 is expressed in the inner membrane of mitochondria that act as precursors of iron sulphur protein and is essential for maintaining iron homeostasis in mitochondria (Lill et al., 2012, Kispal et al., 1997). Membrane topology analysis revealed a slightly different topology in both A1120 and SFL Atm1, with A1120 Atm1 (545 aa long) predicted to possess 4 TMH with N and C terminal outside and SFL Atm1 (710 aa long) possessed 5 TMHs with N and C terminal outside, in comparison to the topology of half size ATM1 transporter having 6 TMH (Tusnády et al., 1997). TMH 1 (from 112_{aa}-142_{aa}) of SFL Atm1 was not found in A1120 Atm1. Insilco analysis showed the presence of completely conserved D^{162aa}, E^{168aa}, E^{176aa}, N^{166aa}, N^{174aa}, N^{175aa}, F^{173aa} (A1120) and D^{306aa}, E^{312aa}, E^{320aa}, N^{310aa}, N^{318aa}, N^{319aa} and F^{317aa} (SFL) in the transmembrane region that could be the potential Cr binding sites. Amino acids G, C, D, E and/or N are present in chromodulin, a low molecular weight chromium-binding peptide known to bind Cr (III) (Chen et al., 2011). Aromatic amino acid phenylalanine (F) is also known to complex with Cr (III) (Yang et al., 2005). Aromatic amino acids are

involved in electron transfer reactions (Xiao et al., 2014, Nunthaboot et al., 2016) therefore, may reduce Cr (VI) to Cr (III). The expression of *Atm1* gene was induced by Cr at both 50 mg L⁻¹ and 100 mg L⁻¹ in SFL strain with the highest level of expression at 24 h. The induction of mitochondrial *Atm1* gene by Cr (VI) with the increase in treatment time as well as concentration, suggests the increased need of the encoded protein with the increase in toxicity. *Atm1* proteins are implicated in heavy metal detoxification processes and mediate heavy metal resistance (Lee et al., 2014). Consistent with the present study, upregulation of *Cds1* gene encoding a mitochondrial half size ATM1 transporter by cadmium has been reported in *Chlamydomonas reinhardtii* (Hanikenne et al., 2005). Chromate reduction takes place in mitochondria with the involvement of electron transport chain. This process generates reactive intermediates like Cr (V) and/or Cr (IV) that contribute to Cr carcinogenicity (Rossi et al., 1988). Thus, an increased expression of mitochondrial *Atm1* might protect SFL from the deleterious effects of Cr by exporting the Cr from mitochondria to the cytosol and hence required for Cr tolerance in SFL. This cytosolic Cr is either exported out of the cell via efflux transporters or may form complex with the chelating compounds and transported to vacuoles. On the contrary, there was no change in expression of *Atm1* in A1120 indicating the inability of A1120 to detoxify Cr out of the mitochondria that probably cause mitochondrial dysfunction and induce cell death/cell lysis (Monaselidze et al., 2006). This suggests the sensitivity of A1120 to Cr (VI).

Sequence similarity analysis of vacuolar heavy metal transporter, *Hmt1* from A1120 and SFL showed 100 % similarity to unnamed protein product from *A. oryzae* and hypothetical protein AOR_1_1188014 from *A. oryzae* respectively. Multiple sequence alignment showed the presence of highly conserved ABC transmembrane domain followed by a nucleotide binding ABCC ATM1 transporter

domain (ATP-binding cassette domain of iron-sulphur clusters transporter, subfamily C; ATM1). This indicates Hmt1 is structurally related to Atm1 proteins (Mendoza-Cózatl et al., 2010, Iwaki et al., 2005), a half size ABC transporter. Membrane topology analysis observations indicated that A1120 Hmt1 possessed 10 TMHs with N and C terminal outside the cell. On the other hand, SFL Hmt1 possessed 4 TMH with N and C terminal outside the cell. TMH1 to TMH6 toward the N terminal region of A1120 Hmt1 were not found in SFL Hmt1 indicating structural differences between A1120 and SFL Hmt1, nonetheless TMH7, TMH8, TMH9 and TMH10 were identical to TMH1 to TMH4 and highly conserved that might impart similar functional property. In *Shizosaccharomyces pombe*, Hmt1 is known to confer cadmium (Cd) tolerance by transporting the cytosolic phytochelatin-Cd and glutathione-Cd complex to the vacuole (Preveral et al., 2009, Ortiz et al., 1995). It is likely that Hmt1 gene might be involved in vacuolar compartmentalisation of cytosolic Cr as a mode of Cr detoxification, however, when the responsiveness of Hmt1 gene was tested against Cr exposure, the expression of Hmt1 gene, was found to be reduced significantly below the basal level after 1 h and 6 h. There was a slight increase in expression after 24 h but with no significant change. This suggests that there is either no or a very slow sequestration of Cr to the vacuole by Hmt1 gene. This further indicates the need of a long term Cr exposure to completely understand the vacuolar sequestration phenomena. The proteins homologous to Hmt1 demonstrated Cd tolerance in different organisms from bacteria to humans (Preveral et al., 2009) including *Caenorhabditis elegans* (Vatamaniuk et al., 2005), *Chlamydomonas reinhardtii* (Hanikenne et al., 2001). Therefore, it can be concluded that Hmt1 gene may not be related to vacuolar compartmentalisation of Cr in *A. flavus*. A different detoxification mechanism/transporter gene might be involved in Cr tolerance in this fungus for

example, an ATPase. *S. cerevisiae* mutants lacking vacuolar (V)-H(+)-ATPase showed high sensitivity to tellurite and chromate (Gharieb and Gadd, 1998) displaying their potential role in Cr tolerance.

Sequence similarity analysis of the ABC efflux transporter from A1120 and SFL showed its closed similarity with pleotropic drug resistance PDR family protein from *A. parasiticus* SU-1. Putative domains, identified during the multiple sequence alignment analysis were found highly conserved across all the species. The P-loop NTPase domain (from 64_{aa}-285_{aa}) is the nucleotide binding domain (NBD) of ABC transporter and is characterised by the presence of conserved Walker A motif (GxxxxGK[S/T] where x is any residue) also known as nucleotide phosphate binding motif, the Walker B motif (hhhh[D/E], where h is a hydrophobic residue), ABC signature motif (LSGGQ), Q-loop, H-loop (Marchler-Bauer A et al., 2015). These conserved motifs are involved in ATP driven transport of substrate. Members of this family of proteins are involved in many different cellular functions including intracellular trafficking, membrane transport etc., (Aravind et al., 2004). ABC2 membrane domain from (376_{aa}-588_{aa}) is the transmembrane region of ABC2 type transporters (Marchler-Bauer A et al., 2015). Predicted membrane topology analysis revealed a reverse ABC transporter topology i.e., the domains are arranged in (NBD-TBD) manner which resembles the domain organisation of fungal pleotropic drug resistance (PDR) transporters (Lamping et al., 2010, Kovalchuk and Driessen, 2010). These observations suggest that ABC efflux transporter gene encodes a pleotropic drug resistance protein that might have a role in conferring resistance to Cr in *A. flavus*. Individual sequence analysis of each transporter showed that in A1120, two NBDs and two TMDs [(NBD-TMD)₂] were present and only one set was found to be highly conserved (NBD-TMD) where as in SFL only one conserved unit of each domain (NBD-TMD) was found. One set of NBD-TMD towards the C

terminal of A1120 transporter was not found in SFL indicating that A1120 ABC efflux transporter is a full size ABC transporter where as SFL ABC efflux transporter is a half molecule transporter that may function as homodimer of two half transporters (Higgins 2001, Piehler et al., 2012). A prototypic full size ABC transporter possess four core domains; two NBD and two TMD arranged in (TBD-NBD)₂ manner where each TMD is represented by 6 transmembrane helices (TMH) (Wilkins et al., 2015, Paumi et al., 2009). However, in A1120, the transmembrane domain prediction demonstrated the presence of 2 TMD each containing 5 and 2 transmembrane helices (TMH) [total 7 TMHs] where as in SFL one TMD with 4 TMHs were found.

Time dependent gene regulation studies showed the expression of ABC efflux transporter significantly reduced upon exposure to Cr after 1 h and 6 h in SFL at both 50 mg L⁻¹ and 100 mg L⁻¹. The initial decrease in expression of ABC efflux transporter indicates accumulation of Cr in the cell. At this stage, the uptake mechanism is activated and chromate may be accumulated inside the cell via the sulphate uptake transporter. After 24 h, the mRNA expression level of this efflux transporter reverted back to approximately the basal level at 50 mg L⁻¹ indicating efflux mechanism might get switched on. There is a possibility that beyond 24 h the expression goes further up in order to initiate the efflux process. However at 100 mg L⁻¹, expression of ABC transporter significantly increased above the basal level indicating the fungal cell start detoxifying process by exporting Cr out of the cell. In contrast to SFL, the expression of efflux transporter in A1120 significantly decreased throughout indicating that this efflux mechanism is not functioning in this strain. Despite higher expression of efflux transporter, SFL displayed higher Cr tolerance and accumulation than A1120. Although the SFL strain accumulates and tolerates Cr it may still need to efflux Cr from the cells in order to prevent toxicity.

A similar result to this was seen where high upregulation of a PDR like ABC transporter gene (Os07g33780) under Cr (VI) stress has been reported in rice root in spite of high Cr accumulation capacity (Dubey et al., 2010). Thus, instead of vacuolar storage Cr is expelled out of the cell by ABC transporter. The reason for the reduction in expression of the ABC efflux transporter in A1120 over 24 hours, both at 50 and 100 mg L⁻¹ is not clear, but it may be a toxicity effect.

To summarise, an increase in expression of sulphate uptake transporter mRNA in both SFL and A1120 strain suggests a potential role for these transporters in Cr accumulation. The data suggest that induction of mitochondrial *Atm1* gene may be a main defence mechanism identified in SFL, to confer tolerance to Cr by preventing mitochondrial damage. In contrast, in A1120, the *Atm1* gene was not active, which may confer Cr sensitivity via mitochondrial damage. Pleiotropic drug resistance ABC efflux transporter might play a role in effluxing Cr out of the cell.

The significant finding of this study was the increase in *Atm1* in SFL in response to Cr treatment, not seen in A1120. This may indicate that mitochondrial toxicity is an important consequence of Cr damage and that the tolerance to Cr shown by the SFL strain is due to its capacity to remove Cr from the mitochondria. However, apart from the four studied genes, there could be other genes as well that might play a role in conferring Cr tolerance in SFL strain. Based on all the observations a model of Cr tolerance mechanism is proposed in Cr tolerant SFL strain of *A. flavus* as described in the Figure 6.23.

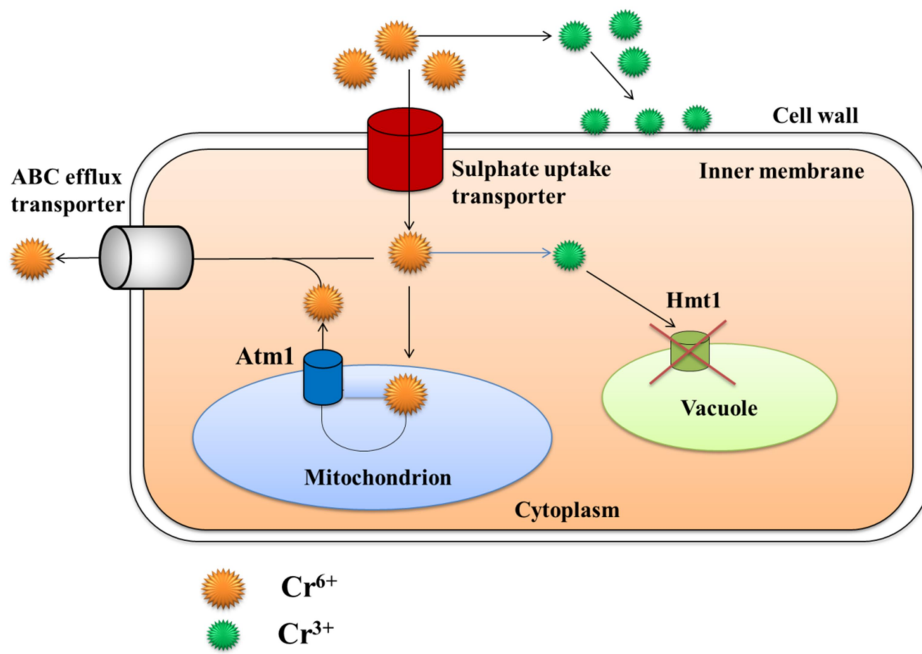


Figure 6.23 Schematic representation of Cr interaction mechanism in SFL strain of *A. flavus*.

CHAPTER 7

Summary and Conclusion

Microorganisms are known to develop tolerance to toxic metals under unfavourable conditions and adapt specific strategies for survival. The ability of microorganisms to tolerate and survive under toxic conditions makes them a potential tool for bioremediation purpose. The mechanisms of metal-microbe interaction play a key role in conferring tolerance to microorganisms.

During this study, the underlying mechanism of interactions of Cr with *A. flavus* was described and the processing of Cr at physiological, topographical and molecular level was compared in a Cr tolerant (SFL) and non-tolerant (A1120) strain of fungus. Divergent functioning of SFL and A1120 with respect to Cr processing was unveiled. The Cr tolerance study suggested that the SFL strain exhibits remarkably high tolerance over a broad range of Cr (VI) concentrations compared to A1120. The dose response study indicated that SFL strain grows and survives well at high Cr (VI) concentrations of 100 mg L⁻¹ whereas the growth of A1120 was impaired in the presence of Cr. The SFL strain was found to be more efficient in depleting Cr from the extracellular medium than A1120 and other reported *Aspergillus* species including *A. niger*, *A. parasiticus*, *A. foetidus* and *A. tubingensis*. The Cr depletion study also suggested that toxic Cr (VI) may be transformed to less toxic Cr (III) during the reduction process as seen by the diminished pale yellow colour of the medium and appearance of greenish colour indicative of Cr (III). The two strains demonstrated differences in Cr uptake mechanism. The tolerant SFL strain displayed metabolism dependent Cr (VI) uptake by sequestration of high Cr inside the cell. On the other hand A1120 showed

metabolism independent Cr adsorption. The decreased uptake of Cr in the presence of metabolic inhibitors confirmed that Cr uptake in the SFL strain is a metabolism driven energy dependent process.

By investigating the physico-chemical interactions between Cr and the fungal cell occurring at the cell surface it was established that the fungal cell surface plays a significant role during the interaction with Cr but there was no significant difference observed between SFL and A1120 strain. SEM-EDX analysis indicated the deposition of Cr on the hyphae as a result of Cr binding to the cell wall. TEM-EDX study further confirmed the localisation of Cr on the fungal cell surface. Intracellular localisation studies in bacteria and filamentous fungi to date have reported the presence of Cr in the cell cytoplasm. This study sheds light for the first time on Cr localisation in the intracellular membrane bound organelles like mitochondria. The different functional groups present on the fungal cell wall serve as binding site to Cr as revealed by FTIR analysis. The XPS study indicated the presence of only one form of Cr i.e., Cr (III) on the cell surface which further suggested prior to its aggregation on the cell surface Cr (VI) is reduced to Cr (III) in the extracellular medium in both SFL and A1120 strain. But at the cellular (proteomic) level, significant differences between SFL and A1120 were observed as suggested by the differential protein expression pattern during the proteomic analysis. With the existing information on the induction of (~25kDa and ~29kDa) protein possibly 'chromate reductase' in Cr treated A1120 and SFL strain and differential expression of (~35kDa) protein possibly 'glutathione synthetase' in A1120 and SFL, it may be assumed that these proteins may have a potential role in the chromate reduction (in both SFL and A1120 strains) and conferring Cr (VI) tolerance (in SFL) by protection against the oxidative damage. For a realistic conclusion, identification, characterisation and functional validation of proteins

expressed under Cr stress need to be examined and would be the area of future research.

The genetic response of A1120 and SFL strain was also studied for a better understanding of the Cr interaction mechanism. Gene regulation studies of short term Cr exposure suggested a potential role of sulphate uptake transporters in chromate uptake process in both SFL and A1120 strain. The main defence mechanism identified in SFL strain was the upregulation of *Atm1* gene, which may mediate Cr tolerance by protecting against the mitochondrial damage, as *Atm1* is known to be localised to mitochondria. Thus the activity of *Atm1* in the SFL strain suggests that the *Atm1* protein may help SFL cells to tolerate and survive at high Cr (VI) concentrations, by avoiding mitochondrial damage. This gene was non-responsive in A1120 after Cr exposures and thus confers chromate sensitivity by mitochondrial toxicity. In contrast to the proposed hypothesis, *Hmt1* gene was not found to be responsible for vacuolar sequestration of Cr, at least not during the short term exposures. ABC efflux transporter might play a role in exporting excessive Cr out of the cell in SFL strain after a certain degree of chromate accumulation may be after 24 h of Cr exposure. However, in A1120 the function of this gene is not completely understood during the study. For conclusive evidence further investigations are needed. The involvement of sulphate transporters in chromate accumulation can be validated by investigating the influence of sulphate anion on Cr uptake capacity of fungi by supplementing the media with sulphate anion. Another approach can be the generation of sulphate transporter knock out mutants and comparison of Cr uptake and reduction rates in the wild type and mutant strains. Similarly, the knock out studies with *Atm1* gene would give a definitive conclusion to its role in stress response to tolerate Cr (VI). To completely understand the function of *Hmt1* gene and ABC efflux genes, gene expression study with long term

Cr (VI) exposure (up to 72 h) is required. Further it would be interesting to study how these Cr tolerance genes are regulated, including analysis of the regulatory 5' regions of the genes and identification of conserved regulatory sequences such as metal binding domains.

Overall this study provided a basic understanding of Cr resistance mechanism in filamentous fungus *A. flavus* and confirms the hypothesis that Cr tolerant SFL strain possesses intrinsic defence mechanism (Cr resistant genes) for high Cr (VI) tolerance, reduction and intracellular accumulation. Overexpression of Cr tolerance genes may help in development of a novel strain best suitable for bioremediation purpose with enhanced Cr accumulation properties and this Cr hyperaccumulator strain may further be used for biomining purpose for the recovery of Cr in nanoform which may have potential applications in pharmaceutical industries. In this direction, further research is needed to explore the possibilities of Cr nanoparticle synthesis by SFL strain.

REFERENCES

Abbas, A., Al-Amer, A. M., Laoui, T., Al-Marri, M. J., Nasser, M. S., Khraisheh, M. and Atieh, M. A. (2016) Heavy metal removal from aqueous solution by advanced carbon nanotubes: Critical review of adsorption applications. *Sep Purif Technol* **157**, 141-161.

Acar, F.N. and Malkoc, E. (2004) The removal of chromium (VI) from aqueous solutions by *Fagus orientalis L.* *Bioresour Technol* **94**, 13–15.

Acevedo-Aguilar, F.J., Espino-Saldana, A.E., Leon-Rodriguez, I.L., Rivera-Cano, MaE., Avila-Rodriguez, M., Wrobel, K., Wrobel, K., Lappe, P., Ulloa, M. and Gutierrez- Corona, J.F. (2006) Hexavalent chromium removal in vitro and from industrial wastes, using chromate-resistant strains of filamentous fungi indigenous to contaminated wastes. *Can J Micro* **52**, 809-815.

Adams, D. J. (2004) Fungal cell wall chitinases and glucanases. *Microbiology* **150** (7), 2029-2035.

Agrawal, A., Kumar, V. and Pandey, B.D. (2006) Remediation options for the treatment of electroplating and leather tanning effluent containing chromium – a review. *Miner Process Extr Metall Rev* **27**, 99–130.

Ahalya, N., Ramachandra, T. V., and Kanamadi, R. D. (2003) Biosorption of heavy metals. *Res J Chem Environ* **7**(4), 71-79.

Ahluwalia, S.S. and Goyal, D. (2010) Removal of Cr (VI) from aqueous solution by fungal biomass. *Eng Life Sci* **10(5)**, 480–485.

Ahmad, A., Senapati, S., Khan, M. I., Kumar, R., Ramani, R., Srinivas, V. and Sastry, M. (2003) Intracellular synthesis of gold nanoparticles by a novel alkalotolerant actinomycete, *Rhodococcus species*. *Nanotechnology* **14(7)**, 824.

Aksu, Z., Sag, Y. and Kutsal, T. (1992) The biosorption of copper by *C. vulgaris* and *Z. ramigera*. *Environ Technol* **13(6)** 579-586.

Aksu, Z., Sag, Y. and Kutsal, T. (1992). The biosorption of copper by *C. vulgaris* and *Z. ramigera*. *Environ Technol* **13(6)**, 579-586.

Alper, S. L. and Sharma, A. K. (2013) The SLC26 gene family of anion transporters and channels. *Mol aspects Med* **34(2)**, 494-515.

Altaf, M. M., Masood, F. and Malik, A. (2008) Impact of long-term application of treated tannery effluents on the emergence of resistance traits in *Rhizobium* sp. isolated from *Trifolium alexandrinum*. *Turkish J Biol* **32**, 1–8.

Alvarez, A. H., Moreno-Sanchez, R. and Cervantes, C. (1999) Chromate efflux by means of the ChrA chromate resistance protein from *Pseudomonas aeruginosa*. *J. Bacteriol* **181**, 7398–7400.

Alvarez, A., Saez, J.M., Costa, J.S.D., Colin, V.L., Fuentes, M.S., Cuozzo, S.A., Benimeli, C.S., Polti, M.A. and Amoroso, M.J. (2017) Actinobacteria: Current

research and perspectives for bioremediation of pesticides and heavy metals. *Chemosphere* **166**, 41-62.

Apte, A.D., Verma, S., Tare, V. and Bose, P. (2005) Oxidation of Cr (III) in tannery sludge to Cr (VI): Field observations and theoretical assessment. *J Hazard Mater* **121**, 215-222.

Arakawa, H., Weng, M. W., Chen, W. C. and Tang, M. S. (2012) Chromium (VI) induces both bulky DNA adducts and oxidative DNA damage at adenines and guanines in the p53 gene of human lung cells. *Carcinogenesis* **33(10)**, 1993-2000.

Aravind, L., Iyer, L. M., Leipe, D. D. and Koonin, E. V. (2004) A novel family of P-loop NTPases with an unusual phyletic distribution and transmembrane segments inserted within the NTPase domain. *Genome biology* **5(5)**, 1.

Aron Marchler-Bauer, A., Derbyshire, M.K., Gonzales, N.R., Shennan, L., Chitsaz, F., Geer, L.Y., Geer, R.C., He, J., Gwadz, M., Hurwitz, D. I., Lanczycki, C.J., Lu, F., Marchler, G.H., Song, J.S., Thanki, N., Wang, Z., Yamashita, R.A., Zhang, D., Zheng, C. and Bryant, S.H. (2015) CDD: NCBI's conserved domain database *Nucl Acids Res* **43 (D1)**, D222-D226.

ATSDR September (2008) Draft toxicological profile for chromium, U.S. Department of Health and Human Services, Public Health Service, Agency for Toxic Substances and Disease Registry. <http://www.atsdr.cdc.gov/toxprofiles/tp7.pdf>.

Aziz, H.A., Adlan, M.N. and Ariffin, K.S. (2008) Heavy metals (Cd, Pb, Zn, Ni, Cu and Cr (III)) removal from water in Malaysia: post treatment by high quality limestone. *Bioresour Technol* **99**, 1578–1583.

Babu, M., Greenblatt, J. F., Emili, A., Strynadka, N. C., Reithmeier, R. A. and Moraes, T. F. (2010) Structure of a SLC26 anion transporter STAS domain in complex with acyl carrier protein: implications for *E. coli* YchM in fatty acid metabolism. *Structure* **18(11)**, 1450-1462.

Bahafid, W., Tahri Joutey, N., Sayel, H., Boularab, I. and El Ghachtouli, N. (2013) Bioaugmentation of chromium-polluted soil microcosms with *Candida tropicalis* diminishes phytoavailable chromium. *J Appl Microbiol* **115(3)**, 727-734.

Bai, R.S., Abraham, T.E., (2001) Biosorption of Cr (VI) from aqueous solution by *Rhizopus nigricans*. *Bioresour Technol* **79**, 73–78.

Bailey, T. L., Boden, M., Buske, F. A., Frith, M., Grant, C. E., Clementi, L., Ren, J., Li, W.W. and Noble, W. S. (2009). MEME SUITE: tools for motif discovery and searching. *Nucleic acids research*, gkp335.

Belchik, S. M., Kennedy, D. W., Dohnalkova, A. C., Wang, Y., Sevinc, P. C., Wu, H., Lin, Y., Lu, H.P., Fredrickson, J.K. and Shi, L. (2011) Extracellular reduction of hexavalent chromium by cytochromes MtrC and OmcA of *Shewanella oneidensis* MR-1. *Appl Environ Microbiol* **77(12)**, 4035-4041.

Beyersmann, D. and Hartwig, A. (2008) Carcinogenic metal compounds: Recent insight into molecular and cellular mechanisms. *Arch. Toxicol* **82(8)**, 493–512.

Biesinger, M. C., Payne, B. P., Grosvenor, A. P., Lau, L. W., Gerson, A. R. and Smart, R. S. C. (2011) Resolving surface chemical states in XPS analysis of first row transition metals, oxides and hydroxides: Cr, Mn, Fe, Co and Ni. *Appl Surf Sci* **257(7)**, 2717-2730.

Blackwell, M. (2011) The Fungi: 1, 2, 3... 5.1 million species? *American J Bot* **98(3)**, 426-438.

Bopp, L. H., Chakrabarty, A. M. and Ehrlich, H. L. (1983) Chromate resistance plasmid in *Pseudomonas fluorescens*. *J. Bacteriol.* **155**, 1105–1109.

Bowman, S. M. and Free, S. J. (2006) The structure and synthesis of the fungal cell wall. *Bioessays*, **28(8)**, 799-808.

Bridgewater, L.C., Manning, F.C., Woo, E.S. and Patierno, S.R. (1994) DNA polymerase arrest by adducted trivalent chromium. *Mol. Carcino* **9**, 122–133.

Brilly, M., Jamnik, B. and Drobne, D. (2003) Chromium contamination of the Ljubijansko Poije aquifer. *RMZ-Mat Geo Environ* **50(1)**, 71-74.

Brown, S. D., Thompson, M. R., VerBerkmoes, N. C., Chourey, K., Shah, M., Zhou, J., Hettich, R.L. and Thompson, D. K. (2006) Molecular dynamics of the *Shewanella oneidensis* response to chromate stress. *Mol Cell Proteomics* **5(6)**, 1054-1071.

Camargo, F.A.O., Okeke, B.C., Bento, F.M. and Frankenberger, W.T. (2003) In vitro reduction of hexavalent chromium by a cell-free extracts of *Bacillus sp.* ES 29 stimulated by Cu^{2+} . *Appl Microbiol Biotechnol* **62**, 569-573.

Cefalu, W. T. and Hu, F. B. (2004) Role of chromium in human health and in diabetes. *Diabetes Care* **27(11)**, 2741-2751.

Cerbasi, I.H. and Yetis, U. (2001) Biosorption of Ni (ii) and Pb (ii) by *Phanerochaete chrysosporium* from binary metal system – Kinetics. *Water Res* **27**, 15–20.

Cervantes, C. and Ohtake, H. (1988) Plasmid-determined resistance to chromate in *Pseudomonas aeruginosa*. *FEMS Microbiol Lett* **56**, 173–176.

Cervantes, C., Campos-García, J., Devars, S., Gutiérrez-Corona, F., Loza-Tavera, H., Torres-Guzmán, J. C. and Moreno-Sánchez, R. (2001) Interactions of chromium with microorganisms and plants. *FEMS Microbiol Rev* **25(3)**, 335-347.

Cervantes, C., Ohtake, H., Chu L., Misra, T. K. and Silver, S. (1990) Cloning, nucleotide sequence, and expression of the chromate resistance determinant of *Pseudomonas aeruginosa* plasmid pUM505. *J Bacteriol* **172**, 287–291.

Chang, F., Tian, C., Liu, S. and Ni, J. (2016) Discrepant hexavalent chromium tolerance and detoxification by two strains of *Trichoderma asperellum* with high homology. *Chem Eng J* **298**, 75-81.

Chang, K. S., Won, J. I., Lee, M. R., Lee, C. E., Kim, K. H., Park, K. Y., Kim, S.K., Lee, J.S. and Hwang, S. (2003) The putative transcriptional activator MSN1 promotes chromium accumulation in *Saccharomyces cerevisiae*. *Mol Cells* **16(3)**, 291-296.

Chatterjee, S., Chatterjee, N. C. and Dutta, S. (2012) Bioreduction of chromium (VI) to chromium (III) by a novel yeast strain *Rhodotorula mucilaginosa* (MTCC 9315) *Afr J Biotechnol*, **11(83)**, 14920-14929.

Chen, G.H. (2004) Electrochemicals technologies in wastewater treatment. *Sep Purif Technol* **38 (1)**, 11–41.

Chen, Y., Watson, H. M., Gao, J., Sinha, S. H., Cassady, C. J. and Vincent, J. B. (2011) Characterization of the organic component of low-molecular-weight chromium-binding substance and its binding of chromium. *J Nutr* **141(7)**, 1225-1232.

Cheng, Y., Xie, Y., Zheng, J., Wu, Z., Chen, Z., Ma, X., Li, B. and Lin, Z. (2009) Identification and characterization of the chromium(VI) responding protein from a newly isolated *Ochrobactrum anthropi* CTS-325. *J Environ Sci* **21**, 1673–1678.

Chloupková, M., Reaves, S. K., LeBard, L. M. and Koeller, D. M. (2004) The mitochondrial ABC transporter Atm1p functions as a homodimer. *FEBS Lett* **569(1-3)**, 65-69.

Chourey, K., Thompson, M. R., Morrell-Falvey, J., VerBerkmoes, N. C., Brown, S. D., Shah, M., Zhou, J., Doktycz, M., Hettich, R.L. and Thompson, D. K. (2006) Global molecular and morphological effects of 24-hour chromium (VI) exposure on *Shewanella oneidensis* MR-1. *Appl Environ Microbiol* **72(9)**, 6331-6344.

Clarkson, D. T., Hawkesford, M. J., Davidian, J. C. and Grignon, C. (1992) Contrasting responses of sulphate and phosphate transport in barley (*Hordeum vulgare* L.) roots to protein-modifying reagents and inhibition of protein synthesis. *Planta* **187(3)**, 306-314.

Clemens, S. (2001) Molecular mechanisms of plant metal tolerance and homeostasis. *Planta* **212**, 475–486.

Codd, R., Rillon, C.T., Levina, A. and Lay, P.A. (2001) Studies on the genotoxicity of chromium: from the test tube to the cell. *Coord Chem Rev* **216**, 217 537–582.

Congeevaram S., Dhanarani, S., Park, J., Dexilin, M., Thamaraiselvi, K. (2007) Biosorption of chromium and nickel by heavy metal resistant fungal and bacterial isolates. *J Haz Mat* **146**, 270–277.

Coreño-Alonso, A., Sole, A. Diestra, E., Esteve, I., Gutiérrez-Corona, J.F., Reyna López, G.E., Fernández, F.J., Tomasini, A. (2014) Mechanisms of interaction of chromium with *Aspergillus niger* var *tubingensis* strain Ed8. *Bioresour Technol* **158**, 188–192.

Corradi, M.G. and Gorbi, G. (1993) Chromium toxicity on two linked trophic levels. II Morphophysiological effects on *Scenedesmus acutus*. *Ecotoxicol Environ Saf* **25**, 72-78.

Corradi, M.G., Gorbi, G. and Bassi, M. (1995a) Hexavalent chromium induces gametogenesis in the freshwater algae *Scenedesmus acutus*. *Ecotoxicol Environ Saf* **30**, 106-110.

Corradi, M.G., Gorbi, G., Ricci, A., Torelli, A. and Bassi, A.M. (1995b) Chromium-induced sexual reproduction gives rise to a Cr-tolerant progeny in *Scenedesmus acutus*. *Ecotoxicol Environ Saf* **32**, 12-18.

Costa M. (2003) Potential hazards of hexavalent chromium in our drinking water. *Toxicol Appl Pharm* **188** 1-5.

CPCB. (2000)-(2001) Environmental standards for Ambient air, automobiles, fuels, industries and noise. Pollution Control Law Series, PCLS/4/(2000)-(2001), Published by Central Pollution Control Board, New Delhi.

Cui, X., Wang, Y., Liu, J., Chang, M., Zhao, Y., Zhou, S. and Zhuang, L. (2015) *Bacillus dabaoshanensis* sp. nov., a Cr (VI)-tolerant bacterium isolated from heavy-metal-contaminated soil. *Arch Microbiol* **197(4)**, 513-520.

Czakó-Vér, K., Batiè, M., Raspor, P., Sipiczki, M. and Pesti, M. (1999) Hexavalent chromium uptake by sensitive and tolerant mutants of *Schizosaccharomyces pombe*. *FEMS microbiology letters* **178(1)**, 109-115.

D'ors, A., Cortés, A. A., Sánchez-Fortún, A., Bartolomé, M. C. and Sánchez-Fortún, S. (2016) Interference of heavy metals on the photosynthetic response from a Cr (VI)-resistant *Dictyosphaerium chlorelloides* strain. *Ecotoxicology*, **25(1)**, 15-21.

Das, S. K. and Guha, A. K. (2009) Biosorption of hexavalent chromium by *Termitomyces clypeatus* biomass: kinetics and transmission electron microscopic study. *J Hazard Mater* **167(1)**, 685-691.

Das, S. K., Das, A. R. and Guha, A. K. (2007) A study on the adsorption mechanism of mercury on *Aspergillus versicolor* biomass. *Environ Sci Technol* **41(24)**, 8281-8287.

Das, S. K., Mukherjee, M. and Guha, A. K. (2008) Interaction of chromium with resistant strain *Aspergillus versicolor*: investigation with atomic force microscopy and other physical studies. *Langmuir* **24(16)**, 8643-8650.

Das, S.K., Mukherjee, Das, A.R., M., Guha, A.K. (2009) Structural and Nanomechanical Properties of *Termitomyces clypeatus* Cell Wall and Its Interaction with Chromium (VI) *J Phys Chem B* **113**, 1485–1492.

Dayan, A. D. and Paine, A. J. (2001) Mechanisms of chromium toxicity, carcinogenicity and allergenicity: Review of the literature from 1985 to (2000) *Hum Exp Toxicol* **20**, 439–451.

Decottignies, A. and Goffeau, A. (1997) Complete inventory of the yeast ABC proteins. *Nature Genet* **15**, 137-145.

Deepa, K. K., Sathishkumar, M., Binupriya, A. R., Murugesan, G. S., Swaminathan, K. and Yun, S. E. (2006) Sorption of Cr (VI) from dilute solutions and wastewater by live and pretreated biomass of *Aspergillus flavus*. *Chemosphere* **62(5)** 833-840.

Deng, L., Zhang, Y., Qin, J., Wang, X. and Zhu, X. (2009) Biosorption of Cr (VI) from aqueous solutions by nonliving green algae *Cladophora albida*. *Miner Eng* **22(4)**, 372-377.

Desai, C., Jain, K. and Madamwar, D. (2008) Hexavalent chromate reductase activity in cytosolic fractions of *Pseudomonas sp.* G1DM21 isolated from Cr (VI) contaminated industrial landfill. *Process Biochem* **43(7)**, 713–721.

Dhakate, R., Singh V. and Hodlur, G. (2008) Impact Assessment of Chromite Mining on Groundwater through Simulation Modeling Study in Sukinda Chromite Mining Area, Orissa, India. *J Hazard Mater* **160 (2-3)** 535-47.

Dhankhar, R. and Hooda, A. (2011) Fungal biosorption—an alternative to meet the challenges of heavy metal pollution in aqueous solutions. *Environ Technol* **32(5)**, 467-491.

Díaz-Pérez, C., Cervantes, C., Campos-García, J., Julián-Sánchez, A. and Riveros-Rosas, H. (2007) Phylogenetic analysis of the chromate ion transporter (CHR) superfamily. *FEBS J* **274**(23), 6215-6227.

Dubey, S., Misra, P., Dwivedi, S., Chatterjee, S., Bag, S. K., Mantri, S., Asif, M.H., Rai, A., Kumar, S., Shri, M. and Tripathi, P. (2010) Transcriptomic and metabolomic shifts in rice roots in response to Cr (VI) stress. *BMC genomics* **11**(1), 1.

Ezzouhri L., Castro, E., Moya, M., Espinola, F. and Lairini, K., 2009. Heavy metal tolerance of filamentous fungi isolated from polluted sites in Tangier, Morocco. *Afr J Microbiol Res* **3**(2) 035-048

Fasulo, M.P., Bassi, M. and Donini, A. (1983) Cytotoxic effects of hexavalent chromium in *Euglena gracilis*. II. Physiological and ultrastructural studies. *Protoplasma* **114**, 35-43.

Fedorovych, D. V., Gonchar, M. V., Ksheminska, H. P., Prokopiv, T. M., Nechay, H. I., Kaszycki, P., Koloczek, H. and Sibirny, A. A. (2009) Mechanisms of chromate detoxification in yeasts. *Microbiol Biotechnol*, **3**, 15-21.

Festa, R. A. and Thiele, D. J. (2011) Copper: an essential metal in biology. *Curr Biol* **21**(21), R877-R883.

Filipović-Kovačević, Ž., Sipos, L. and Briški, F. (2000) Biosorption of chromium, copper, nickel and zinc ions onto fungal pellets of *Aspergillus niger* 405 from aqueous solutions. *Food Technol Biotechnol* **38(3)**, 211-216.

Francisco, R., Moreno, A. and Vasconcelos, Morais, P (2010) Different physiological responses to chromate and dichromate in the chromium resistant and reducing strain *Ochrobactrum tritici* 5bv11. *Biometals* **23** 713-725.

Fu, F. and Wang, Q. (2011) Removal of heavy metal ions from wastewaters: a review. *J Environ Manage* **92(3)**, 407-418.

Fukuda, T., Ishino, Y., Ogawa, A., Tsutsumi, K. and Morita, H. (2008) Cr(VI) reduction from contaminated soils by *Aspergillus sp.* N2 and *Penicillium sp.* N3 isolated from chromium deposits. *J Gen Appl Microbiol* **54**, 295-303.

Gadd, G. M. (Ed.) (2001) *Fungi in bioremediation* (**23**) Cambridge University Press.

Gadd, G. M. and White, C. (1989) Uptake and intracellular compartmentation of thorium in *Saccharomyces cerevisiae*. *Environ Pollut* **61(3)**, 187-197.

Ganguli A. and Tripathi A. K. (2002) Bioremediation of toxic chromium from electroplating effluents by chromate-reducing *Pseudomonas aeruginosa* A2Chr in two bioreactors. *Appl Microbiol and Biotechnol* **58**: 416–420.

Gao, Y. and Xia, J. (2011) Chromium contamination accident in China: Viewing environment policy of China. *Environ Sci Technol* **45**, 8605–8606.

Garg, S.K., Tripathi, M., Singh, S.K. and Singh, A. (2013) Pentachlorophenol dechlorination and simultaneous Cr⁶⁺ reduction by *Pseudomonas putida* SKG-1 MTCC (10510): characterization of PCP dechlorination products, bacterial structure, and functional groups. *Environ Sci Poll Res* **20(4)**, 2288-2304.

Gazdag, Z., Pócsi, I., Belágyi, J., Emri, T., Blaskó, Á., Takács, K. and Pesti, M. (2003) Chromate tolerance caused by reduced hydroxyl radical production and decreased glutathione reductase activity in *Schizosaccharomyces pombe*. *J Basic Microbiol* **43(2)**, 96-103.

Gharieb, M. M. and Gadd, G. M. (1998) Evidence for the involvement of vacuolar activity in metal (loid) tolerance: vacuolar-lacking and-defective mutants of *Saccharomyces cerevisiae* display higher sensitivity to chromate, tellurite and selenite. *Biometals* **11(2)**, 101-106.

Gorbi, G., Corradi, M.G., Torelli, A. and Bassi, M. (1996) Comparison between a normal and a Cr-tolerant strain of *Scenedesmus acutus* as a source food to *Daphnia magna*. *Ecotoxicol Environ Saf* **35**, 109-111.

Gouda, M.K., 2000. Studies on chromate reduction by three *Aspergillus species*. *Fresen Environ Bull* **9**, 799–808.

Gow, N.A.R., Gadd, G.M., 1995. *The Growing Fungus*, 1st ed. Chapman and Hall, London, UK.

Greenberg, A.D., Connors, J.J., Jenkins, D., Franson, M.A. (1981) Standard methods for the examination of water and wastewater, 15th ed. American Public Health Association, Washington, D.C.

Gu, Y., Xu, W., Liu, Y., Zeng, G., Huang, J., Tan, X., Jian, H., Hu, X., Li, F. and Wang, D. (2015) Mechanism of Cr (VI) reduction by *Aspergillus niger*: enzymatic characteristic, oxidative stress response, and reduction product. *Environ Sci Pollut Res* **22**, 6271–6279.

Gupta, V. K., Shrivastava, A. K. and Jain, N. (2001) Biosorption of chromium (VI) from aqueous solutions by green algae *Spirogyra* species. *Water Res* **35(17)**, 4079-4085.

Habi, S. and Daba, H. (2009) Plasmid incidence, antibiotic and metal resistance among enterobacteriaceae isolated from Algerian streams. *Pak J Biol Sci* **12(22)**, 1474-1482.

Han, X., Wong, Y. S., Wong, M. H. and Tam, N. F. Y. (2007) Biosorption and bioreduction of Cr (VI) by a microalgal isolate, *Chlorella miniata*. *J Hazard Mater* **146(1)**, 65-72.

Hanikenne, M., Motte, P., Wu, M. C. S., Wang, T., Loppes, R. and Matagne, R. F. (2005) A mitochondrial half-size ABC transporter is involved in cadmium tolerance in *Chlamydomonas reinhardtii*. *Plant Cell Environ* **28**(7), 863-873.

Hanikenne, M., Matagne, R. F. and Loppes, R. (2001) Pleiotropic mutants hypersensitive to heavy metals and to oxidative stress in *Chlamydomonas reinhardtii*. *FEMS Microbiol Lett* **196**,107–111.

He, Z., Hu, Y., Yin, Z., Hu, Y. and Zhong, H. (2016) Microbial Diversity of Chromium-Contaminated Soils and Characterization of Six Chromium-Removing Bacteria. *Environ Manage* **57**(6), 1319-1328.

Hedayati, M.T., Pasqualotto, A.C., Warn, P.A., Bowyer, P. and Denning, D.W. (2007) *Aspergillus flavus*: human pathogen, allergen and mycotoxin producer. *Microbiol* **153**(6), 1677-1692.

Henne, K. L., Turse, J. E., Nicora, C. D., Lipton, M. S., Tollaksen, S. L., Lindberg, C., Babnigg, G., Giometti, C.S., Nakatsu, C.H., Thompson, D.K. and Konopka, A. E. (2009) Global proteomic analysis of the chromate response in *Arthrobacter sp.* strain FB24. *J Proteome Res* **8**(4), 1704-1716.

Hibbett, D.S. and Taylor, J.W. (2013) Fungal systematics: is a new age of enlightenment at hand?. *Nature Rev Microbiol* **11**(2), 129-133.

Higgins, C. F. (2001) ABC transporters: physiology, structure and mechanism—an overview. *Res Microbiol* **152**(3), 205-210.

Higgins, C.F. (1992) ABC transporters: from microorganisms to man. *Ann Rev Cell Biol* **8**, 67-113.

Higgins, D. G. and Sharp, P. M. (1988) "Clustal: A package for performing multiple sequence alignment on microcomputer." *Gene* **73**, 273-244.

Hlihor, R.M., Figueiredo, H., Tavares, T. and Gavrilescu, M. (2016) Biosorption potential of dead and living *Arthrobacter viscosus* biomass in the removal of Cr (VI): Batch and column studies. *Process Saf Environ*.

Ilias, M., Rafiqullah, I.M., Debnath, B.C., Mannan, K.S.B. and Hoq, M. M. (2011) Isolation and characterization of chromium (VI)-reducing bacteria from tannery effluents. *Indian J Microbiol* **51**, 76–81.

Iram, S., Zaman, A., Iqbal, Z. and Shabbir, R. (2013) Heavy metal tolerance of fungus isolated from soil contaminated with sewage and industrial wastewater. *Pol J Environ Stud* **22(3)**, 691-697.

Iwaki, T., Fujita, Y., Tanaka, N., GIGA-HAMA, Y. and TAKEGAWA, K. (2005) Mitochondrial ABC transporter Atm1p is required for protection against oxidative stress and vacuolar functions in *Schizosaccharomyces pombe*. *Biosci Biotechnol Biochem* **69(11)**, 2109-2116.

Jain. P., Amatullah, A., Alam Rajib, S. and Mahmud Reza, H. (2012) Antibiotic resistance and chromium reduction pattern among Actinomycetes. *American J Biochem Biotech* **8** 111-117.

James, B.R. (2002) Chemical transformations of chromium in soils relevance to mobility, bioavailability and remediation. *The Chromium File* 8.

Joutey, N. T., Sayel, H., Bahafid, W. and El Ghachtouli, N. (2015) Mechanisms of hexavalent chromium resistance and removal by microorganisms. In *Reviews of Environmental Contamination and Toxicology* **233**, 45-69. Springer International Publishing.

Jozefczak, M., Remans, T., Vangronsveld, J. and Cuypers, A. (2012) Glutathione is a key player in metal-induced oxidative stress defenses. *Int J Mol Sci* **13(3)**, 3145-3175.

Juang, R.S. and Shiau, R.C. (2000) Metal removal from aqueous solutions using chitosan -enhanced membrane filtration. *J Membr Sci* **165(2)**, 159-167.

Kaszycki, P., Federovych, D., Ksheminska, H., Babyak, L., Wojcik, D., Koloczek, H. (2004) Chromium accumulation by living yeast at various environmental conditions. *Microbiol Res* **159**, 11-17.

Kayalvizhi, K., Vijayaraghavan, K. and Velan, M. (2015) Biosorption of Cr (VI) using a novel microalga *Rhizoclonium hookeri*: equilibrium, kinetics and thermodynamic studies. *Desalin Water Treat* **56(1)**, 194-203.

Khambhaty, Y., Mody, K., Basha, S. and Jha, B. (2009) Kinetics, equilibrium and thermodynamic studies on biosorption of hexavalent chromium by dead fungal biomass of marine *Aspergillus niger*. *Chem Eng J* **145(3)**, 489-495.

Kılıç, N. K., Stensballe, A., Otzen, D. E. and Dönmez, G. (2010) Proteomic changes in response to chromium (VI) toxicity in *Pseudomonas aeruginosa*. *Bioresour Technol* **101**(7), 2134-2140.

Kirk, P.M., Cannon, P.F., Minter, D.W. and Stalpers, J.A. (2008) Dictionary of the Fungi.

Kispal, G., Csere, P., Guiard, B. and Lill, R. (1997) The ABC transporter Atm1p is required for mitochondrial iron homeostasis. *FEBS Lett* **418**(3), 346-350.

Klich, M.A. (2002) *Identification of common Aspergillus species*. Centraal bureau voor schimmel cultures. AD Utrecht, The Netherlands, 116.

Kobya, M., Demirbas, E., Senturk, E. and Ince, M. (2005) *Bioresour Technol* **96**, 1518-1521.

Kortenkamp, A., Curran, B. and O'Brien, P. (1992) Defining conditions for the efficient in vitro cross-linking of proteins to DNA by chromium (III) compounds. *Carcinogenesis* **13**, 307–308.

Kovacevic, Z.F., Sipos, L., Briski, F. (2000) Biosorption of chromium, copper, nickel and zinc ions onto fungal pellets of *Aspergillus niger* 405 from aqueous solutions. *Food Technol Biotechnol* **38**, 211–216.

Kovalchuk, A. and Driessen, A. J. (2010) Phylogenetic analysis of fungal ABC transporters. *BMC genomics*, **11**(1), 177.

Kozłowski, C.A. and Walkowrak W. (2002) Removal of Cr⁶⁺ from aqueous solutions by polymer inclusion membranes. *Water Res* **36**, 4870-4876.

Kratochvíl, D. and Volesky, B. (1998) Advances in the biosorption of heavy metals. *Trends Biotechnol.* **16**, 291-300.

Krumov, N., Perner-Nochta, I., Order, S., Gotcheva, V., Angelov, A. and Posten, C. (2009) Production of inorganic nanoparticles by microorganisms. *Chem Eng Technol* **32(7)**, 1026-1035.

Ksheminska, H., Fedorovich, D., Honchar, T., Ivash, M., and Gonchar, M. (2008). Yeast tolerance to chromium depends on extra cellular chromate reduction and Cr (III) chelation. *Food Technol Biotechnol* **46(4)**, 420-427.

Ksheminska, H., Jaglarz, A., Fedorovych, D., Babyak, L., Yanovych, D., Kaszycki, P., Koloczek, H. (2003) Bioremediation of chromium by the yeast *Pichia guilliermondii*: toxicity and accumulation of Cr (III) and Cr (VI) and the influence of riboflavin on Cr tolerance. *Microbiol Res* **158**, 59–67.

Ksheminska, H.P., Honchar, T.M., Gayda, G.Z. and Gonchar, M.V. (2006) Extra-cellular chromate-reducing activity of the yeast cultures, *Central Eur J Biol* **1**, 37–149.

Kurniawan, T.A., Chan, G.Y.S., Lo, W.H. and Babel, S. (2006) Physicochemical treatment techniques for wastewater laden with heavy metals. *Chem Eng J* **118**, 83–98.

Kuyucak, N. and Volesky, B. (1988) Biosorbents for recovery of metals from industrial solutions. *Biotechnol Lett* **10 (2)**, 137-142.

Lamping, E., Baret, P. V., Holmes, A. R., Monk, B. C., Goffeau, A. and Cannon, R. D. (2010) Fungal PDR transporters: Phylogeny, topology, motifs and function. *Fungal Genet Biol* **47(2)**, 127-142.

Lee, Hyun-uk., Park, J.B., Lee, H., Chae, K.S., Han, D.M., Jahng, K.Y. (2010) Predicting the chemical composition and structure of *Aspergillus nidulans* hyphal wall surface by atomic force microscopy. *J Microbio.* **48**, 243-248.

Lee, J. Y., Yang, J. G., Zhitnitsky, D., Lewinson, O. and Rees, D. C. (2014) Structural basis for heavy metal detoxification by an Atm1-type ABC exporter. *Science* **343(6175)**, 1133-1136.

Leita, L., Margon, A., Sinicco, T. and Mondini C. (2011) Glucose promotes the reduction of hexavalent chromium in soil. *Geoderma* **164**, 122–127.

Lill, R., Hoffmann, B., Molik, S., Pierik, A. J., Rietzschel, N., Stehling, O. and Mühlenhoff, U. (2012) The role of mitochondria in cellular iron–sulfur protein biogenesis and iron metabolism. *Biochimica et Biophysica Acta (BBA)-Mol Cell Res* **1823(9)**, 1491-1508.

Lindblom, S. D., Abdel-Ghany, S., Hanson, B. R., Hwang, S., Terry, N. and Pilon-Smits, E. A. (2006) Constitutive expression of a high-affinity sulfate

transporter in Indian mustard affects metal tolerance and accumulation. *J Environ Qual* **35(3)**, 726-733.

Linton, K. J. (2007) Structure and function of ABC transporters. *Physiology* **22(2)**, 122-130.

Mala, J. G. S., Sujatha, D. and Rose, C. (2015) Inducible chromate reductase exhibiting extracellular activity in *Bacillus methylotrophicus* for chromium bioremediation. *Microbiol Res* **170**, 235-241.

Malik, A. (2004). Metal bioremediation through growing cells. *Environ Int* **30(2)**, 261-278.

Malik, A. and Jaiswal, R. (2000) Metal resistance in *Pseudomonas* strains isolated from soil treated with industrial wastewater. *World J Microbiol Biotechnol* **16**, 108–117.

Mangala, U.N., Rao, Y.R., Varma, P.K. and Muralidharan, K. (2016) Prevalence and Characterization of *Aspergillus* spp. From Rice grains in South India.

Maqbool, Z., Asghar, H.N., Shahzad, T., Hussain, S., Riaz, M., Ali, S., Arif, M.S. and Maqsood, M. (2015) Isolating, screening and applying chromium reducing bacteria to promote growth and yield of okra (*Hibiscus esculentus* L.) in chromium contaminated soils. *Ecotoxicol Environ Saf* **114**, 343-349.

Marsh, T.L. and McInerney, M.J. (2001) Relationship of hydrogen bioavailability to chromate reduction in aquifer sediments. *Appl Environ Microbiol* **67**, 1517–1521.

Marzluf, G.A. (1970) Genetic and metabolic controls for sulfate metabolism in *Neurospora crassa*: isolation and study of chromate-resistant and sulfate transport-negative mutants. *J Bacteriol* **102**, 716-721.

McLean, J. and Beveridge, T.J. (2001) Chromate Reduction by a *Pseudomonad* Isolated from a Site Contaminated with Chromated Copper Arsenate. *App Env Microbiol* 1076–1084.

McNeill, L. and McLean, J. (2012) State of the science of hexavalent chromium in drinking water. *Pollut Eng* **44**, 5.

Mendoza-Cózatl, D. G., Zhai, Z., Jobe, T. O., Akmakjian, G. Z., Song, W. Y., Limbo, O., Russell, M.R., Kozlovskyy, V.I., Martinoia, E., Vatamaniuk, O.K. and Russell, P. (2010) Tonoplast-localized Abc2 transporter mediates phytochelatin accumulation in vacuoles and confers cadmium tolerance. *J Biol Chem* **285(52)**, 40416-40426.

Middleton, S. S., Latmani, R. B., Mackey, M. R., Ellisman, M. H., Tebo, B. M. and Criddle, C. S. (2003) Cometabolism of Cr (VI) by *Shewanella oneidensis* MR-1 produces cell-associated reduced chromium and inhibits growth. *Biotechnol Bioeng* **83(6)**, 627-637.

Mishra, A. and Malik, A. (2014) Novel fungal consortium for bioremediation of metals and dyes from mixed waste stream. *Bioresour Technol* **171**, 217-226.

Mishra, S. and Bharagava, R. N. (2016) Toxic and genotoxic effects of hexavalent chromium in environment and its bioremediation strategies. *J Environ Sci Health, Part C* **34(1)**, 1-32.

Monaselidze, J., Abuladze, M., Asatiani, N., Kiziria, E., Barbakadze, S., Majagaladze, G., Iobadze, M., Tabatadze, L., Holman, H.Y. and Sapojnikova, N. (2006) Characterization of chromium-induced apoptosis in cultured mammalian cells: A differential scanning calorimetry study. *Thermochimica acta* **441(1)**, 8-15.

Morais, P. V., Branco, R. and Francisco, R. (2011) Chromium resistance strategies and toxicity: what makes *Ochrobactrum tritici* 5bv11 a strain highly resistant. *Biometals* **24(3)**, 401-410.

Morales-Barrera, L. and Cristiani-Urbina, E. (2008) Hexavalent chromium removal by a *Trichoderma inhamatum* fungal strain isolated from tannery effluent. *Water Air Soil Pollut* **187**, 327-336.

Muraleedharan, T.R. and Venkobachar, C. (1990) Mechanism of biosorption of copper (II) by *Ganoderma lucidum*. *Biotechnol Bioen.* **35**, 320-325.

Narayani, M. and Shetty, K. V. (2013) Chromium-resistant bacteria and their environmental condition for hexavalent chromium removal: a review. *Crit Rev Environ Sci Technol*, **43(9)**, 955-1009.

Neal, A. L., Lowe, K., Daulton, T. L., Jones-Meehan, J. and Little, B. J. (2002) Oxidation state of chromium associated with cell surfaces of *Shewanella oneidensis* during chromate reduction. *Appl Surf Sci* **202(3)**, 150-159.

Ngô, C.T.T. (2016) Heavy Metal Resistance and Biosorption of Acid-Tolerant Yeasts Isolated from Tea Soil. *VNU J Sci: Earth Environ Studies*, **29(4)**.

Nies, A., Nies, D. H. and Silver, S. (1989) Cloning and expression of plasmid genes encoding resistance to chromate and cobalt in *Alcaligenes eutrophus*. *J Bacteriol* **171**, 5065–5070.

Nies, A., Nies, D. H. and Silver, S. (1990) Nucleotide sequence and expression of a plasmid-encoded chromate resistance determinant from *Alcaligenes eutrophus*. *J Biol Chem* **265**, 5648–5653.

Nunthaboot, N., Lugsanangarm, K., Nueangaudom, A., Pianwanit, S., Kokpol, S., Tanaka, F. and Kitamura, M. (2016) Photoinduced electron transfer from aromatic amino acids to the excited isoalloxazine in flavin mononucleotide binding protein. Is the rate in the inverted region of donor–acceptor distance not real? *J Photochem Photobiol A Chem* **326**, 60-68.

Ohta, N., Galsworthy, P. R. and Pardee, A. B. (1971) Genetics of sulfate transport by *Salmonella typhimurium*. *J Bacteriol* **105(3)**, 1053-1062.

Ohtake, H., Cervantes, C. and Silver, S. (1987) Decreased chromate uptake in *Pseudomonas fluorescens* carrying a chromate resistance plasmid. *J Bacteriol* **169**, 3853-3856.

Ortiz, D. F., Ruscitti, T., McCue, K. F. and Ow, D. W. (1995) Transport of metal-binding peptides by HMT1, a fission yeast ABC-type vacuolar membrane protein. *J Biol Chem* **270(9)**, 4721-4728.

Park, C.H., Keyhan, M., Wielinga, B., Fendorf, S., Matin, A. (2000) Purification to Homogeneity and Characterization of a Novel *Pseudomonas putida* Chromate Reductase. *App Env Microbiol* 1788–1795.

Park, D., Lim, S.R., Yun, Y.S., Park, J.M., (2007) Reliable evidences that removal mechanism of hexavalent chromium by natural biomaterials is adsorption coupled reduction. *Chemosphere* **70**, 298–305.

Park, D., Yun, Y. S., and Park, J. M. (2004). Reduction of hexavalent chromium with the brown seaweed *Ecklonia biomass*. *Environci Sci Technol* **38(18)**, 4860-4864.

Park, D., Yun, Y.S., Jo, J.H. and Park, J.M., (2005) Mechanism of hexavalent chromium removal by dead fungal, biomass of *Aspergillus niger*, *Water Res.* **39**, 533–540.

Park, D., Yun, Y.-S., Jo, J.H. and Park, J.M. (2005a) Mechanism of hexavalent chromium removal by dead fungal biomass of *Aspergillus niger*. *Water Res* **39**, 533–540.

Park, D., Yun, Y.-S. and Park, J.M. (2005b) Use of dead fungal biomass for the detoxification of hexavalent chromium: screening and kinetics. *Process Biochem* **40**, 2559–2565.

Park, D., Yun, Y.S., Park, J.M. (2008) XAS and XPS studies on chromium-binding groups of biomaterial during Cr (VI) biosorption. *J Colloid Interface Sci* **317**, 54–6.

Passow, H., Rothstein, A. and Clarkson T. W., (1961) The general pharmacology of heavy metals. *Pharmacol Rev* **13**, 185-224.

Paumi, C. M., Chuk, M., Snider, J., Stagljar, I. and Michaelis, S. (2009) ABC transporters in *Saccharomyces cerevisiae* and their interactors: new technology advances the biology of the ABCC (MRP) subfamily. *Microbiol Mol Biol Rev* **73(4)**, 577-593.

Pessoni, R. A., Freshour, G., Rita de Cássia, L., Hahn, M. G. and Braga, M. R. (2005) Cell-wall structure and composition of *Penicillium janczewskii* as affected by inulin. *Mycologia*, **97(2)**, 304-311.

Pesti, M., Gazdag, Z. and Belágyi, J., (2000) In vivo interaction of trivalent chromium with yeast plasma membrane, as revealed by EPR spectroscopy. *FEMS Microbiol Lett* **182**, 375–380.

Piehler, A. P., Özcürümez, M. and Kaminski, W. E. (2012) A-subclass ATP-binding cassette proteins in brain lipid homeostasis and neurodegeneration. *Front Psychiatry* **3**, 17.

Pilon-Smits, E. (2005) Phytoremediation. *Annu Rev Plant Biol* **56**, 15–39.

Piłyk, S. and Paszewski, A. (2009) Sulfate permeases—phylogenetic diversity of sulfate transport. *Acta Biochim Pol* **56(3)**, 375-84.

Poljsak, B., Pócsi, I., Raspor, P. and Pesti, M. (2010) Interference of chromium with biological systems in yeasts and fungi: a review. *J Basic Microbiol* **50**, 21–36.

Polti, M.A., Atjian, M.C., Amoroso, M.J. and Abate, C.M. (2011) Soil chromium bioremediation: Synergic activity of Actinobacteria and plants. *Int Biodeterior Biodegradation* **65**, 1175-1181.

Pramanik, K., Ghosh, P. K., Ghosh, A., Sarkar, A. and Maiti, T. K. (2016) Characterization of PGP Traits of a Hexavalent Chromium Resistant *Raoultella* sp. Isolated from the Rice Field near Industrial Sewage of Burdwan District, WB, India. *Soil Sediment Contam* **25(3)**, 313-331.

Prasenjiti, B. and Sumathi, S. (2005) Uptake of chromium by *Aspergillus foetidus*, *J Mat Cycles Waste Manag* **7(2)**, 88–92.

Prévéral, S., Gayet, L., Moldes, C., Hoffmann, J., Mounicou, S., Gruet, A., Reynaud, F., Lobinski, R., Verbavatz, J.M., Vavasseur, A. and Forestier, C. (2009) A common highly conserved cadmium detoxification mechanism from bacteria to humans heavy metal tolerance conferred by the ATP-binding cassette (ABC) transporter SpHMT1 requires glutathione but not metal-chelating phytochelatin peptides. *J Biol Chem* **284(8)**, 4936-4943.

Puglisi, I., Faedda, R., Sanzaro, V., Piero, A. R. L., Petrone, G. and Cacciola, S. O. (2012) Identification of differentially expressed genes in response to mercury I and II stress in *Trichoderma harzianum*. *Gene* **506(2)**, 325-330.

Pure Earth. (2015) World's Worst Pollution Problems. The New Top Six Toxic Threats. A Priority List for Remediation. Available at <http://www.worstpolluted.org>.

Quiévryn G., Messer J. and Zhitkovich A. (2002) Carcinogenic chromium (VI) induces cross-linking of vitamin C to DNA in vitro and in human lung A549 cells. *Biochem* **41**, 3156–3167.

Quiévryn G., Peterson E., Messer J. and Zhitkovich A. (2003) Genotoxicity and mutagenicity of chromium (VI)/ascorbate-generated DNA adducts in human and bacterial cells. *Biochemistry* **42**, 1062–1070.

Ramirez-Diaz, M.I., Diaz-Perez, C., Vargas, E., Riveros-Rosas, H., Campos-Garcia, J. and Cervantes, C. (2008) Mechanisms of bacterial resistance to chromium compounds. *Biometals* **21**: 321–332.

Ramirez-Ramirez, R., Calvo-Medez, C., Avila-Rodriguez, M., Lappe, P., Ulloa, M., Vaquez-Juarez, R. and Gutierrez-Corona, J.F. (2004) Cr (VI) reduction in a chromate-resistant strain of *Candida maltosa* isolated from the leather industry. *Antonie van Leeuwenhoek* **85**, 63–68.

Ramrakhiani, L., Majumder, R., Khowala, S. (2011) Removal of hexavalent chromium by heat inactivated fungal biomass of *Termitomyces clypeatus*: Surface characterization and mechanism of biosorption. *Chem Eng J* **171**, 1060–1068.

Ran, Z., Bi, W., Cai, Q.T., Li, X.X., Min, L.I.U., Dong, H.U., Guo, D.B., Juan, W. and Chun, F. (2016) Bioremediation of Hexavalent Chromium Pollution by *Sporosarcina saromensis* M52 Isolated from Offshore Sediments in Xiamen, China. *Biomed Environ Sci* **29(2)**, 27-136.

Reynolds M.F., Peterson-Roth E.C., Bessalov I.A., Johnston T., Gurel V.M., Menard H.L. and Zhitkovich A. (2009) Rapid DNA double-strand breaks resulting from processing of Cr-DNA cross-links by both MutS dimers. *Cancer Res* **69**, 1071–1079.

Rossi, S. C., Gorman, N. and Wetterhahn, K. E. (1988) Mitochondrial reduction of the carcinogen chromate: formation of chromium (V). *Chem Res Toxicol* **1(2)**, 101-107.

Rouached, H., Berthomieu, P., El Kassis, E., Cathala, N., Catherinot, V., Labesse, G. Davidian, J.C. and Fourcroy, P. (2005) Structural and functional analysis of the C-terminal STAS (sulfate transporter and anti-sigma antagonist) domain of the *Arabidopsis thaliana* sulfate transporter SULTR1.2. *J Biol Chem* **280(16)**, 15976-15983.

Saha, B. and Orvig, C., 2010. Biosorbents for hexavalent chromium elimination from industrial and municipal effluents. *Coord Chem Rev* **254(23)**, 2959-2972.

Samuel, M. S. and Chidambaram, R. (2015) Hexavalent chromium biosorption studies using *Penicillium griseofulvum* MSR1 a novel isolate from tannery effluent site: Box–Behnken optimization, equilibrium, kinetics and thermodynamic studies. *J Taiwan Inst Chem Eng* **49**, 156-164.

Sandal., N. N. and Marcker, K. A. (1994) Similarities between a soybean nodulin, *Neurospora crassa* sulphate permease II and a putative human tumour suppressor. *Trends Biochem Sci* **19(1)**, 19

Sanghi, R and Srivastava, A. (2010) Long-term chromate reduction by immobilized fungus in continuous column. *Chem Eng J* **162(1)**, 122-126.

Sanghi, R., Sankararamakrishnan, N. and Dave, B. C. (2009) Fungal bioremediation of chromates: conformational changes of biomass during sequestration, binding, and reduction of hexavalent chromium ions. *J Hazard Mater* **169(1)**, 1074-108

Sarı, A. and Tuzen, M. (2008) Biosorption of total chromium from aqueous solution by red algae (*Ceramium virgatum*): equilibrium, kinetic and thermodynamic studies. *J Hazard Mater* **160(2)**, 349-355.

Seidel, A., Waypa, J. J. and Elimelech, M. (2001) Role of charge (Donnan) exclusion in removal of arsenic from water by a negatively charged porous nanofiltration membrane. *Environ Eng Sci* **18(2)**, 105-113.

Sen, M. (2012) A Comparative Study on Biosorption of Cr (VI) by *Fusarium solani* under different growth conditions. *Open J Appl Sci* **2(03)**, 146.

Sharma S. and Adholeya A. (2011) Detoxification and accumulation of chromium from tannery effluent and spent chrome effluent by *Paecilomyces lilacinus* fungi. *Int Biodeterior Biodegradation* **65**, 309–317.

Sharma, I. and D. Goyal, (2010) Adsorption kinetics: Bioremoval of trivalent chromium from tannery effluent by *Aspergillus sp.* Biomass. *Res J Environ Sci* **4**, 1-12.

Sharma, S. and Adholeya, A. (2012) Hexavalent chromium reduction in tannery effluent by bacterial species isolated from tannery effluent contaminated soil. *J Environ Sci Technol* **5(3)**, 142.

Sharma, S. and Malaviya, P. (2016) Bioremediation of tannery wastewater by chromium resistant novel fungal consortium. *Ecol Eng* **91**, 419-425.

Shen, Y., Wang, S., Tzou, Y., Yan, Y. and Kuan, W. (2012) Removal of hexavalent Cr by coconut coir and derived chars the effect of surface functionality. *Bioresour Technol* **104**, 65–172.

Shi W., Becker J., Bischoff M., Turco R.F. and Konopka A.E. (2002) Association of microbial community composition and activity with lead, chromium, and hydrocarbon contamination. *Appl Environ Microbiol* **68**, 3859–3866.

Shibagaki, N. and Grossman, A. R. (2006) The role of the STAS domain in the function and biogenesis of a sulfate transporter as probed by random mutagenesis. *J Bioll Chem* **281(32)**, 22964-22973.

Shugaba, A., Buba, F., Kolo, B.G., Nok, A.J., Ameh, D.A. Lori, J.A. (2012) Uptake and reduction of hexavalent chromium by *Aspergillus niger* and *Aspergillus parasiticus*. *J Pet Environ Biotechnol* **3**, 3.

Shugaba, A., Nok, A. J., Ameh, D. A. Lori, J. A. (2010) Studies on the growth of some filamentous fungi in culture solutions containing hexavalent chromium. *Int J Biotech Biochem* **6**, 715–722.

Sievers, F., Wilm, A., Dineen, D., Gibson, T. J., Karplus, K., Li, W., Lopez, R., McWilliam, H., Remmert, M., Söding, J. and Thompson, J. D. (2011) Fast, scalable generation of high-quality protein multiple sequence alignments using Clustal Omega. *Mol Syst Biol* **7(1)**, 539.

Singh, R. and Bishnoi, N. R. (2015) Biotransformation dynamics of chromium (VI) detoxification using *Aspergillus flavus* system. *Ecol Eng* **75**, 103-109.

Singh, R., Kumar, M. and Bishnoi, N. R. (2016) Development of biomaterial for chromium (VI) detoxification using *Aspergillus flavus* system supported with iron. *Ecol Eng* **91**, 31-40.

Slocik, J. M., Knecht, M. R. and Wright, D. W. (2004), *Encyclopedia Nanosci Nanotechnol* **1**, 293.

Smith, F. W., Hawkesford, M. J., Prosser, I. M. and Clarkson, D. T. (1995) Isolation of a cDNA from *Saccharomyces cerevisiae* that encodes a high affinity sulphate transporter at the plasma membrane. *Mol Gen Genet* **247**, 709–715.

Snow, E.T. and Xu, L.S. (1989) Effect of chromium (III) on DNA replication in vivo. *Biol Trace Elem Res* **21**, 113–117.

Sobol Z. and Schiestl R.H. (2012) Intracellular and extracellular factors influencing Cr(VI) and Cr(III) genotoxicity. *Environ Mol Mutagen* **53**, 94–100.

Srinivasa, S. G. and Govil, P.K. (2008) Distribution of Heavy Metals in Surface Water of Ranipet Industrial Area in Tamil Nadu, India. *Environ Monit Assess* **136(1-3)** 197-207.

Srivastava, S. and Thakur, I.S. (2006) Evaluation of Bioremediation and Detoxification Potentiality of *Aspergillus niger* for Removal of Hexavalent Chromium in Soil Microcosm. *Soil Biol Biochem* **7**, 1904-1911.

S

rivastava, S. and Thakur, I.S. (2006a) Isolation and process parameter optimization of *Aspergillus sp.* for removal of chromium from tannery effluent. *Bioresour Technol* **97**, 1167–1173.

Sturm, G., Jacobs, J., Spröer, C., Schumann, P. and Gescher, J. (2011) *Leucobacter chromiirestiens sp. nov.*, a chromate-resistant strain. *Int J Syst Evol Microbiol* **61(4)**, 956-960.

Summers, A. O. and Jacoby, G.A. (1978) Plasmid-determined resistance to boron and chromium compounds in *Pseudomonas aeruginosa*. *Antimicrob Agents Chemother* **13**, 637–640.

Suzuki, T. O. H. R. U., Miyata, N., Horitsu, H., Kawai, K., Takamizawa, K., Tai, Y. and Okazaki, M. (1992) NAD (P) H-dependent chromium (VI) reductase of

Pseudomonas ambigua G-1: a Cr (V) intermediate is formed during the reduction of Cr (VI) to Cr (III) *J Bacteriol* **174(16)**, 5340-5345.

Tamura, K., Stecher, G., Peterson, D., Filipski, A., and Kumar, S. (2013) MEGA6: molecular evolutionary genetics analysis version 6.0. *Molecular Biol Evol* **30(12)**, 2725-2729.

Terada, H. (1990) Uncouplers of oxidative phosphorylation. *Environ Health Perspect* **87**, 213.

Thacker, U. and Madamwar, D. (2005) Reduction of toxic chromium and partial localization of chromium reductase activity in bacterial isolate DM1. *World J Microbiol Biotechnol* **21**, 891–899.

Thacker, U., Parikh, R., Shouche, Y. and Madamwar, D. (2006) Hexavalent Chromium Reduction by *Providencia* sp. *Process Biochem* **41**, 1332–1337.

Thilakaraj, R., Raghunathan, K., Anishetty, S. and Pennathur, G. (2007) In silico identification of putative metal binding motifs. *Bioinformatics* **23(3)**, 267-271.

Thompson, J. G., McNaughton, C., Gasparini, B., McGowan, L. T. and Tervit, H. R. (2000) Effect of inhibitors and uncouplers of oxidative phosphorylation during compaction and blastulation of bovine embryos cultured in vitro. *J Reprod Fertil* **118(1)**, 47-55.

Toei, M. and Noji, H. (2013) Single-molecule analysis of F₀F₁-ATP synthase inhibited by N, N-dicyclohexylcarbodiimide. *J Biol Chem* **288(36)**, 25717-25726.

Torricelli, E., Gorbi, G., Pawlik-Skowronska, B., di Toppi, L. S. and Corradi, M. G. (2004) Cadmium tolerance, cysteine and thiol peptide levels in wild type and chromium-tolerant strains of *Scenedesmus acutus* (Chlorophyceae). *Aquatic Toxicol* **68(4)**, 315-323.

Tripathi, M., Vikram, S., Jain, R. K., Garg, S. K. (2011) Isolation and growth characteristics of chromium (VI) and pentachlorophenol tolerant bacterial isolate from treated tannery effluent for its possible use in simultaneous bioremediation. *Indian J Microbiol* **51**, 61–69.

Tusnády, G. E., Bakos, É., Váradi, A. and Sarkadi, B. (1997) Membrane topology distinguishes a subfamily of the ATP-binding cassette (ABC) transporters. *FEBS Lett* **402(1)**, 1-3.

U.S. EPA. 2005. Guidelines for Carcinogen Risk Assessment Risk Assessment Forum. Washington, DC:U.S. Environmental Protection Agency.

UdDin, I., Bano, A, and Masood, S. (2015) Chromium toxicity tolerance of *Solanum nigrum L.* and *Parthenium hysterophorus L.* plants with reference to ion pattern, antioxidation activity and root exudation. *Ecotoxicol Environ Saf* **113**, 271-278.

United States Environmental Protection Agency.

<https://www3.epa.gov/>(Accessed May 2016).

USEPA. (2000) Effluent limitations guidelines, pre-treatment standards, commercial hazardous waste combustor subcategory. *Federal Register* vol. 65, No 18, 40 CFR Part 444. USEPA, Washington, DC.

USEPA. Exposure factors handbook 2011 edition (Final); 2011. <http://cfpub.epa.gov/ncea/risk/recordisplay.cfm>.

Valko, M., Morris, H. and Cronin, M.T. (2005) Metals, toxicity and oxidative stress. *Curr Med Chem* **12**, 1161–1208.

Van der Bruggen, B., Mänttari, M. and Nyström, M. (2008) Drawbacks of applying nanofiltration and how to avoid them: a review. *Sep Purif Technol* **63(2)**, 251-263.

Vatamaniuk, O. K., Bucher, E. A., Sundaram, M. V. and Rea, P. A. (2005) CeHMT-1, a putative phytochelatin transporter, is required for cadmium tolerance in *Caenorhabditis elegans*. *J Biol Chem* **280(25)**, 23684-23690.

Verma, T. and Singh, N. (2013) Isolation and process parameter optimization of *Brevibacterium casei* for simultaneous bioremediation of hexavalent chromium and pentachlorophenol. *J basic Microbiol* **53(3)**, 277-290.

Vigneswaran, S., Ngo, H.H., Chaudhary, D.S., Hung, Y.T., (2004) Physico-chemical treatment processes for water reuse. In: Wang, L.K., Hung, Y.T., Shammas, N.K. (Eds.), *Physicochemical Treatment Processes*, vol. 3. Humana Press, New Jersey, 635–676.

Viti, C., Marchi, E., Decorosi, F. and Giovannetti, L. (2014) Molecular mechanisms of Cr (VI) resistance in bacteria and fungi. *FEMS Microbiol Rev* **38(4)**, 633-659.

Volesky, B. (1994) Advances in biosorption of metals: Selection of biomass types. *FEMS Microbiol* **14**, 291-302.

Volesky, B. 1986. Biosorbent Materials, *Biotechnol. Bioeng Symp* **16**, 121-126

Walker, J.E., Saraste, M., Runswick, M.J. and Gay N.J. (1982) Distantly related sequence in alpha- and beta-subunits of ATP synthase, myosin, kinases and other ATP requiring enzymes and a common nucleotide binding fold. *EMBO J* **1(8)**, 945

Wang, H., Xu, Z., Gao, L. and Hao, B. (2009) A fungal phylogeny based on 82 complete genomes using the composition vector method. *BMC Evol Biol* **9(1)**, 1.

Wang, L.K., Vaccari, D.A., Li, Y., Shammas, N.K., (2004) Chemical precipitation. In: Wang, L.K., Hung, Y.T., Shammas, N.K. (Eds.), *Physicochemical Treatment Processes*, vol. 3. Humana Press, New Jersey, 141–198.

White, C. and Gadd, G. M. (1986) Uptake and cellular distribution of copper, cobalt and cadmium in strains of *Saccharomyces cerevisiae* cultured on elevated concentrations of these metals. *FEMS Microbiol Ecol* **2(5)**, 277-283.

WHO (2004) *Guidelines for drinking water quality*. WHO, Geneva.

WHO, World Health Organization, Geneva (2010) *Guideline for drinking water quality recommendations 1*.

Wilkins, S. (2015) Structure and mechanism of ABC transporters. *F1000prime reports* **7**.

Williams, L.E., Pittman, J.K. and Hall, J.L. (2000) Emerging mechanisms for heavy metal transport in plants. *Biochim Biophys Acta* **1465**, 104–126.

Wong, P.K. and Chang, L. (1991) Effects of copper, chromium and nickel on growth, photosynthesis and chlorophyll a synthesis of *Chlorella pyrenoidosa* 251. *Environ Pollut* **72**, 127-139.

Xiao, F., Li, Y., Luoc, L., Xie, Y., Zeng, M., Wang, N., Chen, H. and Zhong, C, (2014) Role of Mitochondrial Electron Transport Chain Dysfunction in Cr(VI)-Induced Cytotoxicity in L-02 Hepatocytes. *Cell Physiol Biochem* **33**, 1013-1025.

Xu, X.R., Li, H.B. and Gu, J.D. (2004) Reduction of hexavalent chromium by ascorbic acid in aqueous solutions. *Chemosphere* **57**, 609–613.

Xu, X.R., Li, H.B., Gu, J-D. and Li, X.Y. (2005) Kinetics of the reduction of chromium (VI) by vitamin C. *Environ Toxicol Chem* **24**, 1310–1314.

Yadav, G.C., Pandey, G.C., Singh, C.S. and Yadav, S.R.A. (2006) Physico-chemical analysis of M/S Narang distillery, Nawabganj and Sugar factory Babhnan, Gonda effluents. *Himalayan J Environ Zoolol* **20(1)**, 71-74.

Yadav, S., Shukla, O. P., and Rai, U. N. (2005). Chromium pollution and bioremediation. *Environews Newsletter of ISEB India*, *11(1)*.

Yan, G. and Viraraghavan, T. (2001) Heavy metal removal in a biosorption column by immobilized *M. rouxii* biomass. *Bioresour Technol* **78(3)** 243-249.

Yang, X., Palanichamy, K., Ontko, A.C., Rao, M., Fang, C.X., Ren, J. and Sreejayan, N. (2005) A newly synthetic chromium complex–chromium 162 (phenylalanine) 3 improves insulin responsiveness and reduces whole body glucose tolerance. *FEBS Lett* **579**, 1458-1464.

Yang, Y., Chen, M., Li, Z., Al-Hatmi, A.M., de Hoog, S., Pan, W., Ye, Q., Bo, X., Li, Z., Wang, S. and Wang, J. (2016) Genome sequencing and comparative genomics analysis revealed pathogenic potential in *Penicillium capsulatum* as a novel fungal pathogen belonging to Eurotiales. *Front Microbiol* **7**.

Zafar, S., Aquil, F. and Ahmad, I. (2007) Metal tolerance and biosorption potential of filamentous fungi isolated from metal contaminated agricultural soil. *Bioresour Technol* **98**, 2557–256.

Zayed, A.M. and Terry, N. (2003) Chromium in the environment: Factors affecting biological remediation. *Plant Soil* **249**, 139–156.

Zhang, K.D. and Li, F.L. (2011) Isolation and characterization of a chromium-resistant bacterium *Serratia sp.* Cr-10 from a chromate-contaminated site. *Appl Microbiol Biotechnol* **90**: 1163–1169.

Zhao, C., Liu, J., Tu, H., Li, F., Li, X., Yang, J., Liao, J., Yang, Y., Liu, N. and Sun, Q., (2016) Characteristics of uranium biosorption from aqueous solutions on fungus *Pleurotus ostreatus*. *Environ Sci Poll Res* **23(24)**, 24846-24856.

Zhitkovich, A., Song, Y., Quievryn, G. and Voitkun, V. (2001) Non-oxidative mechanisms are responsible for the induction of mutagenesis by reduction of Cr (VI) with cysteine: role of ternary DNA adducts in Cr(III)-dependent mutagenesis. *Biochemistry* **40**, 549–560.

Zhou, J., Xia, B., Treves, D.S., Wu, L-Y, Marsh, T.L., O'Neill, R.V., Palumbo, A.V. and Tiedje, J.M. (2002) Spatial and resource factors influencing high microbial diversity in soil. *Appl Environ Microbiol* **68**, 326–334.

Zinicovscaia, I., Cepoi, L., Chiriac, T., Ana Culicov, O., Frontasyeva, M., Pavlov, S., Kirkesali, E., Akshintsev, A. and Rodlovskaya, E. (2016) *Spirulina platensis* as biosorbent of chromium and nickel from industrial effluents. *Desalination and Water Treat* **57 (24)**, 11103-11110.

Zolgharnein, H., Karami, K., Assadi, M.M. and Sohrab, A.D. (2010)
Investigation of heavy metals biosorption on *Pseudomonas aeruginosa* strain
MCCB 102 isolated from the Persian Gulf. *Asian J Biotech* **2(2)**, 99-109.